

GENE EXPRESSION ANALYSIS OF Xrel3-INDUCED  
TUMOURS IN *Xenopus laevis*

CENTRE FOR NEWFOUNDLAND STUDIES

**TOTAL OF 10 PAGES ONLY  
MAY BE XEROXED**

(Without Author's Permission)

REBECCA FORD









## **INFORMATION TO USERS**

**This manuscript has been reproduced from the microfilm master. UMI films the text directly from the original or copy submitted. Thus, some thesis and dissertation copies are in typewriter face, while others may be from any type of computer printer.**

**The quality of this reproduction is dependent upon the quality of the copy submitted. Broken or indistinct print, colored or poor quality illustrations and photographs, print bleedthrough, substandard margins, and improper alignment can adversely affect reproduction.**

**In the unlikely event that the author did not send UMI a complete manuscript and there are missing pages, these will be noted. Also, if unauthorized copyright material had to be removed, a note will indicate the deletion.**

**Oversize materials (e.g., maps, drawings, charts) are reproduced by sectioning the original, beginning at the upper left-hand corner and continuing from left to right in equal sections with small overlaps.**

**Photographs included in the original manuscript have been reproduced xerographically in this copy. Higher quality 6" x 9" black and white photographic prints are available for any photographs or illustrations appearing in this copy for an additional charge. Contact UMI directly to order.**

**ProQuest Information and Learning  
300 North Zeeb Road, Ann Arbor, MI 48106-1346 USA  
800-521-0600**

**UMI<sup>®</sup>**

## **NOTE TO USERS**

**This reproduction is the best copy available.**

UMI<sup>®</sup>



**National Library  
of Canada**

**Acquisitions and  
Bibliographic Services**

**395 Wellington Street  
Ottawa ON K1A 0N4  
Canada**

**Bibliothèque nationale  
du Canada**

**Acquisitions et  
services bibliographiques**

**395, rue Wellington  
Ottawa ON K1A 0N4  
Canada**

*Your file Votre référence*

*Our file Notre référence*

**The author has granted a non-exclusive licence allowing the National Library of Canada to reproduce, loan, distribute or sell copies of this thesis in microform, paper or electronic formats.**

**The author retains ownership of the copyright in this thesis. Neither the thesis nor substantial extracts from it may be printed or otherwise reproduced without the author's permission.**

**L'auteur a accordé une licence non exclusive permettant à la Bibliothèque nationale du Canada de reproduire, prêter, distribuer ou vendre des copies de cette thèse sous la forme de microfiche/film, de reproduction sur papier ou sur format électronique.**

**L'auteur conserve la propriété du droit d'auteur qui protège cette thèse. Ni la thèse ni des extraits substantiels de celle-ci ne doivent être imprimés ou autrement reproduits sans son autorisation.**

**0-612-62384-X**

**Canada**

# **Gene Expression Analysis of *Xre/3*-induced Tumours in *Xenopus laevis***

**By**

**Rebecca Ford, B. Sc. (Hons.)**

**A dissertation submitted to the School of Graduate Studies in partial fulfilment of the requirement for the degree of Master of Science.**

**Division of Basic Medical Sciences  
Faculty of Medicine  
Memorial University of Newfoundland**

**November, 2000**



## **Abstract**

*Xenopus rel3 (Xrel3)* is one of five *Xenopus* members of the Rel/Nuclear Factor kappa B (NF- $\kappa$ B) family of transcriptional activators. The role of *Xrel3* in early embryonic development is unclear, however, its spatially and temporally restricted pattern of expression in larval and tadpole stages suggests a potential role in embryonic patterning. Overexpression of synthetic *Xrel3* messenger RNA (mRNA) in the animal pole of *Xenopus* embryos induces the formation of tumours on the surface of embryos. Reverse transcription polymerase chain reaction (RT-PCR) was used in this study to investigate and identify genes that are activated in response to *Xrel3* overexpression. My results show that *sonic hedgehog (shh)*, *gli1*, *otx-2* and the fibroblast growth factors, *fgf-8* and *efgf(ii)*, are upregulated in response to *Xrel3* overexpression. Interestingly, these genes are axial patterning genes required for the development of dorsal and anterior body structures, whose normal expression patterns overlap that of *Xrel3* in neurula and larval stage embryos. In addition, *Gli1*, *Shh* and *Fgfs* play normal roles in promoting cell proliferation and regulating the cell cycle. This suggests that perhaps the role of *Xrel3* in development is to regulate cell proliferation and hence the differentiation of certain structures of the nervous system. The effect of *Xrel3* overexpression on the levels of *gli1*, *shh* and *otx-2* was not an immediate one, but the use of the differential display technique has led to the identification of a potentially novel gene activated by *Xrel3*. The identification and characterization of the specific components of the *Xrel3* signalling pathway and the biochemical nature by which *Xrel3* exerts its influence will provide us with an insight into the mechanism by which it functions in development and cancer.

# **Acknowledgements**

I would like to express my deepest feelings of gratitude to my supervisor, Dr. Ken Kao, for providing me with the opportunity to gain laboratory and research experience in the fields of molecular and developmental biology. Throughout the course of my graduate career, Dr. Kao has always made himself readily available for any problems or questions I might have and has been a constant source of encouragement and inspiration. Even though it may not have seemed like it at the time, I sincerely appreciate all the little extra pushes that Dr. Kao gave me to help keep me on track and focused.

I would also like to say a special thank you to Dr. Laura Gillespie and Dr. Karen Mearow for all their positive advice and suggestions. Thanks also go out to Trudy Toms, for providing technical assistance with the differential display and Corinne Mercer, for trouble-shooting assistance with RT-PCR. I would also like to thank Blue Lake, Artee Luchman, Gordon Nash, Janine Post, Lori Ann Foley, Olga Skhirtladze and everyone else at the Terry Fox Cancer Research Laboratories for their friendship and advice and, in general, for providing a great working environment.

Last, but by no means least, I would like to say a special thank you to my parents, particularly my father, for their continued support and encouragement in everything I do, for all their advice and for all their pep talks when I was feeling down.

# **Preface**

The work in this thesis (Chapter 3, sections 3.1-3.5 and Chapter 4, sections 4.2-4.3) pertaining to the RT-PCR analysis of *Xrel3*-induced tumours has been accepted for publication in *Development*. In this paper I am a joint-first author with Blue Lake. I provided Figures 2-4 in the paper and was involved with writing the Materials and Methods and the Results sections pertaining to these figures.

# Table of Contents

Abstract.....	i
Acknowledgements.....	ii
Preface .....	iii
List of Tables .....	vi
List of Figures .....	vii-x
Abbreviations.....	xi-xii
 <b>1. Introduction</b>	
<b>1.1 General</b> .....	1
<b>1.2 <i>Xenopus laevis</i> as a developmental model</b> .....	2
<b>1.3 <i>Xenopus</i> development</b> .....	3-30
1.3.1 Oogenesis.....	3-6
1.3.2 Fertilization and post-fertilization events .....	6-8
1.3.3 Early Cleavage Stages .....	9
1.3.4 Body patterning in the early embryo .....	9-24
1.3.4.1 Mesoderm induction .....	10-14
1.3.4.2 Molecular events that pattern the mesoderm .....	14-20
1.3.4.3 Gastrulation and Neurulation .....	20-22
1.3.4.4 Neural Induction.....	23-24
1.3.5 Organogenesis.....	24-26
1.3.6 Metamorphosis and limb formation in <i>Xenopus</i> .....	26-30
<b>1.4 <i>Xenopus laevis</i> as a tumour model</b> .....	30-33
<b>1.5 The Rel family of proteins</b> .....	32,34-41
1.6.1 Rel/NF- $\kappa$ B structure.....	34-37
1.6.2 Regulation of rel/NF- $\kappa$ B activity .....	38-41
<b>1.6 The role of Rel proteins in development</b> .....	41-45
<b>1.7 The role of Rel in oncogenesis</b> .....	45-47
<b>1.8 Objectives</b> .....	47-49
 <b>2. Materials and Methods</b>	
<b>2.1 <i>In vitro</i> fertilization of mature <i>Xenopus</i> oocytes</b> .....	50-52
<b>2.2 <i>In vitro</i> transcription of <i>Xrel3</i></b> .....	53-55
<b>2.3 <i>Xenopus</i> embryo microinjections</b> .....	55
<b>2.4 <i>Xenopus</i> embryo dissections/extractions</b> .....	56-57
2.4.1 Animal cap dissections .....	56
2.4.2 Skin and tumour extractions.....	57
2.4.3 Limb bud amputations .....	57



<b>2.5 RNA extraction .....</b>	<b>58-59</b>
<b>2.6 Reverse Transcription Polymerase Chain Reaction (RT-PCR) ....</b>	<b>59-64</b>
2.6.1 Reverse transcription of isolated RNA.....	59-61
2.6.2 PCR of reverse transcription products (cDNAs) .....	62-64
<b>2.7 Differential Display.....</b>	<b>65-78</b>
2.7.1 Reverse transcription of skin and tumour RNA .....	65-67
2.7.2 PCR of skin and tumour cDNA .....	67-68
2.7.3 Polyacrylamide gel electrophoresis .....	68-70
2.7.3.1 100bp end-labelling reaction .....	69-70
2.7.4 Differential Display DNA recovery.....	70-71
2.7.5 Re-amplification of eluted differential display bands .....	71
2.7.6 Characterization of Differential Display PCR products .....	71-78
2.7.6.1 TA cloning.....	71-74
2.7.6.2 DNA minipreparation .....	74-75
2.7.6.3 DNA Sequencing.....	76-77
2.7.6.4 Sequence Analysis.....	77-78
2.7.6.5 Primer design.....	78
 <b>3. Results</b>	
<b>3.1 Overexpression of <i>Xrel3</i> induces tumorigenesis .....</b>	<b>79,80</b>
<b>3.2 Tissue origin of the tumours .....</b>	<b>79-81</b>
<b>3.3 <i>Xrel3</i>-induced tumours express body patterning genes .....</b>	<b>81-83</b>
<b>3.4 <i>Xrel3</i>-induced tumours at different stages in development .....</b>	<b>83-84,85</b>
<b>3.5 Marker expression does not require any inductive interactions from         underlying tissue .....</b>	<b>84,86-87</b>
<b>3.6 A potential role for FGFs in <i>Xrel3</i>-induced tumour formation ....</b>	<b>87,88-89</b>
<b>3.7 A number of differences in gene expression between normal skin         and tumour sections .....</b>	<b>87,90-92</b>
<b>3.8 A potentially novel gene upregulated in response to <i>Xrel3</i>         overexpression .....</b>	<b>90,93-95</b>
<b>3.9 Expression of differential display product in <i>Xrel3</i>-induced         tumours .....</b>	<b>93,96-101</b>
 <b>4. Discussion</b>	
<b>4.1 The use of RT-PCR in gene expression studies .....</b>	<b>102-103</b>
<b>4.2 <i>Xrel3</i> and tumorigenesis.....</b>	<b>103-110</b>
4.2.1 Overexpression of <i>Xrel3</i> leads to the formation of tumour-like lesions .....	103-105
4.2.2 <i>Xrel3</i> -induced tumours express genes involved with promoting cell proliferation .....	105-110
<b>4.3 <i>Xrel3</i> and neural patterning .....</b>	<b>110-112</b>
<b>4.4 Relationship between Rel/NF-<math>\kappa</math>B signalling and FGFs .....</b>	<b>112-117</b>
<b>4.5 Identification of novel downstream targets of <i>Xrel3</i> .....</b>	<b>118-121</b>
<b>4.6 Conclusion .....</b>	<b>121-122</b>
 <b>References.....</b>	<b>123-144</b>

# List of Tables

<b>Table 2.1: Composition of Normal Amphibian Medium .....</b>	<b>51</b>
<b>Table 2.2: Xenopus developmental stages used in the course of this study .....</b>	<b>52</b>
<b>Table 2.3: Reverse transcription reaction mixture volumes and final concentrations in a 22µl total.....</b>	<b>61</b>
<b>Table 2.4: Volumes and final concentrations of the PCR components in a 50µl reaction mixture.....</b>	<b>63</b>
<b>Table 2.5: Oligonucleotide Primers used for RT-PCR Assay .....</b>	<b>64</b>
<b>Table 2.6: Volumes and final concentrations of the differential display reverse transcription components in a 42µl reaction mixture.....</b>	<b>67</b>
<b>Table 2.7: Volumes and final concentrations of the differential display PCR components in a 20µl reaction mixture .....</b>	<b>68</b>
<b>Table 3.1: The sizes and expression of a number of genes, identified from differential display gels after PCR amplification with either one of five primer sets, that are either upregulated (↑) in the skin/control animal caps or tumours/<i>Xrel3</i> injected animal caps.....</b>	<b>92</b>

## List of Figures

- Figure 1.1:** The life cycle of the amphibian *Xenopus laevis* showing the major stages in development and the approximate time scale involved (reproduced from Wolpert et al., 1998) .....4
- Figure 1.2:** An illustration of cortical rotation in the amphibian embryo showing the development of the future dorsal side opposite the site of sperm entry. **A.** Fertilization of the egg. **B.** 30° cortical rotation. V – ventral; D – dorsal (adapted from Wolpert et al., 1998) .....8
- Figure 1.3:** Mesoderm Induction. **A.** A fate map of the *Xenopus* blastula (lateral view), illustrating the normal fates of the different blastula regions. **B.** The four-signal model of mesoderm induction, showing the origins, actions and examples of the potential signal-types involved. Signals 1 and 2 originate from the vegetal region and act on the overlying animal tissue to specify dorsal and ventral mesoderm respectively. Signal 3 originates from the ventral region and signal 4 originates from the Spemann Organizer, both of which act to subdivide the ventral mesoderm into more intermediate-type mesoderm (adapted from Wolpert et al., 1998) ..... 13
- Figure 1.4:** An illustration of the morphogenetic movements involved during gastrulation. Gastrulation is initiated by the elongation and invagination of dorsal vegetal cells (presumptive endodermal cells) to form a blastopore. The internalization of cells continues with the involution of the mesoderm. At the same time, the animal cells undergo epiboly and spread downwards. Additional involution occurs ventrally, where presumptive endodermal and mesodermal cells become internalized as well (reproduced from Wolpert et al., 1998) .....21
- Figure 1.5:** Overexpression of *Xrel3* mRNA in *Xenopus* embryos induces tumorigenesis. 0.5-1ng of synthetic *Xrel3* mRNA was injected into two-cell stage embryos. The blue arrow indicates the presence of a tumour .....33
- Figure 1.6:** A schematic representation of the structural domains of Rel/NF- $\kappa$ B proteins. At the amino terminal end is the highly conserved RHD, which contains the nuclear localization site (N) and the PKA site (RRXS) at its carboxy terminus. In Class I Rel proteins, the carboxy terminal end consists of the transactivation domain, while in Class II Rel proteins the carboxy terminus consists of multiple copies of ankyrin repeats .....35
- Figure 1.7:** A diagrammatic representation of Rel/NF- $\kappa$ B activation in the cell. One of many external stimuli binds to receptors on the surface of the cell, leading to the activation of a signalling cascade. Activation of the IKK complex leads to the phosphorylation of the inhibitory subunits I $\kappa$ B or p105 and targets them for polyubiquitination. The I $\kappa$ B subunit is then rapidly degraded by a proteasome

complex, while the p105 subunit is proteolytically processed and the cleaved, ubiquitinated carboxy terminus is degraded. The resulting active NF- $\kappa$ B complex produced then translocates to the nucleus, where it binds DNA and affects downstream transcription (Thanos and Maniatis, 1995; Gilmore, 1999).....	39
<b>Figure 2.1:</b> The CS2+ expression vector containing the <i>Xrel3</i> coding region in its multiple cloning site after digestion with the restriction enzymes EcoRI and XhoI .....	54
<b>Figure 2.2:</b> A diagrammatic representation of blastula Stage 8 <i>Xenopus</i> animal cap dissections. A. A Stage 2 embryo injected with <i>Xrel3</i> mRNA in each of the cells. B. A blastula Stage 8 embryo. C. A median section through a blastula embryo revealing three distinct regions. D. An isolated animal cap region of a blastula embryo after dissection .....	56
<b>Figure 2.3:</b> Two <i>Xenopus</i> hind limb buds as staged according to Nieuwkoop and Faber (1969). A. A stage 52 hind limb bud. B. A stage 53 hind limb bud .....	57
<b>Figure 2.4:</b> A schematic diagram outlining RT-PCR analysis .....	60
<b>Figure 2.5:</b> A schematic representation of Differential Display .....	66
<b>Figure 2.6:</b> Map of the TA cloning pCR2.1 vector, showing the sequence of the multiple cloning site and the position of the DNA insert. The red and green highlighted regions, either side of the insert, represent the primers used in the sequencing reactions.....	73
<b>Figure 3.1:</b> Expression analysis of <i>Xrel3</i> -induced St. 20 tumours as observed through RT-PCR. A. Twenty tumour and twenty skin samples were excised and analysed for the expression of total exogenous ( <i>Xrel3</i> ) and endogenous ( <i>Xrel3e</i> ) <i>Xrel3</i> . B. mRNA expression levels from twenty tumour and skin samples of various terminally differentiated tissues - muscle mesoderm (cardiac actin), neural ( <i>Nrp-1</i> and <i>HoxB9</i> ) and epidermis (epidermal keratin). Histone levels were used as a standard for RNA loading.....	80
<b>Figure 3.2:</b> Expression of various body patterning genes in St. 20 <i>Xrel3</i> -induced tumours as observed through RT-PCR analysis. RNA was extracted and analyzed for expression from each of twenty excised skin samples and tumours. Histone levels were used as a standard for RNA loading .....	82
<b>Figure 3.3:</b> RT-PCR analysis of St. 16/17 (A) and St. 26/27 (B) tumours for the expression of the body patterning genes sonic hedgehog ( <i>Shh</i> ), <i>Gli1</i> , <i>Otx-2</i> and <i>Twist</i> , after RNA extraction from fifteen to twenty excised tumours and skin samples. A. <i>Gli1</i> and <i>Twist</i> levels were not affected by increased levels of <i>Xrel3</i> in St. 16/17 tumours. B. Levels of <i>Shh</i> , <i>Gli1</i> , <i>Otx-2</i> and <i>Twist</i> were all upregulated in the St. 26/27 tumours. Histone levels were used as a standard for	



RNA loading.....	85
<b>Figure 3.4:</b> Expression analysis of <i>Xrel3</i> injected animal caps (AC) that have been allowed to develop to St. 10 (A) and St. 20 (B). RNA was extracted from ten to twelve injected <i>Xrel3</i> and control ACs. A. Expression of the body patterning genes Shh, Gli1, Otx-2 and Twist (not shown) are not affected by the increased levels of <i>Xrel3</i> in the <i>Xrel3</i> injected ACs. B. Expression of the body patterning genes Shh, Gli1, and Otx-2 are upregulated in response to elevated levels of <i>Xrel3</i> , while endogenous levels of <i>Xrel3</i> ( <i>Xrel3<sub>e</sub></i> ) and cardiac actin (Actin) are not. Histone was used as a standard for RNA loading.....	86
<b>Figure 3.5:</b> RT-PCR analysis of Stage 52-53 <i>Xenopus</i> hind limb buds, showing expression of <i>Xrel3</i> ( <i>Xrel3<sub>e</sub></i> and <i>Xrel3<sub>nc</sub></i> ). RNA was extracted and analyzed from eight to ten limb buds. The expression of various vertebrate limb bud markers (Shh, Gli1, Twist, Fgf-8, R-fng, Wnt-7a) served as positive controls .....	88
<b>Figure 3.6:</b> Expression of vertebrate limb bud markers in St. 20 <i>Xrel3</i> -induced tumours. RNA was extracted from each of fifteen to twenty excised tumours and skin samples. Fgf8 and efgf(ii) are upregulated in the tumours. Histone served as a control for RNA loading .....	89
<b>Figure 3.7:</b> An example of a differential display gel showing multiple banding patterns in the skin (S), tumour (T), injected (I) or control (C) animal caps from three stages of <i>Xenopus</i> embryos, after PCR amplification with the primer sets AP1/AP1 and T <sub>11</sub> AC/AP2. The red arrow points to one type of band that is upregulated in the tumours and the green arrow points to another type of band that is upregulated in the skin.....	91
<b>Figure 3.8:</b> Nucleotide sequence of the differential display cDNA product A1.1aT that was upregulated in tumours.....	94
<b>Figure 3.9:</b> DNA translation of the differential display product A1.1aT in three reading frames. Asterisks represent stop codons. No open reading frame was found ..	95
<b>Figure 3.10:</b> RT-PCR analysis of <i>Xrel3</i> -induced tumours (A) and <i>Xrel3</i> -injected ACs (B) for the expression of the isolated differential display product A1.1aT. A. In RNA extracted from fifteen to twenty excised tumours and skin samples, the differential display product is expressed in only the tumours. B. In RNA extracted from ten to twelve ACs, at St. 10 in development, two PCR products were obtained in the <i>Xrel3</i> injected ACs. The lower PCR product was also expressed in the whole embryo and control ACs .....	96

**Figure 3.11:** Nucleotide sequences of the two PCR products obtained from RT-PCR analysis of St. 10 *Xrel3* injected ACs, with nested A1.1aT primers. The higher PCR product is designated 'Tumour', while the lower PCR product is designated 'Embryo' .....98

**Figure 3.12:** Sequence alignments between the original differential display sequence (A1.1aT) and the two sequences (Embryo and Tumour) obtained from the St. 10 *Xrel3* injected PCR sample. The sequence alignment analysis shows that the Tumour and A1.1aT sequences are the same, while the Embryo and Tumour/A1.1aT sequences are different. The blue sequence represents regions of similarity .....99

**Figure 3.13:** DNA translation of the higher PCR product sequenced from the St. 10 *Xrel3* injected sample, in three reading frames. Asterisks represent stop codons. No open reading frame was found.....100

**Figure 3.14:** DNA translation of the lower PCR product from the St.10 *Xrel3* injected sample, in three reading frames. Asterisks represent stop codons. The green lettering represents an open reading frame.....101

**Figure 4.1:** The Hedgehog (Hh)/Sonic hedgehog (Shh) signalling pathway, established primarily from *Drosophila*. Full length cubitus interruptus (*ci*<sup>155</sup>) or the vertebrate counterpart Gli, forms a complex with Fused (Fu), Costal-2 (COS-2) and Suppressor of fused (Su(fu)), and associates with a microtubule complex. In the absence of Hh/Shh induction, *ci*<sup>155</sup> is targeted for proteasomal cleavage and *ci*<sup>75</sup> is released. Translocation of this molecule to the nucleus leads to the repression of transcription. The binding of Hh/Shh to Ptc inactivates Ptc and releases Smo from repression. COS-2 and Fu become phosphorylated and the complex dissociates from the microtubules. Cleavage of *ci*<sup>155</sup> is blocked and this full-length form or some other related form translocates to the nucleus, where it associates with CREB-binding protein (CBP) and activates downstream target genes such as Ptc, decapentaplegic (*dpp*; BMP in vertebrates) and wingless (*wg*; Wnt in vertebrates; Ingham, 1998; Ming et al., 1998) .....107

**Figure 4.2:** A schematic representation of a developing limb bud, illustrating some of the possible signalling events involved. A=Anterior; P=Posterior; Pr=Proximal; D=Distal; AER=Apical Ectodermal Ridge; ZPA=Zone of Polarizing Activity.114

## List of Abbreviations

<b>AC</b>	animal cap
<b>AER</b>	apical ectodermal ridge
<b>APS</b>	ammonium persulfate
<b>BMP</b>	bone morphogenetic protein
<b>bp</b>	base pair
<b>BCC</b>	basal cell carcinoma
<b>cAMP</b>	cyclic adenosine monophosphate
<b>cDNA</b>	complementary deoxyribonucleic acid
<b>CNS</b>	central nervous system
<b>DEPC</b>	diethyl pyrocarbonate
<b>ddNTPs</b>	dideoxyribonucleotide triphosphates
<b>dH<sub>2</sub>O</b>	distilled water
<b>dNTPs</b>	deoxyribonucleotide triphosphates
<b>EDTA</b>	ethylenediamine tetraacetic acid
<b>ESTs</b>	expressed tag sequences
<b>FGF</b>	fibroblast growth factor
<b>FGFR</b>	fibroblast growth factor receptor
<b>FOG</b>	friend of GATA
<b>GSK-3</b>	glycogen synthase kinase 3
<b>HEPES</b>	N-2-hydroxyethylpiperazine-N'-2-ethanesulfonic acid
<b>I<math>\kappa</math>B</b>	I kappa B
<b>IKK</b>	I $\kappa$ B kinase
<b>IL-1</b>	interleukin-1
<b>LPS</b>	lipopolysaccharide
<b>MBT</b>	midblastula transition
<b>ml</b>	millilitres
<b>MPF</b>	maturation promoting factor
<b>mRNA</b>	messenger ribonucleic acid
<b>MS222</b>	methanesulfonate
<b>NAM</b>	normal amphibian medium
<b>ng</b>	nanograms
<b>NBCCS</b>	nevroid basal cell carcinoma syndrome
<b>NETS</b>	sodium chloride, EDTA, Tris-HCl, sodium dodecyl sulfate
<b>NF-<math>\kappa</math>B</b>	nuclear factor kappa B
<b>NLS</b>	nuclear localization signal
<b>pg</b>	picograms
<b>PKA</b>	protein kinase A
<b>PKAc</b>	catalytic subunit of protein kinase A
<b>PTC</b>	patched
<b>RHD</b>	rel homology domain
<b>rpm</b>	revolutions per minute
<b>RT</b>	room temperature
<b>RT-PCR</b>	reverse transcription-polymerase chain reaction

<b>Shh</b>	sonic hedgehog
<b>SMO</b>	smoothened
<b>TGF-<math>\beta</math></b>	transforming growth factor beta
<b>TH</b>	thyroid hormone
<b>TNF-<math>\alpha</math></b>	tumour necrosis factor alpha
<b><math>\mu</math>l</b>	microlitres
<b>UV</b>	ultraviolet
<b>Xbra</b>	brachyury
<b>Xlefty</b>	<i>Xenopus</i> lefty
<b>XMMR</b>	<i>Xenopus</i> molecular marker resource
<b>Xrel3</b>	<i>Xenopus</i> rel3
<b>Xrel3<sub>c</sub></b>	Xrel3 coding region
<b>Xrel3<sub>e</sub></b>	endogenous Xrel3
<b>Xrel3<sub>nc</sub></b>	Xrel3 non-coding region
<b>ZPA</b>	zone of polarizing activity



# **Chapter 1: Introduction**

## **1.1 General**

Although progress is being made in many areas of cancer research in terms of prevention and treatments, cancer still remains a devastating class of diseases that will afflict many of us. It has long been established that cancers arise as defects in the normal constraints of cell division, differentiation and growth that are placed upon cells. The identification and characterization of proto-oncogenes and tumour suppressor genes has provided considerable information on the regulation of cell growth and proliferation. Mutation of these genes by base substitution/deletion, gene amplification and chromosomal rearrangement can lead to uncontrolled clonal proliferation of cells which can result in carcinogenesis. Over the years, developmental biology has played a significant role in cancer research, as many of these tumour suppressor genes and proto-oncogenes play important roles in the development of organisms. Gene expression and regulation, how cells differentiate and how cells interact with one another are all paramount to understanding developmental biology and cancer.

One such family of genes involved in both development and oncogenesis is the Rel/NF- $\kappa$ B family of transcriptional activators. Indeed NF- $\kappa$ B, to date, has been associated with several human cancers, including breast cancer, non-small cell lung carcinoma, thyroid cancer, T- or B-cell lymphocyte leukemia and several virally-induced tumours. However, what remains in question is whether or not NF- $\kappa$ B plays a direct role in the induction of these cancers and also what genes are targeted and are ultimately influenced by NF- $\kappa$ B in oncogenesis. This study involves the investigation of one such Rel/NF- $\kappa$ B family member, *Xrel3*.

## 1.2 *Xenopus laevis* as a developmental model

Over the years there have been a few extensively studied species that have provided us with most of our knowledge about developmental mechanisms. These include sea urchins, amphibians, such as *Xenopus laevis*, mice, chickens, zebrafish, the fruit fly *Drosophila melanogaster* and the nematode worm *Caenorhabditis elegans*. Each species has its advantages and disadvantages as a developmental model.

Some amphibians, like *Xenopus laevis*, make good model organisms because the females are oviparous and lay a great number of large (1-2 millimetre) eggs at one time, thus making them quite suitable for microdissection and microinjection procedures, as well as for molecular and biochemical manipulations. Being oviparous confers a great advantage on embryological studies, as artificial fertilizations can be performed, thereby allowing for the exact time of fertilization to be known (for review, see Jones & Smith, 1999).

*Xenopus laevis* has been singled out as the standard amphibian for embryological work due to the ease with which it can be maintained and induced to spawn (for review, see Jones & Smith, 1999). In fact, it was its ability to spawn when induced with gonadotropic hormone that led to its common usage for human pregnancy tests in the 1950s (for reviews, see Burstein & Braunstein, 1995; Jones & Smith, 1999). An injection of pregnancy urine, which contains chorionic gonadotropic hormone, into the dorsal lymph sac of a female frog would induce spawning. In addition, *Xenopus* embryos are quite vigorous and their development is relatively rapid compared to other anuran amphibian species (for review, see Jones & Smith, 1999).

### **1.3 *Xenopus* development**

The basic body plan of any animal is laid down very early in development and provides the framework from which all the morphological and histological characteristics of an organism become established. Following fertilization, the zygote undergoes rapid cell division leading to the production of a blastula or hollow ball of cells. The embryo then proceeds through gastrulation, which establishes the primary germ layers: ectoderm, endoderm and mesoderm, followed by formation of the nervous system and major body systems (neurulation) and their elaboration through organogenesis (Figure 1.1).

#### **1.3.1 Oogenesis**

Oogenesis is the process whereby female gametes (ova) are produced. This process involves the maturation and growth of oocytes by which the oocyte cytoplasm acquires yolk, mitochondria, enzymes and precursors for DNA, RNA and protein synthesis, stored mRNAs and structural and regulatory proteins, all of which are required to initiate and maintain metabolism during early development (Smith et al., 1991).

Prior to oogenesis, primordial germ cells undergo a small number of mitotic cell divisions as they migrate to the genital ridge (future gonad; for review, see Saffman & Lasko, 1999). Germ cell differentiation into eggs is initiated upon entry into meiosis, after which the primary oocytes become arrested at the diplotene stage of the first meiotic cell division. It is at this time that ribosomal and transfer RNAs needed for protein synthesis until mid-blastula stage are made and all the maternal mRNA for early development is transcribed.

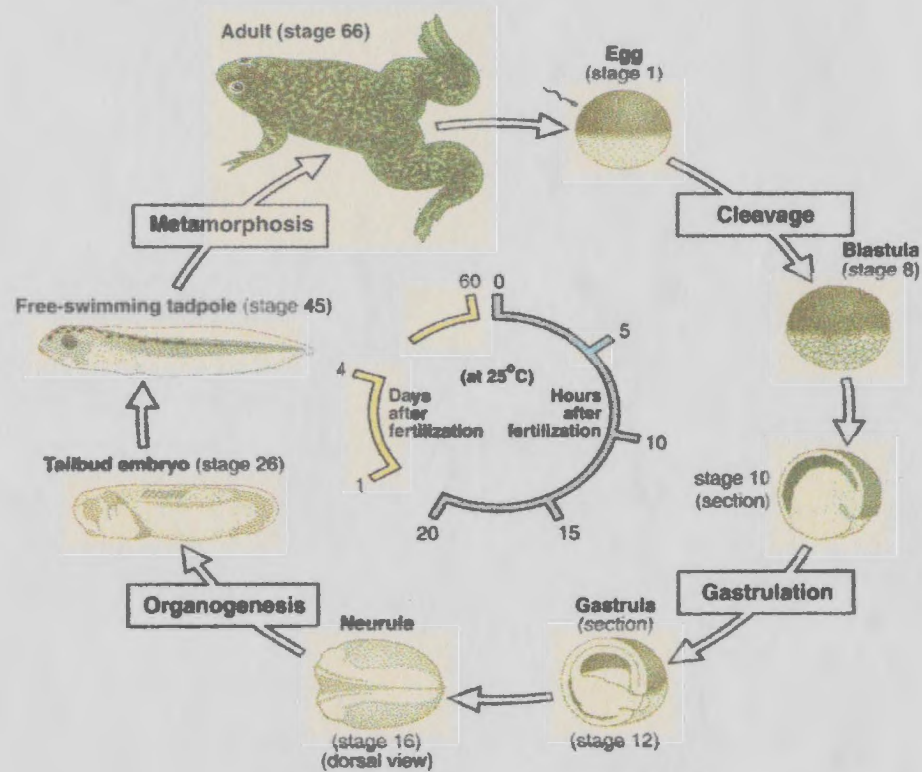


**Figure 1.1:** The life cycle of the amphibian *Xenopus laevis* showing the major stages in development and the approximate time scale involved (reproduced from Wolpert et al., 1998).

Most eggs are highly asymmetric with respect to their constituents and it is during oogenesis that translocation events occur which help to specify the animal-vegetal polarity of the egg. In *Xenopus* and *Rana*, the animal hemisphere is characterized by pigmentation, while the vegetal hemisphere remains unpigmented. This typically occurs during a process known as 'Vitellogenesis' or the yolk synthesis and deposition stage of oogenesis (Danilchik & Gerhart, 1987).

Yolk is the main source of nutrition for the developing embryo. The major component of yolk is the protein vitellogenin. Vitellogenesis occurs when the oocyte reaches the diplotene stage of meiosis I and is triggered by environmental cues that initiate ovarian growth (Danilchik & Gerhart, 1987). These external signals stimulate the hypothalamus to secrete gonadotropin-releasing hormone, which in turn stimulates the release of gonadotropins from the pituitary. The gonadotropins circulate in the blood and stimulate the follicle cells of the ovary to synthesize and secrete oestrogen. Oestrogen is then carried to the liver in the blood where vitellogenin is made and transported to the ovaries for uptake by the oocytes (Skipper & Hamilton, 1977).

Initially, vitellogenin is uniformly distributed around the circumference of the oocyte, but as vitellogenesis progresses, the oocyte cytoplasm becomes highly stratified. Cortical granules, mitochondria and pigment granules are found around the periphery of the cell, generating what is known as the oocyte cortex. The yolk platelets, containing the vitellogenin, become displaced toward the centre of the vegetal hemisphere (Danilchik & Gerhart, 1987). Glycogen granules, ribosomes, lipochondria, endoplasmic reticulum and the germinal vesicle (nucleus) become translocated towards the animal

pole. In addition specific cytoplasmic mRNA stores become localised to certain regions of the oocyte (Danilchik & Gerhart, 1987; Chang et al., 1999).

As vitellogenesis comes to an end and the oocyte reaches maturity, genes stop actively transcribing and the chromosomes condense. This stage can last for several months. Resumption of meiosis in the primary oocyte and hence ovulation is achieved via progesterone stimulation (for reviews, see Sagata, 1998; Ferrell, 1999). Again, responding to environmental cues, this hormone is released by the follicle cells surrounding the oocytes and within six hours germinal vesicle breakdown occurs. The oocyte then completes its first round of meiotic division and is ovulated (Hunt, 1989; for reviews, see Sagata, 1998; Ferrell, 1999).

### **1.3.2 Fertilization and post-fertilization events**

Successful fertilization in *Xenopus* is achieved when sperm penetrates the egg surface at any point solely on the animal hemisphere (Elinson, 1975). The egg has two surface coats around its plasma membrane, the vitelline envelope and the outer jelly coat. Fusion of the sperm and egg plasma membranes causes a rapid release in free calcium ions from the egg's endoplasmic reticulum into the egg cytoplasm. This rise in calcium ion levels leads to depolarisation of the egg membrane and activation of the enzyme, calmodulin-dependent protein kinase II. This enzyme causes the degradation of the cyclin component of maturation promoting factor (MPF). As a result MPF levels decline and the egg re-enters the meiotic cell cycle (Nuccitelli, 1991; Watanabe et al., 1991; Runft et al., 1999).

Another consequence of elevated intracellular calcium is the release of cortical granules via exocytosis into the space between the vitelline membrane and the egg. This, in combination with the transient depolarisation of the egg plasma membrane, is responsible for establishing polyspermy blocks (Nuccitelli, 1991; Runft et al., 1999).

Once the egg completes the second meiotic division, the egg and sperm pro-nuclei fuse to form a diploid zygotic nucleus. The vitelline membrane then elevates from the egg surface and allows the egg to rotate due to gravity, so that the animal pole points upwards and the vegetal pole downwards.

About 30-45 minutes after fertilization (approximately halfway between fertilization and first cleavage), the cortical cytoplasm of the egg relative to the inner cytoplasm, shifts about 30° towards the point of sperm entry (Figure 1.2). This cortical rotation is extremely important to the future development of the zygote because now the dorsal-ventral polarity of the egg is determined. The area opposite the point of sperm entry becomes the future dorsal side, while the site of sperm entry becomes the future ventral side. This cortical rotation also causes extensive movements within the inner cytoplasm of the egg, so that by the end of the first cleavage the cytoplasmic constituents of the presumptive dorsal side are distinctly different from those of the ventral side (Gerhart et al., 1981; Vincent & Gerhart, 1987; Gerhart et al., 1989). Experiments have shown that ultraviolet (UV)- irradiation of *Xenopus* embryos, through disruption of microtubule arrays, prevents cortical/cytoplasmic rotation and yields axis-deficient embryos that lack dorsal and anterior structures, such as the head, central nervous system (CNS) and notochord (Grant & Wacaster, 1972; Malacinski et al., 1975; Kao & Elinson, 1988).

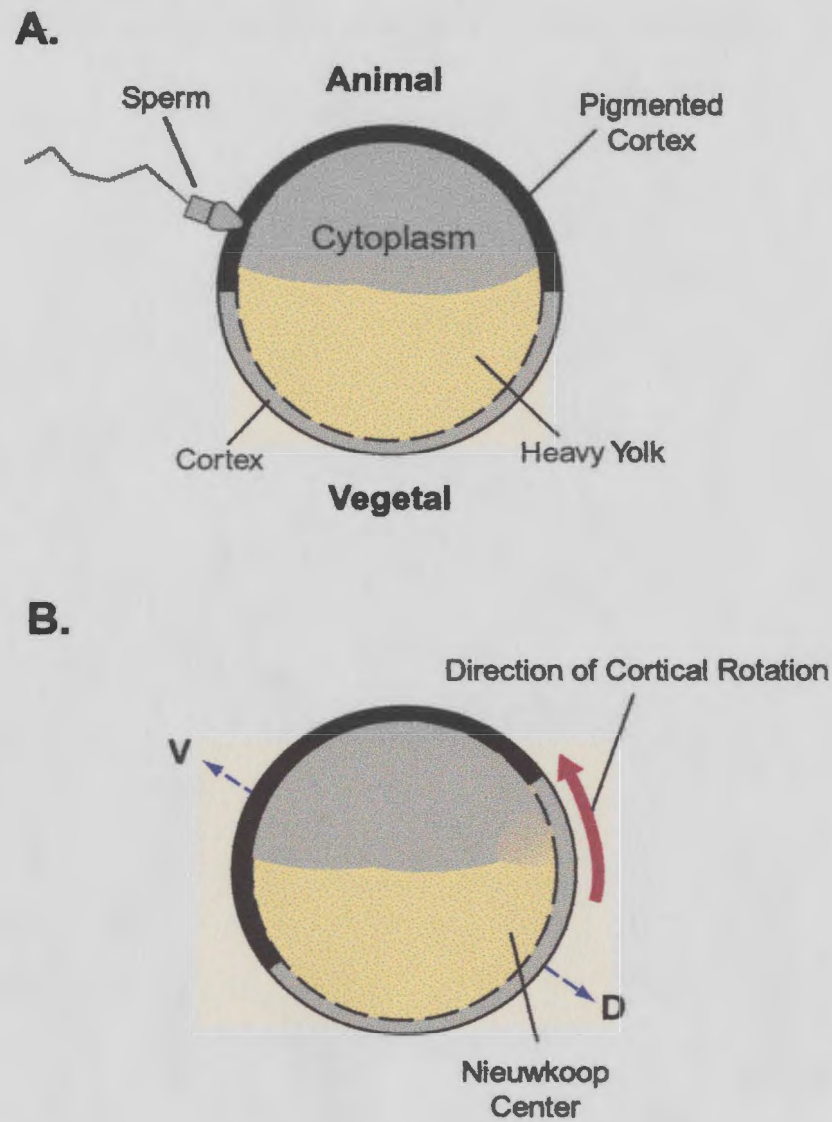


**Figure 1.2:** An illustration of cortical rotation in the amphibian embryo showing the development of the future dorsal side opposite the site of sperm entry. **A.** Fertilization of the egg. **B.** 30° cortical rotation. V – ventral; D – dorsal (adapted from Wolpert et al., 1998).



### 1.3.3 Early Cleavage Stages

Once fertilization has been achieved, the egg undergoes cleavage. Cleavage in *Xenopus* is radial and holoblastic. About 90 minutes after fertilization, the first cleavage furrow starts to form, which initiates in the animal pole and divides the cell into equal halves. Subsequent cleavages occur at approximately 30 minute intervals. The second cleavage occurs at right angles to the first and separates the future dorsal and ventral halves. The third cleavage is equatorial and separates the animal and vegetal poles. The unequal distribution of yolk within the embryo causes an asymmetrical division of the embryo into small animal and large vegetal cells by the end of the third cleavage. Thus two major embryonic regions become established, a rapidly dividing region of animal cells and a more slowly dividing region of vegetal cells. During these early cleavage stages, a small space forms and becomes larger as the cleavages proceed to eventually form the blastocoel (fluid-filled cavity), at which time the embryo is referred to as a blastula (for review, see Jones & Smith, 1999).

At about the twelfth cell division, approximately 6-7 hours after fertilization, the cleavage rate slows down and the cell divisions become asynchronous. This is referred to as the Midblastula Transition (MBT). This period in development is characterized by the onset of zygotic transcription and cell motility (Newport & Kirschner, 1984; Kimelman et al., 1987; Masui & Wang, 1998).

### 1.3.4 Body patterning in the early embryo

The establishment of a body plan in *Xenopus* relies extensively upon inductive interactions, in which the fates of groups of cells becomes determined. Induction is the

process where by one group of cells produces a signal or signals that affects the fate of another group of cells.

Two major inductive events during early *Xenopus* development are mesoderm and neural induction. These two inductive events help to establish the dorsal-ventral and anterior-posterior embryonic body axes, thus creating an organism that is bilaterally symmetrical.

#### *1.3.4.1 Mesoderm induction*

Mesoderm formation and the establishment of dorsoventral and anteroposterior embryonic axes are critical processes in *Xenopus* development. As a consequence, much embryological and developmental research has been devoted to the molecular aspects of these two processes.

The blastula consists of two cell types, animal and vegetal, which are separated from each other by the blastocoel except at the outer equatorial region. The animal cells form both presumptive mesoderm and ectoderm; the middle and outer primary germ layers respectively. The vegetal cells form the presumptive endoderm, the innermost primary germ layer.

The outer ectodermal layer eventually differentiates into the epidermis (skin), nervous system and sensory organs. The mesodermal layer develops into muscle, connective tissue, skeletal tissue, and the circulatory and excretory systems. The endodermal layer eventually differentiates into the gut and associated organs, such as the liver and the pancreas.

Perhaps one of the most important and prominent discoveries about mesoderm induction and embryonic axis formation was achieved in an earlier experiment by Spemann and Mangold (1924). Through transplantation experiments, in which dorsal marginal zone or equatorial cells were transplanted into ventral tissue, they obtained an organism with two body axes. In essence, their experiment showed that the cells of the dorsal marginal zone were responsible for the formation of dorsal mesodermal structures such as the notochord and neural tube, in addition to organizing or specifying the anterior-posterior body axis. More importantly, their experiments showed that cells of one type, mainly dorsal mesoderm, could induce the formation of other mesoderm and neural tissue in other cells. Consequently, the dorsal marginal zone is now referred to as 'Spemann's organizer'.

The differentiation of the mesodermal embryonic germ layer is now considered to be controlled by inductive cell interactions between the animal and vegetal hemispheres. Nieuwkoop (1969) demonstrated that vegetal cells induce the adjacent animal cells to form mesoderm. He isolated midblastula animal and vegetal cap cells and found that neither produced mesodermal tissue. However, when the two caps were combined and cultured together, many of the animal cap cells generated mesodermal tissue.

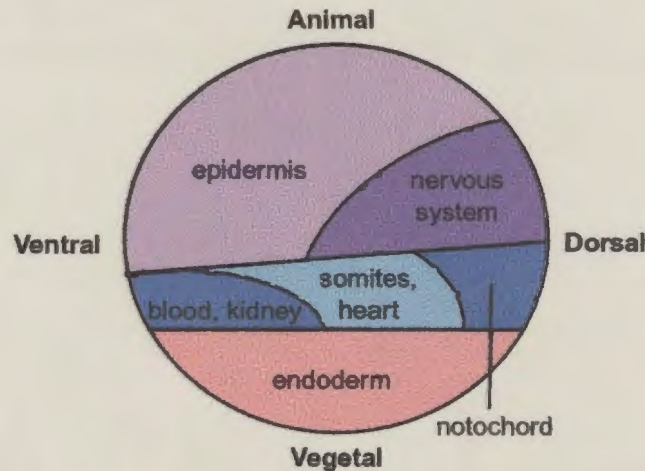
In a follow up experiment Nakamura and Takasaki (1970) removed the equatorial region of the midblastula embryo and found that it formed mesoderm in culture. However, prior to the 64-cell stage, they found that the same equatorial region differentiated into epidermis instead.

Based on these experiments it became evident that vegetal cells indeed possessed some sort of factor that was capable of activating or inducing mesoderm formation in animal cells and that the mesodermal fates of the equatorial animal cells were determined prior to the onset of gastrulation, but not before the blastula stage.

A popular model (Slack, 1994; Wolpert et al., 1998) to explain mesoderm induction and axis determination involves a four-signal system and is outlined in figure 1.3. Shortly after fertilization the inner cytoplasmic movements of the egg, due to cortical rotation, causes the division of the vegetal cytoplasm into ventrovegetal and dorsovegetal regions. As cleavage progresses, factors in the ventrovegetal region induce the marginal cells above to broadly specify ventral-type mesoderm (mesenchyme, mesothelium and blood). The second signal, acting either simultaneously or a little later, in the dorsovegetal region or Nieuwkoop centre (named after its founder) induces organizer activity in the dorsal marginal region above, and induces dorsal marginal cells to specify axial mesoderm. By the onset of gastrulation, two further sets of signals help to pattern the ventral mesoderm along the dorso-ventral axis by subdividing it into prospective muscle, kidney and blood. The third signal emanates from the ventral region, while a fourth signal, from the organizer, inhibits the action of the third signal and dorsalizes the ventral mesoderm closest to it (Figure 1.3).

Recent attempts to identify and characterize the molecules involved in mesoderm induction and axial patterning, however, have further complicated this model. It has now been suggested, for instance, that dorsal animal and equatorial cells, not just dorsal vegetal cells produce dorsalizing signals (Heasman, 1997; Moon & Kimelman, 1998). In

A.



B.

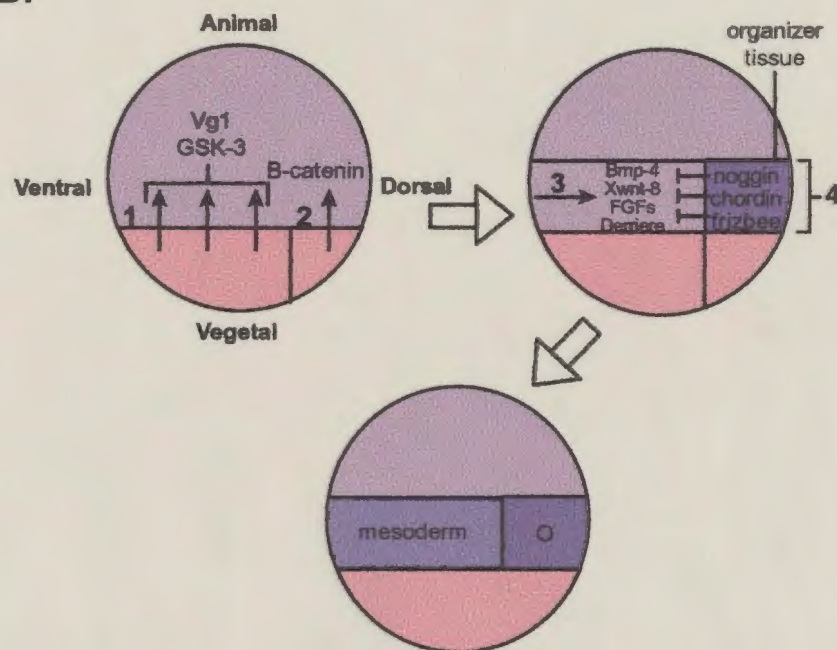


**Figure 1.3: Mesoderm Induction.** **A.** A fate map of the *Xenopus* blastula (lateral view), illustrating the normal fates of the different blastula regions. **B.** The four-signal model of mesoderm induction, showing the origins, actions and examples of the potential signal-types involved. Signals 1 and 2 originate from the vegetal region and act on the overlying animal tissue to specify dorsal and ventral mesoderm respectively. Signal 3 originates from the ventral region and signal 4 originates from the Spemann Organizer, both of which act to subdivide the ventral mesoderm into more intermediate-type mesoderm (adapted from Wolpert et al., 1998).

addition, recent evidence now suggests that *Xenopus* mesoderm induction may be a posttranscriptional event, in which the localization of maternal transcription factors to the vegetal hemisphere is the underlying event involved in patterning the mesoderm (Zhang et al., 1998; Kofron et al., 1999).

#### *1.3.4.2 Molecular events that pattern the mesoderm*

The molecular nature of mesoderm inducers and the inductive response still remains largely obscure. A modified version of Nieuwkoop's experiment, in which isolated animal and vegetal cell fragments are cultured together but separated by a filter with pores too small to allow cell contacts to develop, indicated that mesoderm induction in *Xenopus* is due to some sort of secreted, diffusible molecule or molecules produced by the vegetal region (Slack, 1991).

As previously mentioned, the animal-vegetal axis is maternally determined and established prior to fertilization with the asymmetrical distribution of cytoplasmic constituents. The localization of some of the maternal mRNAs to specific regions of the developing oocyte are of extreme significance, as the proteins encoded by these mRNAs belong to developmentally important families of signalling molecules. This, therefore, makes them strong candidates for signals involved in specifying early polarity and inducing the mesoderm.

An obvious candidate for a mesoderm-inducing signal is the protein Vg1. Vg1 is a maternally expressed member of the transforming growth factor beta (TGF- $\beta$ ) family of proteins and is localized to the vegetal region of the *Xenopus* embryo. Characteristic of the TGF- $\beta$  family, Vg1 is processed as a precursor molecule and has to be proteolytically

cleaved to be activated. Mature, processed Vg1 protein, when injected into animal cap explants, induces mesoderm (Thomsen & Melton, 1993; Kessler & Melton, 1994; Forristall et al., 1995). One obstacle to the attractiveness of Vg1 being a mesoderm-inducer, however, has been the unsuccessful attempts of researchers to detect processed forms of Vg1 in the developing embryo.

Activin, another member of the TGF- $\beta$  family, also has potent mesoderm-inducing capabilities. Isolated animal caps, when treated with activin, form mesodermal tissue (Hemmati-Brivanlou & Melton, 1992; Kessler & Melton, 1994). However, activin mRNA is not present in the zygote and is therefore unlikely to be the initial mesoderm-inducing signal. Members of the bone morphogenetic proteins (BMPs), the FGFs, and noggin, are all present in the zygote, with the BMPs and FGFs also being capable of generating mesoderm. However, their lack of vegetal localization and, in the case of noggin, its inability to induce mesoderm in animal pole explants, has cast doubt as to their role as general mesoderm inducers (Amaya et al., 1991; Smith et al., 1993; Kessler & Melton, 1994).

With the advent of a posttranscriptional view of mesoderm induction, a localized maternal transcription factor, VegT, to the vegetal hemisphere of the mature oocyte and early embryo has recently emerged. VegT is required for vegetal cells of the blastula to produce the endogenous vegetal signal(s) that cause animal caps to form mesoderm (Zhang et al., 1998; Kofron et al., 1999). Since VegT is a transcription factor, it is unable to activate transcription of target genes until after the MBT. Thus, in this situation, zygotic factors downstream of VegT, not maternal signalling factors, initiate the endogenous vegetal signal(s) first described by Nieuwkoop (1969).

The molecule  $\beta$ -catenin, a member of the Wnt signalling pathway, has been recently identified as a potential early dorsal determinant that is involved in inducing organizer activity and potentially represents the second signal in the four signal model.  $\beta$ -catenin is present in the *Xenopus* egg and early embryo and is capable of rescuing UV-irradiated eggs. During the early cleavage stages,  $\beta$ -catenin becomes enriched in the cytoplasm on the prospective dorsal side of the embryo. By the 16 to 32 cell stages, however, it is detected in the dorsal, but not ventral, nuclei (Heasman, 1997; Moon & Kimelman, 1998). How  $\beta$ -catenin accumulates on the prospective dorsal side is unclear, although it is thought that the suppression of ventralizing signals in the future dorsal region is involved.

A candidate ventralizing signal believed to be involved in the establishment and functioning of the Nieuwkoop center is the protein kinase, Glycogen Synthase Kinase-3 (GSK-3). Indeed, blocking GSK-3 activity in *Xenopus*, by either the injection of dominant-negative GSK-3 mutants (He et al., 1995) or lithium treatment (Klein & Melton, 1996; Chen et al., 2000), leads to the development of an embryo that is almost completely dorsalized. Evidence has accumulated to suggest that GSK-3 functions to regulate the levels of  $\beta$ -catenin in the *Xenopus* embryo. GSK-3 is uniformly expressed in the blastula. However after fertilization, GSK-3 activity is likely to be greater on the prospective ventral side than on the dorsal side. What normally suppresses GSK-3 on the dorsal side is uncertain, but there is evidence to suggest Wnt signalling proteins are likely to be involved (Heasman, 1997; Moon & Kimelman, 1998; Chen et al., 2000).

A departure from the traditional four-signal model comes from the finding that  $\beta$ -catenin becomes localized to dorsal animal, equatorial and vegetal cells, not just dorsal



vegetal cells. In addition, it has been discovered that, on the dorsal side of the embryo,  $\beta$ -catenin binds the HMG Box factor, XTcf-3, which directly binds the *siamois* promoter and activates the gene. *Siamois* is a homeobox gene that encodes a transcription factor (Lemaire et al., 1995). As such, dependency of Nieuwkoop signalling upon zygotic gene transcription is implied. *Siamois* is therefore likely to play a major role in specifying the formation of Spemann's organizer (Heasman, 1997; Moon & Kimelman, 1998).

The patterning of the mesoderm and its subsequent division into subdomains involves a number of signalling proteins such as BMP-4, Xwnt-8, chordin, noggin, frizbee and FGFs (Figure 1.3).

BMP-4, a TGF- $\beta$ -related protein, is expressed throughout the late blastula. As gastrulation proceeds, however, BMP-4 is no longer expressed in dorsal regions. BMP-4 induces ventral mesoderm, suppresses induction of dorsal mesoderm by activin and inhibits dorsoanterior development of embryos, suggesting that it is a ventralizing factor and a likely candidate for the third signal in the four-signal model. In addition, expression of a dominant-negative BMP-4 receptor prevents ventralization of embryos (Kessler & Melton, 1994; Piccolo et al., 1996). Another ventralizing factor present in the embryo is Xwnt-8, which is localized to the equatorial cells (future mesoderm; Kessler & Melton, 1994; Heasman, 1997; Moon et al., 1997). The activity of these ventralizing factors is thought to be controlled by dorsalizing signals (the so-called fourth class of signals) emanating from the organizer. These include noggin, chordin and frizbee. Noggin's mode of action is to interact with BMP-4, thus preventing it from binding to its receptor (Kessler & Melton, 1994; Zimmerman et al., 1996). Chordin acts in a similar

manner, while frizbee acts by interacting with Wnt proteins (Piccolo et al., 1996; Leyns et al., 1997).

Members of the FGF family have been implicated in lateroventral mesoderm induction (Slack et al., 1987). This is a family of heparin-binding proteins that consists of both secreted and non-secreted forms (for reviews, see Slack et al., 1996; Isaacs, 1997). The type of mesoderm induced by FGFs is concentration dependent, such that at low doses ventral mesoderm forms (eg. mesothelium), while at higher doses more lateral type mesoderm forms (eg. muscle; Slack et al., 1987; Slack et al., 1988). Expression of a dominant-negative FGF receptor inhibits mesoderm induction in animal cap explants and causes defects in trunk and posterior development, while not affecting anterior development (Amaya et al., 1991; Kessler & Melton, 1994). Of the known *Xenopus* FGFs, four are expressed in the mesoderm. However, only three (bFGFs, eFGF and FGF-9) are maternally expressed, thus making them prime candidates for mesoderm-inducing factors (Issacs et al., 1992; Tannahill et al., 1992; Song & Slack, 1994; Song & Slack, 1996). Since bFGF lacks a signal peptide and is therefore unable to be secreted efficiently, it is unlikely that it plays a major role in mesoderm induction (Mignatti et al., 1992; Isaacs et al., 1994).

A novel member of the TGF- $\beta$  family has recently been identified and found to play a role in mesodermal patterning. Derrière is most closely related to Vg1, however, unlike Vg1, it is zygotically expressed and is initially expressed throughout the presumptive mesoderm. When misexpressed dorsally, derrière suppresses head formation. Expression of a dominant interfering derrière protein leads to posterior

truncation in embryos, including defects in blastopore lip formation, gastrulation and neural tube closure (Sun et al., 1999).

For induction to occur, the signalling molecules must bind specific cell surface receptors of competent (responsive) cells. In this way, one or more signal transduction pathways, in the responding cell, become activated, leading to the eventual mobilization of transcriptional activators, which translocate to the nucleus where they activate the transcription of specific genes.

Two early response zygotic genes coding for transcription factors that are involved with characterizing mesoderm are *Brachyury (Xbra)* and *goosecoid*. *Xbra* is initially transcribed throughout the presumptive mesoderm and later becomes restricted to the notochord and posterior mesoderm. Overexpression studies have shown that it specifies ventro-posterior mesoderm differentiation. In addition, maintenance of *Xbra* depends upon the expression of an FGF and is itself responsible for activating FGF (Issacs et al., 1994; Schulte-Merker & Smith, 1995).

*Goosecoid* is expressed in the organizer region of the embryo and is involved with the specification of dorsal mesoderm. It is a downstream target of *siamois* and is itself responsible for activating the dorsal signalling gene *chordin* (Heasman, 1997; Moon & Kimelman, 1998). Other genes in the organizer region that encode transcription factors are *pintallavis*, *HNF-3 $\beta$* , *Xnot* and *Xlim-1* (Taira et al., 1992; von Dassow et al., 1993; Ang & Rossant, 1994; O'Reilly et al., 1995). While the functions of these genes remains unknown, they are likely to be involved with the activation of genes that encode secreted proteins, such as *noggin*, *chordin* and *frizbee*.

VegT, as well as being maternally expressed, is also zygotically expressed. Zygotic transcripts are restricted to equatorial, presumptive mesodermal cells and its expression pattern appears to be identical to that of *derrière*. Several lines of evidence suggest that *derrière* and VegT form a regulatory loop, in which *derrière* is a downstream target of maternal VegT and that later, *derrière* may be required for zygotic VegT expression. In addition, there is evidence to suggest that *derrière* may function in conjunction with FGF signalling to promote the formation of posterior regions (Zhang et al., 1998; Sun et al., 1999).

#### *1.3.4.3 Gastrulation and Neurulation*

Gastrulation, as summarized in figure 1.4, is characterized by extensive cellular movements. It is initiated at the future dorsal side of the embryo in the dorsal vegetal quadrant, just below the marginal zone. The prospective endodermal cells of the dorsovegetal region involute to form a blastopore. As these endodermal cells pass into the interior of the embryo, they become elongated and become known as bottle cells. These bottle cells line the initial archenteron or primitive gut and later become the pharyngeal cells of the foregut.

The next cells to involute are the dorsal marginal cells, which eventually form the head mesodermal and notochord structures. They involute under the roof of the blastocoel. As this is occurring, the animal cells undergo epiboly or spreading and converge at the blastopore (Keller et al., 1992; Shih & Keller, 1994). In other words, the region occupied by cells of the animal hemisphere expands down towards the vegetal hemisphere, thus vegetally displacing and enlarging the blastopore. Meanwhile ventral

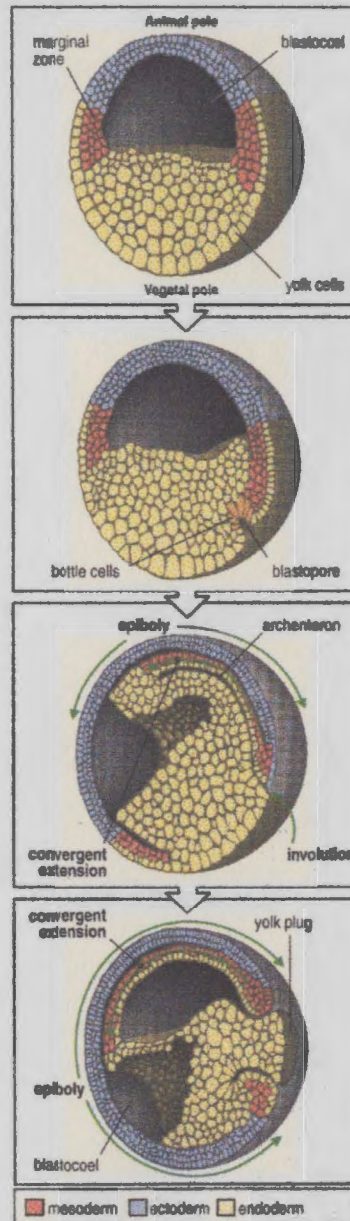


**Figure 1.4:** An illustration of the morphogenetic movements involved during gastrulation. Gastrulation is initiated by the elongation and invagination of dorsal vegetal cells (presumptive endodermal cells) to form a blastopore. The internalization of cells continues with the involution of the mesoderm. At the same time, the animal cells undergo epiboly and spread downwards. Additional involution occurs ventrally, where presumptive endodermal and mesodermal cells become internalized as well (reproduced from Wolpert et al., 1998).

and lateral lips develop over which ventral and lateral mesodermal precursor and presumptive endodermal cells become internalized (Keller et al., 1992; Shih & Keller, 1994).

With all this movement and internalization of cells an archenteron is formed at the expense of the blastocoel, which becomes increasingly displaced and eventually obliterated as gastrulation progresses (Shih & Keller, 1994).

The last thing to become internalized is a small patch of presumptive endoderm known as a yolk plug (Shih & Keller, 1994). On completion of gastrulation, the embryo is surrounded by former animal cap tissue or ectoderm. The yolky vegetal cells of the vegetal hemisphere have become endoderm in the interior and the former marginal zone has become a layer of mesoderm in between the ectodermal and endodermal layers.

Neurulation is the process whereby a specific region of ectoderm is induced to form a hollow neural tube, which later develops into the brain and spinal cord (Schoenwolf & Smith, 1990; Phillips, 1991). This induction involves the interaction between the dorsal mesoderm (inducer) and the region of ectodermal tissue (responder) above through vertical and planar signalling (Poznanski et al., 1997). The involuting dorso-anterior mesoderm induces the adjacent mesoderm to form anterior neural tissue. As the mesoderm migrates toward the former animal pole, it contacts progressively more overlying ectoderm, which is also induced to form anterior neural tissue. As involution proceeds, ectoderm is progressively contacted by more posterior mesoderm, which induces more posterior neural elements. Thus, the anteroposterior character of the neural ectoderm is dependent upon corresponding differences in the underlying dorsal mesoderm.

#### ***1.3.4.4 Neural Induction***

It was initially thought that the formation of epidermis was the default fate of the ectoderm. This was based on experiments in which animal cap explants, when cultured in isolation, formed epidermis. When these same explants were then recombined with organizer grafts, neural tissue formed instead. However, a number of groups have shown that prolonged dissociation of animal cap cells, in the absence of signals from the organizer, induces neural tissue formation (Godsave & Slack, 1989; Grunz & Tacke, 1989; Sato & Sargent, 1989). Thus, the current model regarding neural induction is that the formation of neural tissue is the embryonic default state of the ectoderm and that in the absence of an epidermal inducing signal, ectoderm differentiates as neural tissue (for reviews, see Tiedemann et al., 1998; Weinstein & Hemmati-Bivanlou, 1999).

BMP-4, in addition to being involved with mesodermal patterning, is a potent epidermal inducer (Wilson & Hemmati-Brivanlou, 1995; Suzuki et al., 1997; for review, see Dale & Jones, 1999). Prolonged attenuation of BMP signalling in ectodermal explants is sufficient to induce neuralization (Hawley et al., 1995; Xu et al., 1995). BMP-4 transcripts are present throughout the blastula ectoderm, but become excluded from the dorsal ectoderm by midgastrula stages. This is consistent with the notion that BMP-4 has anti-neuralizing activity and that BMP signalling within the ectoderm is inhibited by secreted factors from the organizer (Sasai & DeRobertis, 1997).

Proposed neural inducers that antagonize BMP-4 activity in the dorsal ectoderm during gastrulation are noggin, chordin, follistatin, cerebus and Xnr3. Noggin, chordin and cerebus act antagonistically by binding BMP-4 directly, preventing it from binding to its receptor (Piccolo et al., 1996; Zimmerman et al., 1996; Piccolo et al., 1999; Connolly

et al., 2000; Larrain et al., 2000; Liu et al., 2000). Follistatin appears to form a complex with BMP-4 and its receptor, preventing the activation of the BMP signalling cascade (Iemura et al., 1998; Connolly et al., 2000). The mode of action of Xnr3 is unknown, but may compete with BMP-4 for receptor binding (Hansen et al., 1997). All five molecules tend to induce neural tissue of anterior character as illustrated by the expression of anterior and general neural markers such as Otx-2 and N-CAM.

Potential factors involved in the posteriorization of neural ectoderm include FGFs, retinoic acid, Xbra3 and members of the Wnt family, such as Wnt-3a (McGrew et al., 1997; Sasai & DeRobertis, 1997; Shum et al., 1999; Strong et al., 2000). Over the last few years there has been a great deal of controversy over the role of FGFs in neural induction (for review, see Doniach, 1995; Hongo et al., 1999). What seems to be the consensus for the time being is that rather than acting as a neural inducer, FGFs caudalize neural tissue (Xu et al., 1997; Holowacz & Sokol, 1999). For instance, treatment of forebrain with FGF will induce a mid/hindbrain fate. Similarly, treatment of hindbrain with FGF will induce spinal cord markers (Cox & Hemmati-Brivanlou, 1995).

### 1.3.5 Organogenesis

The development of most organs begins with aggregates of precursor cells, which then migrate in response to orientation and positional cues. Once in their defined positions, extensive variations in cell adhesion, proliferation and apoptosis occurs which helps to shape the organ. Organogenesis in *Xenopus* has not been extensively studied, with concentrations primarily on the development of the gut, heart, kidney, spleen and blood. Most recent reports have focused mainly on the molecular aspects of



organogenesis, such as in the left-right asymmetry of organs (for reviews, see Ramsdell & Yost, 1998; Capdevila & Izpisua Belmonte, 2000).

In *Xenopus*, two antagonistic TGF- $\beta$ -related signalling pathways exist. A left-sided Vg1/anti-BMP/Nodal signalling pathway and a right-sided BMP/ALK2/Smad signalling pathway (Ramsdell & Yost, 1999; Branford et al., 2000). Both of these pathways are involved with regulating left-right asymmetry in the gut and heart. The recent identification of *Xenopus lefty* (*Xlefty*), a member of the Lefty subfamily of TGF- $\beta$  signalling molecules has provided evidence for cross talk between these two pathways (Branford et al., 2000). It is now proposed that on the left-side, *Xlefty* functions downstream of *Vg1*, along with *Xnr-1* and *Xpitx2*, to specify left-sided development. In addition, *Xlefty* interacts bilaterally with BMP-4 in either a positive or negative manner to help establish and/or maintain left-right axis formation of the heart and gut (Branford et al., 2000). Further complicating this is the identification of isoforms of the *pitx2* gene, *pitx2a* and *pitx2c*. The distinct expression patterns of these two isoforms suggests that they are regulated by different genetic pathways and that *pitx2c* may be primarily involved with regulating gut laterality, while *pitx2a* is involved with heart asymmetry (Essner et al., 2000).

BMP signalling has also been found to be important for heart formation by maintaining the expression of *XNkx2-5*, a homeobox gene required for cardiac specification, prior to differentiation, and by regulating the expression of differentiated heart markers, such as *XMLC* and *XcTnl* (Shi et al., 2000).

In spleen development, splenic precursor cells are found symmetrically on both sides of the embryo and express *XNkx2-5*. Unlike gut and heart precursor cells, pre-

splenic cells do not migrate or undergo differential apoptosis to form the spleen. Instead, only the pre-splenic tissue on the left goes on to form the spleen, presumably by following a different developmental pathway. *XNkx2-5* is thought to play a role in establishing the asymmetry of the spleen, perhaps by acting downstream of *pitx2* and *nodal* in the laterality pathway (Patterson et al., 2000).

Members of the GATA family of zinc-finger transcription factors have been implicated in red blood cell (RBC) proliferation and differentiation (Orkin, 1992). Recently, a *Xenopus* version of friend of GATA (xFOG) has been cloned, and is thought to mediate the switch from progenitor proliferation to maturation and differentiation during erythropoiesis by interacting with and regulating GATA-1 and GATA-2 activity (Deconinck et al., 2000). Additional attempts to isolate other *Xenopus* FOG genes has proven unsuccessful and based upon its pattern of expression it is likely to be involved with the development of other organs, such as the spleen, heart, kidney and the brain, where it again interacts with and regulates GATA proteins (Deconinck et al., 2000).

### **1.3.6 Metamorphosis and limb formation in *Xenopus***

The final event in the *Xenopus laevis* life cycle is metamorphosis. This is a post-embryonic process that involves the transformation of a free-swimming tadpole into an adult organism. Indeed, during this transition many structural changes occur, however, the most dramatic and obvious are the growth and differentiation of limbs and the death and resorption of the tadpole's tail.

Metamorphosis in *Xenopus* is triggered by environmental cues, such as nutrition, light and temperature and is controlled by thyroid hormone (TH; for review, see Tata,

1996). During early development of the tadpole, the pituitary produces and secretes prolactin, which inhibits metamorphosis (Yamashita et al., 1993; Yamamoto et al., 2000). The thyroid gland appears shortly after the tadpole begins to feed. When environmental conditions are favourable, the hypothalamus releases thyrotropin-releasing hormone, which acts on the pituitary and causes the release of thyroid-stimulating hormone. This in turn stimulates the release of the THs, tri-iodothyronine ( $T_3$ ) and thyroxine ( $T_4$ ) from the thyroid gland, which promote metamorphosis (Tata, 1993; for review, see Tata, 1999).

A great deal of research has been conducted recently into the mechanisms of *Xenopus* tail resorption and limb development in response to THs, with particular emphasis on identifying the TH response genes (Brown et al., 1996; Berry et al., 1998; Furlow & Brown, 1999; Damjanovski et al., 2000).

In *Xenopus*, the hind limbs develop first from limb buds, which start off as small protrusions arising from the body wall of the embryo. The limb bud is composed of two types of tissue – mesenchyme, derived from the lateral plate and somitic mesoderm, and epidermis, derived from the ectoderm. With the initiation and progression of the limb bud, a region, known as the progress zone, develops. This is a region at the tip of the limb bud that consists of proliferating mesenchymal cells. It is responsible for inducing the overlying ectoderm to differentiate into a specialized structure, the apical ectodermal ridge (AER). Limb bud outgrowth is initiated and maintained through reciprocal signalling between the ridge and zone of proliferation. Only when cells leave the progress zone do they begin to differentiate into the various limb structures (for review, see Johnson & Tabin, 1997; Zeller & Duboule, 1997; Riddle & Tabin, 1999).

Much of what is currently known about limb development comes from chick and mouse embryos. However, several features appear to be conserved in *Xenopus*. A key molecule in the AER involved with maintaining proliferation in the progress zone is FGF-8. In *Xenopus*, FGF-8 is first detected at Stage 49, when the hind limbs are already visible. Even though, at this stage, there is no morphological AER, the confined expression of FGF-8 to a narrow band along the apical dorsoventral margin of the limb bud epidermis, indicates the presence of a pseudo-ridge (Christen & Slack, 1997; Yokoyama et al., 1998). At around Stage 51, a small thickening of the apical epidermis does become apparent and corresponds with FGF-8 expression. Through regeneration experiments it has been shown that FGF-8, in *Xenopus*, is an important factor in determining whether an amputated limb can regenerate and for maintaining continued outgrowth (Christen & Slack, 1997). Only those ablated limb bud tips that were able to correctly re-establish FGF-8 expression could successfully regenerate.

Another FGF that plays an important role in limb bud development is FGF-10. FGF-10 is expressed in the proliferating mesenchymal region of the developing limb and is thought to be the main initiator of limb bud development, working synergistically with FGF-8 in the AER to help maintain limb elongation (Xu et al., 1998). In *Xenopus*, this role of FGF-10 appears to be conserved. Again, through regeneration experiments, the mesenchyme of the limb bud has been shown to be the primary region controlling regeneration, with FGF-10 being the likely candidate molecule involved (Yokoyama et al., 2000). In recombinant limbs, derived from regenerative limb mesenchyme and non-regenerative limb epidermis, FGF-8 expression was re-established in the epidermis due to the influence of the underlying regenerative mesenchyme, resulting in limb elongation.

In order for limbs to regenerate, the expressions of both FGF-8 and FGF-10 have to be re-established (Yokoyama et al., 2000).

Another important signalling centre in the developing limb bud is a region of the posterior mesenchyme known as the zone of polarizing activity (ZPA). This region is located in the marginal portion of the limb bud and is essential for establishing the anteroposterior axis. When grafted onto the anterior margin of a second limb, the ZPA can induce mirror-image duplications. It is hypothesized that the ZPA releases a signal (morphogen), which forms a concentration gradient across the limb bud, such that those cells receiving high concentrations of morphogen will form more posterior structures, while those receiving low concentrations of morphogen will form more anterior structures (Endo et al., 1997; Riddle et al., 1993). A candidate molecule for the ZPA morphogen is Shh (Riddle et al., 1993).

The existence of a ZPA in developing *Xenopus* limb buds was demonstrated by Cameron and Fallon (1977), who conducted various limb rotation experiments and developed a ZPA map for the hind limb bud. In chick and mouse limb buds, *shh* expression is localized to the posterior margin of the limb bud, directly corresponding with the ZPA (Echelard et al., 1993; Riddle et al., 1993). In *Xenopus*, however, despite the fact that *shh* is also expressed in the posterior margin of the limb bud, its expression domain does not correspond directly with the ZPA map. It tends to be expressed in the distal portion of the ZPA and at Stage 53, *shh* expression was not observed in the ZPA region at all, but in a region more distal to it (Endo et al., 1997). Additional 180° limb rotation experiments, however, have confirmed that the ZPA in *Xenopus* limb buds is accompanied by *shh* expression and that, most likely, the portion of the ZPA that actually

functions in the development of the limb bud is the portion that expresses *shh* (Endo et al., 1997).

#### **1.4 *Xenopus laevis* as a tumour model**

Although ‘cancer’ is a general term that refers to an extensive array of diseases, all of which have their own unique and distinctive features, the basic processes involved with tumorigenesis in most cancers are essentially the same. Tumour development initiates with a single cell that has undergone a genetic alteration, enabling it to outgrow its neighbours. The altered cell and its progeny continue to divide uncontrollably with the acquisition of additional genetic aberrations that further promote proliferation and block terminal differentiation. Eventually these cells will start to appear abnormal in shape and orientation. As long as these neoplastic cells remain in a discrete clump, the tumour is said to be benign. If, however, the cells of a tumour acquire the ability to break loose and invade the surrounding tissue then the tumour is said to be malignant and considered a cancer (for review, see Weinberg, 1996).

The genetic alterations involved with tumour development and progression, typically affect the regulation of the cell cycle and apoptosis, involving both stimulatory and inhibitory control molecules that regulate normal proliferation and ultimately differentiation. These control molecules tend to belong, for the most part, to the proto-oncogene and tumour suppressor gene classes. For a tumour to be considered cancerous, at least six mutations must occur in the cells’ growth-controlling genes (for review, see Weinberg, 1996).

With the advent of cancer being referred to as a developmental disorder (for review, see Pierce et al., 1986; Dean, 1998; for review, see Edwards, 1999), *Xenopus laevis* has proven to be a useful tool to study the mechanisms of development. More recently, it has become evident that *Xenopus* embryos might in fact make model systems to study the mechanisms of neoplasia.

Three different groups, through the course of their investigations into the early developmental events that occur in *Xenopus*, have successfully generated tumour phenotypes (for review, see Wallingford, 1999). Typically these investigations have involved the normal developmental roles that known tumour suppressor genes and proto-oncogenes play.

Mutations in p53, a known tumour suppressor gene, is the most common genetic anomaly in human cancers. Its normal role in the cell is that of a cell cycle checkpoint molecule. P53 is responsible for arresting the cell cycle in response to DNA damage and in some cases inducing apoptosis, if the damage is irreparable. Overexpression of a dominant negative form of the human p53 gene blocked cell differentiation early in *Xenopus* embryos, resulting in the formation of cellular masses, which resembled tumours. Overexpression of the *Xenopus* form of the proto-oncogene mdm2, a negative regulator of p53, produced a very similar phenotype. Co-injection of wild type *Xenopus* or human p53 was able to rescue the mutant p53 phenotype (Wallingford et al., 1997).

Dahmane et al. (1997) showed that overexpression of the proto-oncogene *gli1* in the epidermis of *Xenopus* embryos, produced tumours, reminiscent of basal cell carcinomas (BCC). Gli1 is a zinc finger transcription factor and is a downstream target of the Shh signalling pathway, which has been implicated as a causal agent of BCC.

Indicative of tumours, the *gli1* overexpressing cells failed to distribute themselves normally, resulting in cellular masses. In addition, molecular marker analysis of these *gli1*-induced tumours revealed a close similarity to human BCCs.

Our lab recently showed tumour forming ability by a *Xenopus* Rel family member (Yang et al., 1998). *Xrel3*, when ectopically expressed in the epidermis of *Xenopus* embryos produced densely pigmented patches on the surfaces of embryos (Figure 1.5). Interestingly, these tumour-like lesions closely resembled those formed from *gli1* overexpression. Subsequent tumour analysis has revealed that, as with the *gli1* overexpressing cells, *Xrel3* overexpressing cells fail to distribute normally and remain as discrete clumps (Kao et al., manuscript in progress). In addition, increased cellular proliferation can be observed in the *Xrel3*-induced tumours as compared to control embryo epidermis (Kao et al., manuscript in progress).

Regardless of the mechanisms involved, which remain to be elucidated, these three groups have illustrated that *Xenopus laevis* is a sensitive enough and simple system to study tumour development and progression.

## 1.5 The Rel family of proteins

Rel proteins were first identified in the late 1950's with the discovery of *v-rel*, the oncogene carried by avian reticuloendotheliosis virus strain T. *V-rel* was initially isolated from the liver of diseased turkeys and is responsible for inducing leukemia in juvenile birds (Sevoian et al., 1964; Theilen et al., 1966). Since then the Rel family has greatly expanded with members identified in a number of species of organisms, including



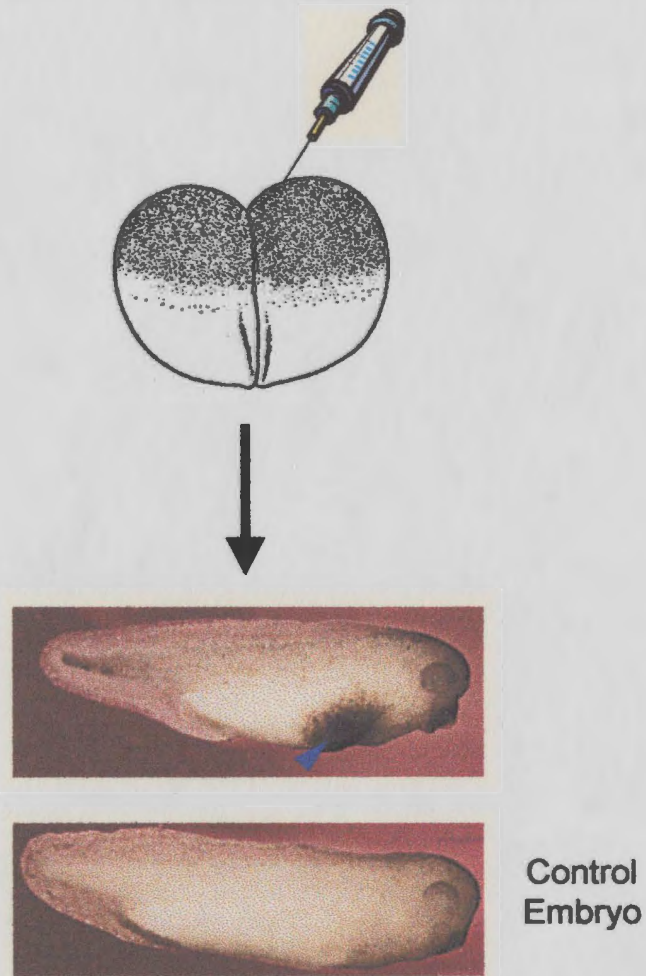


**Figure 1.5:** Overexpression of *Xrel3* mRNA in *Xenopus* embryos induces tumorigenesis. 0.5-1ng of synthetic *Xrel3* mRNA was injected into two-cell stage embryos. The blue arrow indicates the presence of a tumour.

the normal cellular homolog of *v-rel*, the proto-oncogene *c-rel*. Of the Rel/NF- $\kappa$ B family members, mammalian NF- $\kappa$ B has been the most extensively studied and was identified in the mid-80's as a nuclear factor that bound to an enhancer region of the B-cell immunoglobulin kappa light chain gene after stimulation with bacterial lipopolysaccharide (LPS; Sen and Baltimore, 1986).

Rel proteins, over the years, have been found to exist in most cell and tissue types and are involved in myriad biological processes. As such they can be induced by a wide spectrum of external stimuli, including mitogens, cytokines, bacterial and viral proteins and UV light. Likewise, being transcription factors, they target and influence an extensive array of genes (for review, see Pahl, 1999).

### 1.6.1 Rel/NF- $\kappa$ B structure

Common to all Rel/NF- $\kappa$ B family members is a highly conserved region of about 300 amino acids in the amino terminus (Figure 1.6). This region is referred to as the Rel Homology Domain (RHD) and has been shown to be required for DNA binding, homo- or hetero-dimerization with other Rel proteins and nuclear localization (Thanos & Maniatis, 1995; May & Ghosh, 1998; Chen & Ghosh, 1999).

In cells, Rel proteins typically exist as dimers. Only certain pairs have been found to exist *in vivo*, the most common form being the p50/p65(RelA) heterodimer (NF- $\kappa$ B). Rel complexes are responsible for activating transcription from target genes by binding to DNA sequences, known as  $\kappa$ B sites, with a decameric consensus of GGGRNNTYCC (where R is G or A, Y is C or T and N is any nucleotide; Chen & Ghosh, 1999; de Martin et al., 1999). In this way, Rel dimers have different binding affinities for different  $\kappa$ B

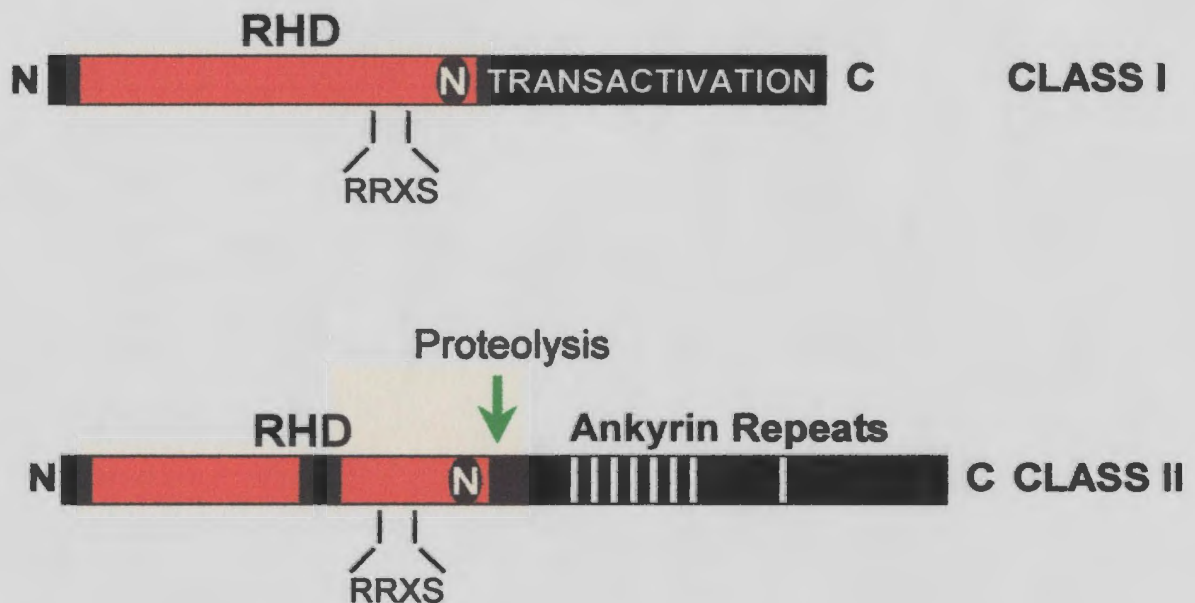


**Figure 1.6:** A schematic representation of the structural domains of Rel/NF- $\kappa$ B proteins. At the amino terminal end is the highly conserved RHD, which contains the nuclear localization site (N) and the PKA site (RRXS) at its carboxy terminus. In Class I Rel proteins, the carboxy terminal end consists of the transactivation domain, while in Class II Rel proteins the carboxy terminus consists of multiple copies of ankyrin repeats.

elements and the genes containing  $\kappa$ B elements in their regulatory regions are selectively targeted by certain Rel dimer complexes.

Rel complexes can activate transcription in either a constitutive or inducible manner. In general, however, Rel dimeric complexes tend to exist in the cytoplasm of quiescent cells in an inactive or uninduced state by the action of inhibitory subunits of the I $\kappa$ B family, which block the nuclear localization sequence (NLS) in the Rel complexes (Thanos & Maniatis, 1995; May & Ghosh, 1998; Chen & Ghosh, 1999).

An additional feature of most Rel proteins is the presence of a consensus recognition sequence (RRXS) for protein kinase A (PKA). This site is located toward the carboxy terminal end of the RHD, approximately 25 amino acids N-terminal to the NLS (Mosialos & Gilmore, 1992; Zhong et al., 1997; Zhong et al., 1998). This site when phosphorylated by PKA, typically on the serine residue, has been shown to enhance the transcriptional activity of Rel complexes (Zhong et al., 1997; Zhong et al., 1998; Chen & Ghosh, 1999). The effect of PKA on Rel complexes presumably involves a conformational change, which in turn affects the way in which Rel complexes bind to DNA. It is thought that the N-terminal and C-terminal domains of Rel proteins normally interact with one another, decreasing the ability of the Rel complex from binding DNA and also masking sites that interact with transcriptional co-activators, such as CBP/p300 (Zhong et al., 1998; Chen & Ghosh, 1999). Phosphorylation of the PKA site could change the conformation of the Rel complex, thereby altering DNA binding activity and increasing transcriptional efficiency.

PKA normally exists in the cytosol as a tetrameric complex consisting of two regulatory and two catalytic subunits ( $R_2C_2$ ). Intracellular increases in cyclic AMP

(cAMP) levels leads to the binding of cAMP to the regulatory subunits of PKA, which causes a conformational change in the tetrameric complex and results in the subsequent release of the catalytic subunits (Zhong et al., 1997). In an attempt to identify the mechanism by which PKA regulates Rel/NF- $\kappa$ B activity, it has recently been demonstrated that the PKA catalytic subunit (PKAc) alone binds I $\kappa$ B proteins and is associated with the Rel/NF- $\kappa$ B complex. In this association, the N-terminal portion of PKAc interacts with the ankyrin motifs of I $\kappa$ B proteins and most likely I $\kappa$ B-like proteins, which blocks its catalytic activity. In this configuration, PKAc activity is unresponsive to changes in cAMP levels (Zhong et al., 1997; Zhong et al., 1998).

The carboxy terminus, on the other hand, is highly variable among the Rel family members and is not very well understood (Figure 1.6). Rel members can be divided into two classes based on the structure of the C-terminus. The first class consists of NF- $\kappa$ B1 (p105), NF- $\kappa$ B2 (p100) and *Drosophila* Relish, which are translated as precursor molecules with long C-terminal domains that contain multiple copies of ankyrin repeats (Thanos & Maniatis, 1995; de Martin et al., 1999; Gilmore, 1999). As such, the unprocessed forms resemble I $\kappa$ B inhibitory proteins and activation requires proteasome-mediated proteolytic cleavage of the C-terminus. The second class consists of Rel proteins such as c-Rel, RelA (p65), RelB and *Drosophila* Dorsal and Dif, which possess transactivation domains in their C-termini (Thanos & Maniatis, 1995; de Martin et al., 1999; Gilmore, 1999). In general, members of the first class of Rel/NF- $\kappa$ B transcription factors activate transcription only when they dimerize with members of the second class.

### **1.6.2 Regulation of rel/NF- $\kappa$ B activity**

In its inactive or quiescent state, Rel complexes are typically found in the cytosol of cells in either of two forms. Either Rel Class II homo- or heterodimer complexes are bound to a member of the I kappa B (I $\kappa$ B) family of inhibitory proteins or a mature Rel Class II protein dimerizes with an unprocessed Class I Rel protein (Thanos & Maniatis, 1995; Gilmore, 1999). As with Class I Rel proteins, I $\kappa$ B proteins also possess multiple ankyrin repeat domains, which forms the core of the protein. I $\kappa$ Bs also possess an N-terminal regulatory domain and a C-terminal PEST domain, which is involved in I $\kappa$ B turnover (de Martin et al., 1999; Karin, 1999).

Upon extracellular stimulation by inducing agents such as tumour necrosis factor alpha (TNF $\alpha$ ), interleukin 1 (IL-1) and bacterial LPS, a phosphorylation cascade ensues in which all external stimuli eventually converge on and activate I $\kappa$ B kinase (IKK) complexes (Figure 1.7; Thanos & Maniatis, 1995; May & Ghosh, 1998; de Martin et al., 1999; Mercurio & Manning, 1999).

Not much is known about the individual signal transduction pathways activated by the various inducing signals prior to convergence on IKK complexes, except that receptor binding proteins such as TNF receptor associated factors (TRAFs) or MyD88, intermediate kinases such as NF- $\kappa$ B inducing kinase (NIK) and Il-1 receptor associated kinases (IRAKs) and direct activators of the IKK complex such as mitogen-activated protein kinase kinase kinases (eg. MEKK-1) and the small GTPases Rac1 and Cdc42 are likely to be involved (May & Ghosh, 1998; de Martin et al., 1999; Gilmore, 1999; Mercurio & Manning, 1999).

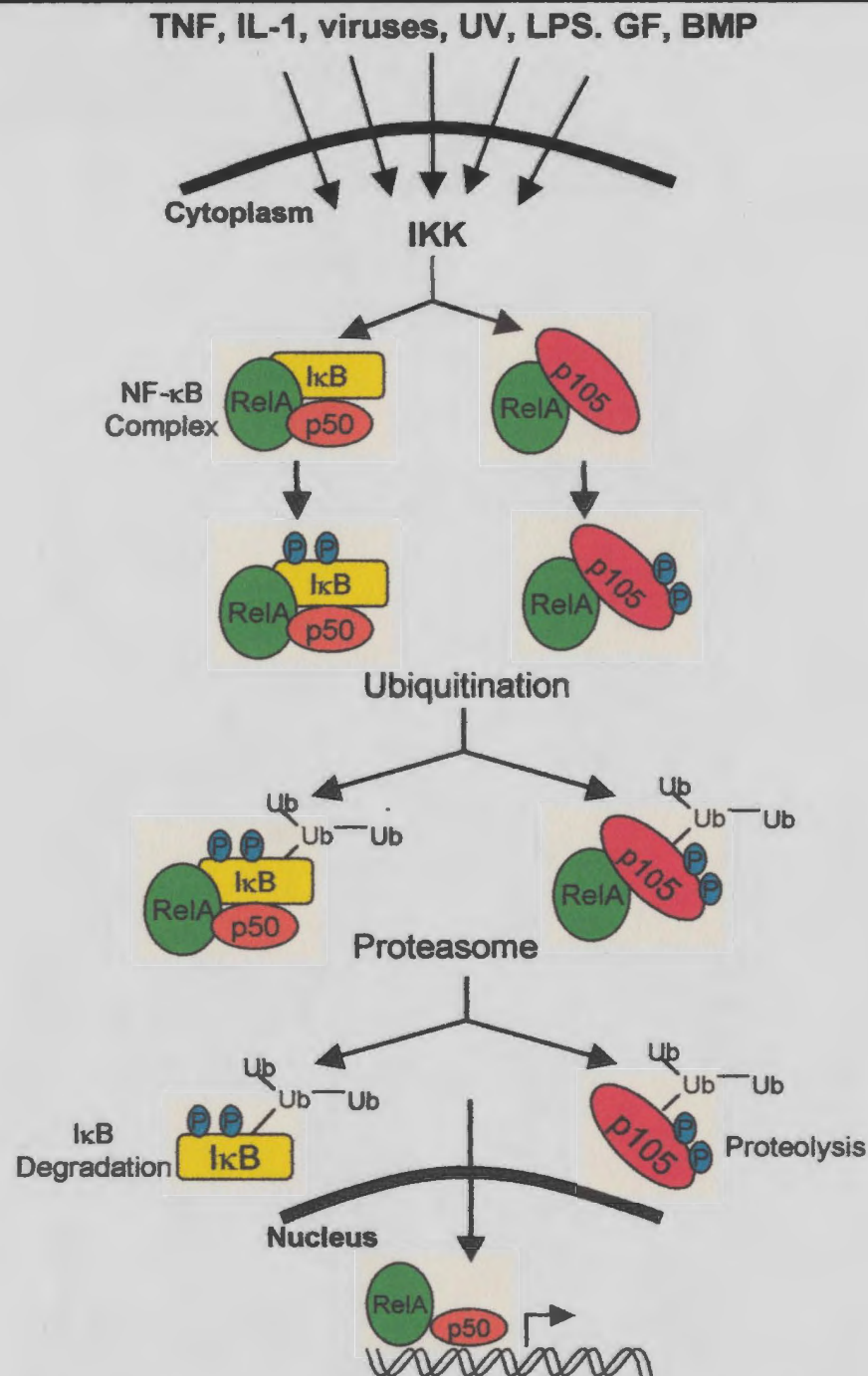


**Figure 1.7:** A diagrammatic representation of Rel/NF-κB activation in the cell. One of many external stimuli binds to receptors on the surface of the cell, leading to the activation of a signalling cascade. Activation of the IKK complex leads to the phosphorylation of the inhibitory subunits IκB or p105 and targets them for polyubiquitination. The IκB subunit is then rapidly degraded by a proteasome complex, while the p105 subunit is proteolytically processed and the cleaved, ubiquitinated carboxy terminus is degraded. The resulting active NF-κB complex produced then translocates to the nucleus, where it binds DNA and affects downstream transcription (Thanos and Maniatis, 1995; Gilmore, 1999).

The IKK complex consists of a number of subunits, three of which have been isolated so far. IKK $\alpha$  and IKK $\beta$  make up the catalytic component of the complex, while IKK $\gamma$  serves as a regulatory subunit. IKKs are serine/threonine kinases and function in the Rel/NF- $\kappa$ B signalling cascade to phosphorylate I $\kappa$ Bs, typically on two conserved serine residues in the N-terminal regulatory domain (May & Ghosh, 1998; de Martin et al., 1999; Karin, 1999; Mercurio & Manning, 1999).

Phosphorylation of I $\kappa$ Bs targets them for polyubiquitination in which ubiquitin molecules covalently conjugate, in general, to neighbouring N-terminal lysine residues. This then triggers rapid degradation of the I $\kappa$ B protein by the multicatalytic 26S proteasome complex (May & Ghosh, 1998; de Martin et al., 1999; Karin, 1999; Mercurio & Manning, 1999). As a result, the NLS becomes unmasked and PKAc becomes activated. Rel/NF- $\kappa$ B complexes then translocate to the nucleus where they bind  $\kappa$ B elements and affect downstream transcription of target genes (Figure 1.7).

Additional levels of complexity arise from findings that different I $\kappa$ B isoforms (eg. I $\kappa$ B $\alpha$  and I $\kappa$ B $\beta$ ) appear to target different combinations of Rel proteins and that different inducers cause the degradation of different I $\kappa$ B isoforms (May & Ghosh, 1998; de Martin et al., 1999; Karin, 1999; Mercurio & Manning, 1999). Whether PKAc is always associated with Rel/NF- $\kappa$ B - I $\kappa$ B complexes in the cytoplasm remains to be determined, as this could have dire consequences as to the regulation of Rel/NF- $\kappa$ B complexes (Zhong et al., 1997). The fact that some Rel family members do not possess PKA sites suggests that an alternate mode of activity regulation exists. In addition, there is evidence to suggest that alternate pathways leading to Rel/NF- $\kappa$ B activation may also be utilized. For instance, NF- $\kappa$ B activation by UV irradiation does not appear to use the



IKK complex and phosphorylation of I $\kappa$ B $\alpha$ , in response to anoxia, occurs on tyrosine residues, rather than serine residues (Imbert et al., 1996; Li & Karin, 1998).

Due to the complex nature of the Rel/NF- $\kappa$ B signalling pathway(s), Rel/NF- $\kappa$ B activity can be regulated at a number of different levels, such as inhibiting I $\kappa$ Bs, proteasomes or dimerization, blocking phosphorylation of I $\kappa$ Bs and disrupting Rel/NF- $\kappa$ B interaction with transcriptional co-activators or basal transcriptional machinery. One important level of control in the case of NF- $\kappa$ B, however, is that one of the downstream targets of NF- $\kappa$ B is I $\kappa$ B. Certain I $\kappa$ Bs, such as I $\kappa$ B $\alpha$ , contain both an NLS and a nuclear export sequence (NES). In this way, newly synthesized I $\kappa$ B $\alpha$  can enter the nucleus, remove NF- $\kappa$ B dimers from the DNA and transport them from the nucleus to the cytoplasm via exportin-mediated transport (Sachdev et al., 1998; Karin, 1999).

## 1.6 The role of Rel proteins in development

I have been interested in the early events that pattern the vertebrate embryo and in particular the role that Rel proteins play. Members of the Rel/NF- $\kappa$ B family are transcriptional activators that have been implicated in a wide variety of physiological and pathological processes, such as embryonic development, apoptosis, the immune response, differentiation and oncogenesis.

Embryologically speaking, the role of Rel proteins is best characterized in the invertebrate *Drosophila*, where Dorsal, a Rel/NF- $\kappa$ B family member is crucial to the specification of the dorso-ventral axis (for review, see Govind, 1999). Initially, Dorsal protein is uniformly distributed along the dorso-ventral axis of the embryo, where it is restricted to the cytoplasm. However, upon ventral activation of the Spätzle/Toll

signalling pathway, Dorsal, in ventral cells becomes activated and translocates to the nucleus. Thus a gradient is established, with the concentration of Dorsal being highest in the ventral nuclei and absent from the dorsal nuclei (Drier et al., 2000). Dorsal, in turn, is then responsible for activating patterning genes such as *twist* and *snail* which give rise to mesoderm. At lower concentrations, in lateral nuclei, Dorsal activates neuroectodermal patterning genes (Drier & Steward, 1997).

The role of Rel proteins in early vertebrate body patterning, however, is not clear. Through knockout studies in mice, Rel proteins have been found to be primarily involved with the immune system and haematopoiesis. In addition, RelA and c-Rel appear to have anti-apoptotic effects (for review, see Gerondakis et al., 1999).

Mice deficient in both p50 and p105 (both of which are encoded by the *nfkb1* gene) develop normally, although multiple defects in the function of the immune system eventually form, primarily due to B-cell proliferation defects (Sha et al., 1995). Like NF- $\kappa$ B1 deficient mice, NF- $\kappa$ B2 (p52/p100) deficient mice also develop normally. However, unlike, NF- $\kappa$ B1, NF- $\kappa$ B2 deficient mice show major defects in the structural integrity of haematopoietic organs such as the spleen and lymph node (Caamaño et al., 1998; Franzoso et al., 1998). In this case, the resulting immune deficiencies observed are primarily due to defects in antigen presentation (Franzoso et al., 1998).

Again, mice deficient in either c-Rel or Rel B do not exhibit abnormal embryogenesis. Mice deficient in c-Rel show an increase in B- and T-cell proliferation (Grumont et al., 1998). In Rel B deficient mice, in addition to a structural disruption of the thymus, populations of splenic and thymic dendritic cells become greatly reduced, affecting both acquired and innate immunity (Wu et al., 1998).

Rel A deficient fetal mice, on the other hand, die of extreme levels of apoptosis in fetal liver cells (Barkett & Gilmore, 1999; Foo & Nolan, 1999; Chen et al., 2000). The death of these mice is believed to be due to an increase in sensitivity to the cytotoxic effects of TNF- $\alpha$  (Doi et al., 1999). These studies indicate a role for NF- $\kappa$ B as an anti-apoptotic factor.

In the majority of knockouts, mouse embryos develop normal body patterning, suggesting that Rel proteins are not required for embryogenesis. However, it is clear from multiple knockout studies that there is a lot of functional overlap and redundancy among the Rel family members that may account for this observation (Gerondakis et al., 1999).

Recent evidence involving avian embryogenesis has shown that the Rel/NF- $\kappa$ B family of transcription factors could play a significant role in vertebrate limb development. Using the chick embryo as a model, *c-rel* was found to be expressed in the progress zone of the developing limb bud. Sequestration of c-Rel in the cytoplasm with a transdominant inhibitor (IkB- $\alpha\Delta$ N), led to limb truncations with a general loss of normal AER structure and reductions in *shh* and *twist* expression (Bushdid et al., 1998; Kanegae et al., 1998). Removal of the AER led to a rapid loss of *c-Rel* expression, with subsequent reductions in *shh* and *twist* expression. When FGF-soaked beads were applied to the truncated limbs, after ridge removal, *c-Rel* expression was restored (Kanegae et al., 1998). This provides evidence for a positive feedback loop between Rel/NF- $\kappa$ B and FGF signalling molecules and also that Rel/NF- $\kappa$ B activity could be critical for mesenchymal maintenance of the AER.

In amphibians, Rel/NF- $\kappa$ B proteins are likely to play a role in embryogenesis due to the developmentally restricted patterns of expression of some of its members. Of the five known *Xenopus laevis* Rel family members, only *XrelA* (Kao & Lockwood, 1996), *Xp100* (Suzuki et al., 1998) and *Xrel3* (Yang et al., 1998) are expressed in a developmentally restricted pattern.

The mRNA of *XrelA*, a *Xenopus* homologue of the mammalian *relA* gene, is expressed in both *Xenopus* oocytes and early embryos. The mRNA is uniformly expressed throughout the entire embryo during the early embryonic stages, but becomes localized to the animal and equatorial regions during the MBT stage (Bearer, 1994), thus suggesting a possible involvement in head and tail formation of the early embryo. In addition, overexpression experiments, in which *XrelA* mRNA is injected into the dorsal side of embryos, resulted in a significant reduction in the development of dorsal structures and attenuation of dorsal morphogenetic movements during gastrulation (Kao & Lockwood, 1996). This demonstrates a possible role in dorsoventral patterning of the embryo.

*Xp100* is the *Xenopus* homolog of mammalian p100/NF- $\kappa$ B2. Initial studies have shown that *Xp100* mRNA is maternally expressed throughout the oocyte and early embryo. However, these transcripts decline during gastrulation with a subsequent rise during neurulation. *Xp100* transcripts persist and are present in all adult tissues. Throughout embryogenesis, *Xp100* transcripts are ubiquitously expressed, except in neurula stages, where they become enriched in the somitogenic mesoderm. This localization suggests that *Xp100* might be involved in the development of somites (Suzuki et al., 1998).

*Xrel3* most closely resembles mammalian c-Rel and shares a high degree of similarity with *Xrel2*. *Xrel3* mRNA is expressed in a spatiotemporally restricted manner. Maternal messages accumulate within the early embryo up to the late blastula stage and are ubiquitously expressed. There does appear to be an enrichment of *Xrel3* mRNA in the equatorial region of blastula stage embryos. During gastrulation, however, a dramatic decline is observed. Transcripts reappear again in the embryos undergoing neural development and accumulate in the notochord, forebrain, mid-hindbrain and otic placode. Later on in tadpole stages, messages accumulate in the forebrain, dorsal aspect of the mid-hindbrain and otocysts (Yang et al., 1998). This pattern of expression suggests that *Xrel3* may have a role in neural patterning, particularly the dorsoanterior aspects of the nervous system.

## **1.7 The role of Rel in oncogenesis**

Consistent with mechanisms involved in oncogenesis, chromosomal amplification, overexpression and rearrangement of genes encoding Rel/NF- $\kappa$ B proteins have been identified in many forms of human cancer (for review, see Rayet & G  linas, 1999). To date, c-Rel, RelA, NF- $\kappa$ B1 and NF- $\kappa$ B2 have been implicated in various forms of haematopoietic and solid tumours. Due to the oncogenic nature of its viral counterpart (v-Rel), c-Rel became attractive as a factor that might be involved in tumorigenesis. Indeed amplification and rearrangement of the *c-rel* gene has been found in several leukemias and lymphomas (Barth et al., 1998; Rao et al., 1998). To a lesser extent, overexpression of *c-rel* has been associated with human non-small cell lung carcinomas (Mukhopadhyay et al., 1995).

Chromosomal rearrangement and amplification of the *rela* gene have also been implicated in a number of lymphoid tumours, such as non-Hodgkin's lymphomas and multiple myelomas (Houldsworth et al., 1996; Trecca et al., 1997). However, these genetic aberrations tend to occur rather infrequently. In addition amplification of *rela* has been identified in a number of carcinomas, including the head, neck, breast and stomach, although a definitive correlation between *rela* gene alterations and carcinomas has yet to be elucidated (Mathew et al., 1993; Visconti et al., 1997).

Few alterations in structure and expression of the *nfkb1* gene have been found in leukemias and lymphomas so far. However, one chromosomal rearrangement has been associated with certain human T-cell acute leukemias (Ferrier et al., 1999). Overexpression of the mature processed form of *nfkb1*, the p50 subunit of NF- $\kappa$ B, on the other hand, has been found to have a high correlation with non-small cell lung carcinomas. In addition, overexpression of p50 has also been found in transformed cells from colon, prostate, breast, bone and brain carcinomas (Mukhopadhyay et al., 1995).

Unlike *nfkb1*, a number of *nfkb2* gene rearrangements have been found in a variety of lymphomas, such as cutaneous T-cell lymphoma, B-cell non-Hodgkin's lymphoma, and multiple myeloma (Thakur et al., 1994; Neri et al., 1995). Overexpression of both the processed and unprocessed forms of *nfkb2*, p52 and p100 respectively, have also been reported in a number of breast and colon carcinomas (Dejardin et al., 1995; 1999).

Not only have aberrations in Rel genes been linked to human cancers, but it is clear that in some instances, misregulation of components of the Rel/NF- $\kappa$ B signalling pathway are involved. For instance, anomalies in members of the I $\kappa$ B family have been

noted in some cases (Michaux et al., 1997; Cabannes et al., 1999; Krappmann et al., 1999; Newton et al., 1999), in which a potential outcome could be the constitutive activation of Rel/NF- $\kappa$ B complexes. Indeed, persistent nuclear localization and hence activity of NF- $\kappa$ B has been found in numerous leukemias, lymphomas and carcinomas (Wood et al., 1998; Cabannes et al., 1999; Dejardin et al., 1999; Devalaraja et al., 1999; Krappmann et al., 1999), primarily due to defects in I $\kappa$ B $\alpha$  activity.

Regardless of the progress that has been made over the last few years in identifying the components of the Rel/NF- $\kappa$ B pathway and how Rel/NF- $\kappa$ B activity is regulated, it remains unclear how the misregulation of this pathway contributes to tumorigenesis. At present, the founding member, v-Rel, still remains the only Rel protein that is truly oncogenic both *in vitro* and *in vivo* (Gilmore, 1999).

## 1.8 Objectives

The primary objective of this study was to characterize the tumours formed from *Xrel3* overexpression in an attempt to identify some of the genes that are involved and ultimately regulated by *Xrel3*. In this way, perhaps an insight can be gained into how *Xrel3* normally functions in development.

**Objective 1:** To determine if there is a relationship between Rel/NF- $\kappa$ B and the Shh/Gli1 signalling pathway.

The spatiotemporally restricted expression pattern of *Xrel3* in *Xenopus* embryos suggests that it may have a distinct and defined role in embryogenesis (Yang et al., 1998). A common technique used in developmental studies to elucidate the function of genes

and gene products is to overexpress them. Interestingly, when *Xrel3* was overexpressed in the animal pole of *Xenopus* embryos, rather than getting the expected over-exaggeration of dorsal and anterior structures, pigmented patches on the surfaces of embryos formed instead, which developed into abnormal growths, or tumours (Yang et al., 1998). These tumours closely resembled those formed from *gli1* overexpression in a previous study (Dahmane et al., 1997), suggesting that perhaps Gli1 was involved in our *Xrel3*-induced tumours. In addition, the aberrant regulation of the Shh/Gli1 signalling pathway has been associated with BCC, the most commonly occurring cancer in humans, and with a number of developmental tumours of neural origin, where it promotes increased cellular proliferation.

**Objective 2:** To determine if a parallel can be drawn between the role of Rel/NF- $\kappa$ B in limb development and neoplasia, in terms of regulating differentiation.

A key aspect of cancers, in addition to uncontrolled cellular proliferation, is a reversion to a less differentiated, more developmentally primitive state. In the developing vertebrate limb, Rel/NF- $\kappa$ B has been shown to play an important role in the maintenance and perhaps initiation of limb bud outgrowth. Rel/NF- $\kappa$ B is expressed in a region of proliferating mesenchymal cells at the tip of a growing limb bud. This proliferating region is essential for limb outgrowth. During limb morphogenesis, there is evidence to suggest that Rel/NF- $\kappa$ B is involved with regulating *twist* and *shh* expression, in addition to being involved with FGF activity (Bushdid et al., 1998; Kanegae et al., 1998). Perhaps the role of Rel/NF- $\kappa$ B in the limb is to regulate proliferation of the mesenchymal cells before they differentiate and leave the progress zone. This would



therefore suggest that perhaps, in *Xrel3*-induced tumours, *Xrel3* promotes proliferation and prevents the differentiation of the *Xrel3* overexpressing cells into normal epidermal cells.

**Objective 3:** To isolate and identify novel genes activated by *Xrel3* induction of tumours.

At present very little is known about the *Xrel3* signalling pathway and in particular the genes it targets. With the aid of differential display technology, perhaps some of these target genes can be identified.

Differential display is a PCR-based technique for measuring changes in gene expression levels (Liang and Pardee, 1992). Total RNA, from two cell types to be compared, is extracted, from which subpopulations of mRNA can then be isolated and reverse transcribed with the use of anchored oligo d(T) primers. These anchored primers anneal to the 3' end of the mRNA molecules making use of the characteristic feature of most mRNAs, the polyadenylated tail. Amplification of partial complementary DNA (cDNA) sequences from these mRNA sub-populations ensues with the use of arbitrary primers, which are capable of annealing to a number of different positions. The resulting cDNA sequences are then displayed on a DNA polyacrylamide sequencing gel, generating what are referred to as "expression profiles". In this way a comparative analysis between *Xrel3* overexpressing and non-expressing cells can be achieved.

## Chapter 2: Materials and Methods

### 2.1 *In vitro* fertilization of mature *Xenopus* oocytes

A day before *Xenopus* embryos were required, female *Xenopus*, (Nasco, WI, USA), were induced to ovulate with a subcutaneous injection, towards the cloaca, into the upper portion of one of the hind legs, of 400-500 I.U. (0.4-0.5ml) of Human Chorionic Gonadotropin (HCG, Sigma Chemical Co., MO, USA). The females were left at room temperature (RT) and after about 12-14 hours began ovulating.

Testes were obtained after sacrificing a male *Xenopus* (Nasco). The male frog was injected, subcutaneously on its dorsal side, with a lethal dose of the anaesthetic Methanesulfonate (MS222, Sigma). An incision was made down the middle of its ventral side and the testes were removed from under the fat bodies. The testes were then cleaned by rinsing in fresh 1 times Normal Amphibian Medium (1X NAM) before being stored in 1XNAM at 4°C (see Table 2.1 for composition).







For fertilization, a portion of the testes was removed and macerated in a few millilitres (ml) of 1X NAM solution with forceps to form a sperm suspension in a 100x15mm Fisher brand disposable petri dish. Before fertilization, the suspension was always checked under a compound microscope in a drop of sterile water (H<sub>2</sub>O) to make sure the sperm were viable. Eggs were squeezed from the ovulating female into the sperm suspension. The eggs and sperm were mixed together by shaking briefly and then left at RT to allow fertilization to commence. After 5 minutes the petri dish was slowly flooded with NAM/20 solution (Table 2.1) to rinse excess sperm off the eggs.

**Table 2.1: Composition of Normal Amphibian Medium**

		g/l (in 10X solution)	Final Concentration in 1X NAM (mM)	Final Concentration in NAM/20 (mM)
<b>10X NAM salts</b>	<b>NaCl</b>	65	110	5.5
	<b>KCl</b>	1.5	2	0.1
	<b>Ca(NO<sub>3</sub>)<sub>2</sub>·4H<sub>2</sub>O</b>	2.4	1	0.05
	<b>MgSO<sub>4</sub>·7H<sub>2</sub>O</b>	2.5	1	0.05
	<b>0.5M EDTA, pH 8.0</b>	2ml	0.1	0.005
	<b>1M HEPES, pH 7.5</b>	100ml	10	0.005
<b>0.1M NaHCO<sub>3</sub></b>		–	1	0.05
<b>Gentamycin</b>		–	12.5mg	1.25mg

Approximately 15 minutes later, eggs that were successfully fertilized rotated so that the darkly pigmented animal pole was visible from the top. At this time the NAM/20 solution was poured off and 2.0-2.3% Cysteine-HCl (Sigma), pH 7.5-8.0 was added, with shaking, to remove the jelly coat from the embryos. Removal of the outer jelly coat was completed as indicated by close-packing of the embryos. The dejelling solution was then gradually diluted with H<sub>2</sub>O and the embryos were rinsed 3 times with NAM/20. Embryos were cultured in NAM/20 at RT, 14°C or 18-20°C, and staged according to Nieuwkoop and Faber (1994; see Table 2.2 for stages used).

**Table 2.2: *Xenopus* developmental stages used in the course of this study**

<b>Nieuwkoop and Faber stages of <i>Xenopus</i> embryos</b>	<b>Description of stages</b>
Stage 2 	Approximately 1 hr. 30 min. after fertilization, showing the completion of the first cleavage furrow (ventral view).
Stage 8 	Approximately 5 hr. after fertilization. First indication of a distinction between animal, marginal and vegetal regions (blastula embryo; dorsal view).
Stage 10 	Approximately 9 hr. after fertilization and representing the initial gastrula stage. The first appearance of the blastopore (vegetal view).
Stage 16 	Approximately 18 hr. and 15 min. after fertilization, showing a mid neurula stage embryo. Can see a distinct elevation of neural folds (posterior-dorsal view).
Stage 20 	Approximately 21 hr. and 45 min. after fertilization, showing the fusion of the neural folds and the flattening of the lateral outline of the embryo (late neurula; dorsal view).
Stage 26 	Approximately 1 day, 5 hr. and 30 min. after fertilization, showing the ear vesicle, primary eye vesicle, pronephros, cement gland and myotomes (larval stage; lateral view).
Stage 52/53	Approximately 21-24 days after fertilization. Presence of both fore- and hind limbs, with the hind limbs being further developed (tadpole stage during metamorphosis).

## 2.2 *In vitro* transcription of *Xrel3*

The *Xrel3* coding domain had been previously subcloned into the CS2+ expression vector (Figure 2.1). Synthetic *Xrel3* mRNA was transcribed and capped, after linearization with the restriction endonuclease NotI (Pharmacia Biotech, PA, USA), with the use of a large scale SP6 RNA Ribomax kit (Promega Corporation, WI, USA) and cap analogue (New England Biolabs, Inc., Mississauga, Ontario). The cap analogue is a 7-methyl guanine residue which is added onto the 5' terminus of the RNA to increase its stability and to allow for efficient translation.

In a 1.5ml eppendorf tube, the following reagents from the kit were assembled: 10 microlitres ( $\mu$ l) SP6 5X transcription buffer, 2.5 $\mu$ l each 100mM rATP, rUTP and rCTP, 0.3 $\mu$ l 100mM rGTP, 15 $\mu$ l 10mM cap analogue, 5 micrograms ( $\mu$ g) linear pCS2+/*Xrel3* template, 5 $\mu$ l SP6 RNA polymerase enzyme mix and nuclease-free H<sub>2</sub>O up to a final volume of 50 $\mu$ l. After gently pipetting up and down and centrifuging briefly, the reaction mix was incubated in a 37°C H<sub>2</sub>O bath for 2 hours. Subsequently, 5U (5 $\mu$ l) of RQ1 RNase free DNase (Promega) was added to the mix and further incubated at 37°C for 20 minutes. Addition of 100 $\mu$ l of nuclease-free H<sub>2</sub>O ensued, followed by phenol/chloroform extraction with equal volumes of buffer saturated phenol and water saturated chloroform (155 $\mu$ l of each). The remaining top aqueous layer from the extractions was then precipitated overnight at -70°C with one tenth the volume of 3M sodium acetate, pH 5.2, 2.5 volumes of 95-100% ethanol and 0.02mg (1 $\mu$ l) glycogen (Boehringer Mannheim Canada, Laval, Québec). After pelleting the RNA with centrifugation at 4°C for 15 minutes in a Fisher Scientific Model 235C Microcentrifuge,

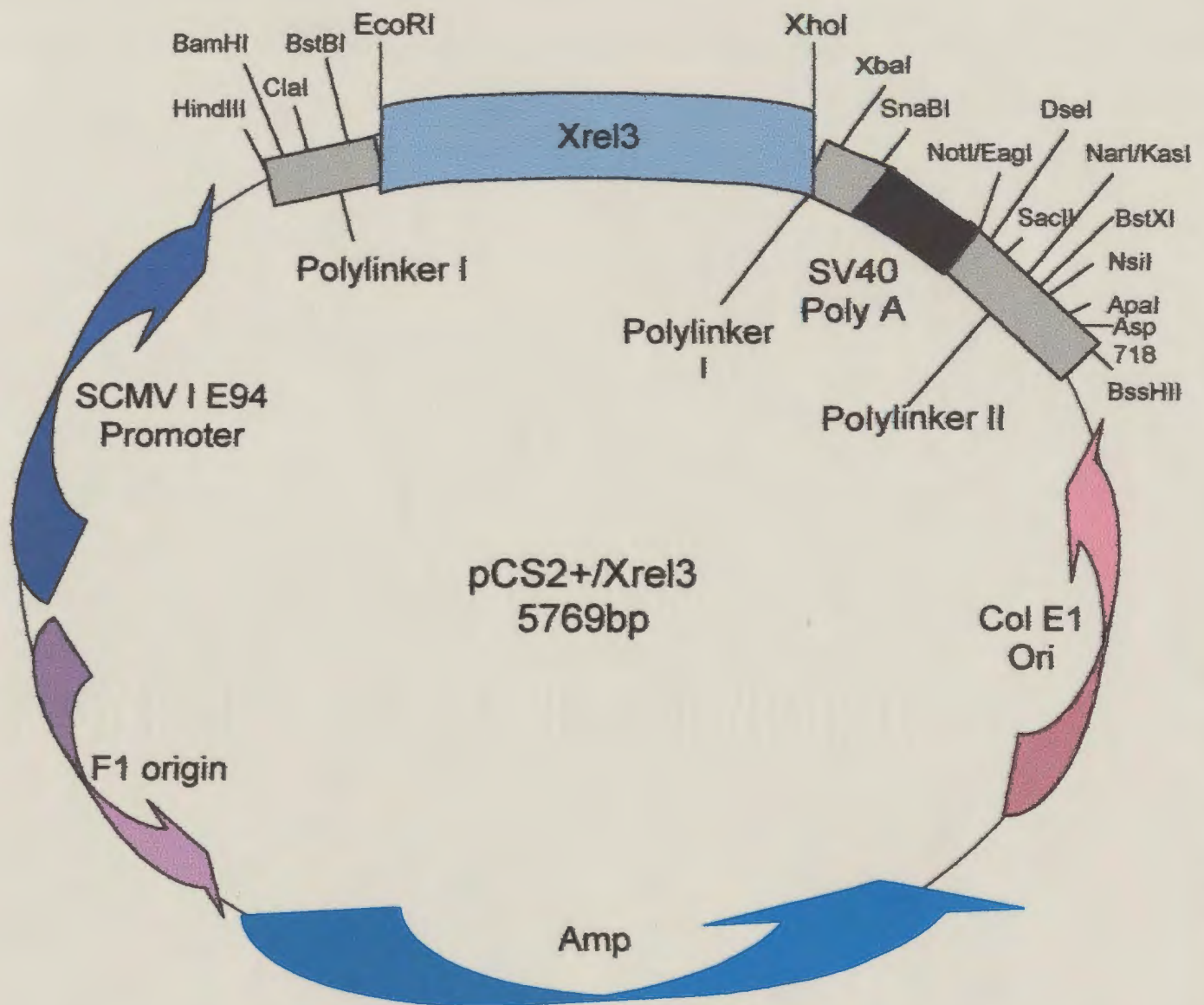


**Figure 2.1:** The CS2+ expression vector containing the *Xrel3* coding region in its multiple cloning site after digestion with the restriction enzymes EcoRI and XhoI.

the pellet was washed three times with 70% ethanol and vacuum dried briefly. The pellet was resuspended in 50µl of nuclease-free H<sub>2</sub>O and 1µl was used for each of agarose (Gibco BRL, Life Technologies Inc., N.Y., USA) gel electrophoresis analysis and optical density readings at wavelengths of 260 and 280 (OD<sub>260</sub> and OD<sub>280</sub>), to check for concentration, purity and integrity. An OD<sub>260</sub>/OD<sub>280</sub> ratio of greater than or equal to 2.0 indicated that the RNA was pure. The presence of primarily a single band of about 850-1000bp in size indicated that the RNA was in tact. The RNA was stored at -70°C.

### **2.3 *Xenopus* embryo microinjections**

Synthetic *Xrel3* mRNA was typically injected into the animal pole of *Xenopus* embryos just after first cleavage (Stage 2; Table 2.2), approximately 90 minutes after fertilization, using a Drummond “Nanoinject” Microinjector (Kao & Lockwood, 1996). The injection needles were made from 3<sup>1</sup>/<sub>2</sub>” Drummond glass capillary tubes (Fisher Scientific, Whitby, Ontario), which were pulled vertically using a Narishige Model PB-7 micropipette puller. The tips of the needles were bevelled at a 20° angle with a Narishige EG-40 grinder.

During the injection procedure the embryos were positioned within a plastic mesh grid cut from a plastic kitchen strainer and fused with chloroform to the bottom of a 60x15mm Fisher brand disposable petri dish. Through an injection volume of about 4.6 nanolitres (nl), each embryo received 500 picograms (pg)-1 nanogram (ng) of *Xrel3* mRNA or a control RNA (250-500pg per cell) while in NAM/2, 4% Ficoll 400. The embryos were then left to culture at RT, 14°C, or 18-20°C until they reached the desired stage in development (refer to Table 2.2).

## 2.4 *Xenopus* embryo dissections/extractions

### 2.4.1 Animal cap dissections

In some instances, once the injected and control embryos had reached the blastula stage (Table 2.2), the embryos were transferred on to a 1.5% agar bed in 60x15mm petri dishes and immersed in NAM/2. After removal of the fertilization membranes, animal tissue, that is destined to form ectoderm when cultured in isolation (animal caps), was dissected with the use of fine forceps (Fine Scientific Tools, North Vancouver, British Columbia). The animal cap explants were left to culture in NAM/2 at 18-20°C until they reached the right stage in development (refer to Table 2.2), as determined by co-culturing whole embryo counterparts. The caps were then subjected to RNA extraction (refer to section 2.5).

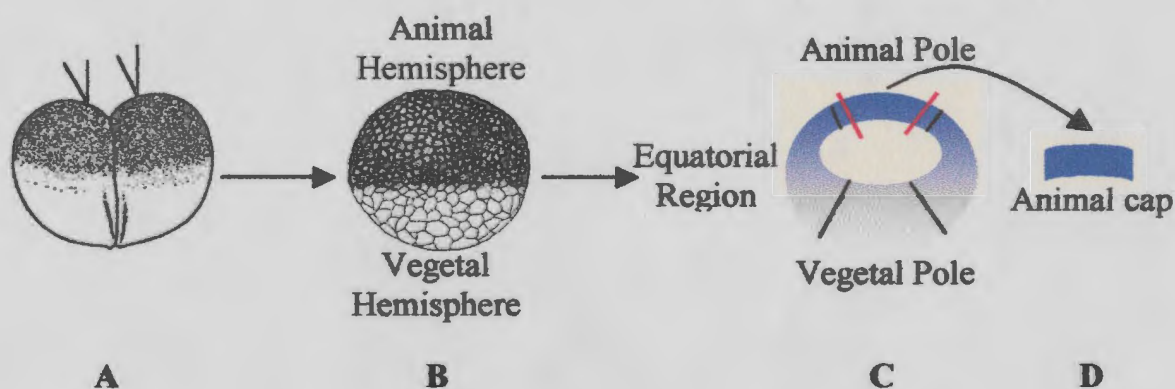


**Figure 2.2:** A diagrammatic representation of blastula Stage 8 *Xenopus* animal cap dissections. **A.** A Stage 2 embryo injected with *Xrel3* mRNA in each of the cells. **B.** A blastula Stage 8 embryo. **C.** A median section through a blastula embryo revealing three distinct regions. **D.** An isolated animal cap region of a blastula embryo after dissection.



### 2.4.2 Skin and tumour extractions

In other instances, *Xrel3* injected and control embryos were left to culture until tumours appeared on the injected embryos. The embryos were again transferred to 1.5% agar dishes containing NAM/2, where the tumours were dissected away from the embryo using fine forceps. Corresponding skin samples were extracted from control embryos from approximately the same regions as the tumours were found to occur in. Tumour and skin samples were taken from embryos at various stages in development (refer to Table 2.2). These sections were processed for RNA as soon as they were extracted (refer to section 2.5).

### 2.4.3 Limb bud amputations

Tadpoles at around Stages 52-53 in development (Figure 2.3; refer to Table 2.2) were anaesthetized in a 1:5000 dilution of MS222 dissolved in Holfreter's solution (60mM NaCl, 0.6mM KCl, 0.9mM CaCl<sub>2</sub>, 0.2mM NaHCO<sub>3</sub>). Hind limb buds were amputated by grasping the limb buds with a pair of forceps and slicing with a sharp, fine ophthalmological scalpel (Fisher). Amputated limb buds were then processed for RNA extraction (refer to section 2.5).

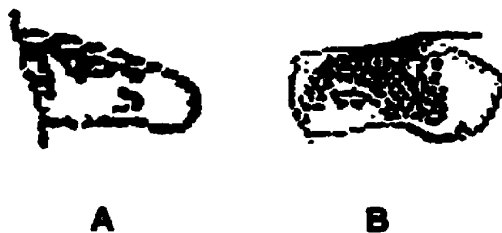


**Figure 2.3:** Two *Xenopus* hind limb buds as staged according to Nieuwkoop and Faber (1969). A. A stage 52 hind limb bud. B. A stage 53 hind limb bud.

## **2.5 RNA extraction**

Two whole embryos, 15-20 skin and tumour samples, 10-12 animal caps and 8-10 limb buds, at the appropriate stages, were transferred to 1.5ml eppendorf tubes containing 200 $\mu$ l of NETS (100mM sodium chloride, 10mM ethylenediamine tetraacetic acid (EDTA), 10mM Tris-HCl, pH 8.0 and 0.2% sodium dodecyl sulfate) plus 10 $\mu$ l of 20mg/ml Proteinase K (Boehringer Mannheim) and homogenized with a micropipette. In the case of the limb buds, a glass homogenizing rod was used to help break up the tissue. In some instances the homogenates were not used immediately and were stored at -70°C. Those homogenates that were frozen were allowed to thaw out on ice before use. They were then transferred to a 50-60°C Fisher H<sub>2</sub>O bath and left to incubate for 30 minutes, after which 200 $\mu$ l of buffer saturated phenol and 20 $\mu$ l of 2M sodium acetate, pH 5.1 were added. The tubes were then vortexed and centrifuged, in an IEC Micromax Digital microcentrifuge, at RT for 5 minutes at 13200 revolutions per minute (rpm). The aqueous phase was extracted and 200 $\mu$ l of isopropanol added to it. The tubes were then placed at -70°C for a minimum of 30 minutes to allow for precipitation. A pellet of nucleic acids was obtained after centrifugation at 4°C for 10 minutes in a Fisher Scientific Model 235C Microcentrifuge. The pellets were washed with 70% ethanol and vacuum dried briefly.

In order to remove DNA present in the samples, the dried pellets were resuspended in 50 $\mu$ l of Diethyl Pyrocarbonate (DEPC, Sigma) treated distilled H<sub>2</sub>O (dH<sub>2</sub>O) plus 50 $\mu$ l of 5M lithium chloride and left to incubate on ice for a minimum of 1 hour, after which they were centrifuged at 4°C for 15 minutes to obtain a pellet. Again the pellets were washed with 70% ethanol and vacuum dried. The pellets were then

resuspended in 39 $\mu$ l of DEPC-treated dH<sub>2</sub>O on ice. To remove remaining traces of DNA, 0.1U (1 $\mu$ l) of RNAGuard RNase inhibitor (Pharmacia), 5 $\mu$ l 10X transcription buffer (400mM Tris-HCl, pH 7.5, 60mM magnesium chloride, 20mM Spermidine; Gibco BRL) and 5U (5 $\mu$ l) RQ1 RNase free DNase were added. The tubes were vortexed, centrifuged briefly and left to incubate in a 37°C Fisher H<sub>2</sub>O bath for 20-30 minutes. The final volume of each tube was brought up to 100 $\mu$ l by adding 50 $\mu$ l of DEPC-treated dH<sub>2</sub>O and phenol/chloroform extracted with equal volumes of buffer saturated phenol and H<sub>2</sub>O saturated chloroform (100 $\mu$ l of each). The remaining aqueous layer was then precipitated with 2.5 volumes of 95-100% ethanol, one tenth of a volume of 3M sodium acetate, pH 5.2 and 0.02mg (1 $\mu$ l) of glycogen at -20°C for a minimum of 2.5 hours. Tubes were centrifuged at 4°C for 10 minutes at 13200rpm. The ethanol supernatants were removed and the pellets washed in 70% ethanol. Once vacuum dried, the pellets were resuspended in 10 $\mu$ l of DEPC dH<sub>2</sub>O and stored at -70°C. The concentration and integrity of the RNA was always checked before use through a combination of optical density readings at a wavelength of 260(OD<sub>260</sub>) and gel electrophoresis. The presence of two distinct bands on an agarose gel, one around 1650bp and the other around 850bp, corresponds to the 28s and 18s subunits respectively and indicated that the RNA was in tact and had not degraded.

## **2.6 Reverse Transcription Polymerase Chain Reacion (RT-PCR)**

### **2.6.1 Reverse transcription of isolated RNA**

cDNA was synthesized (Figure 2.4) from about 1 $\mu$ g of extracted RNA, which was diluted to a final volume of 10 $\mu$ l with DEPC dH<sub>2</sub>O in 0.5ml eppendorf tubes. If the RNA

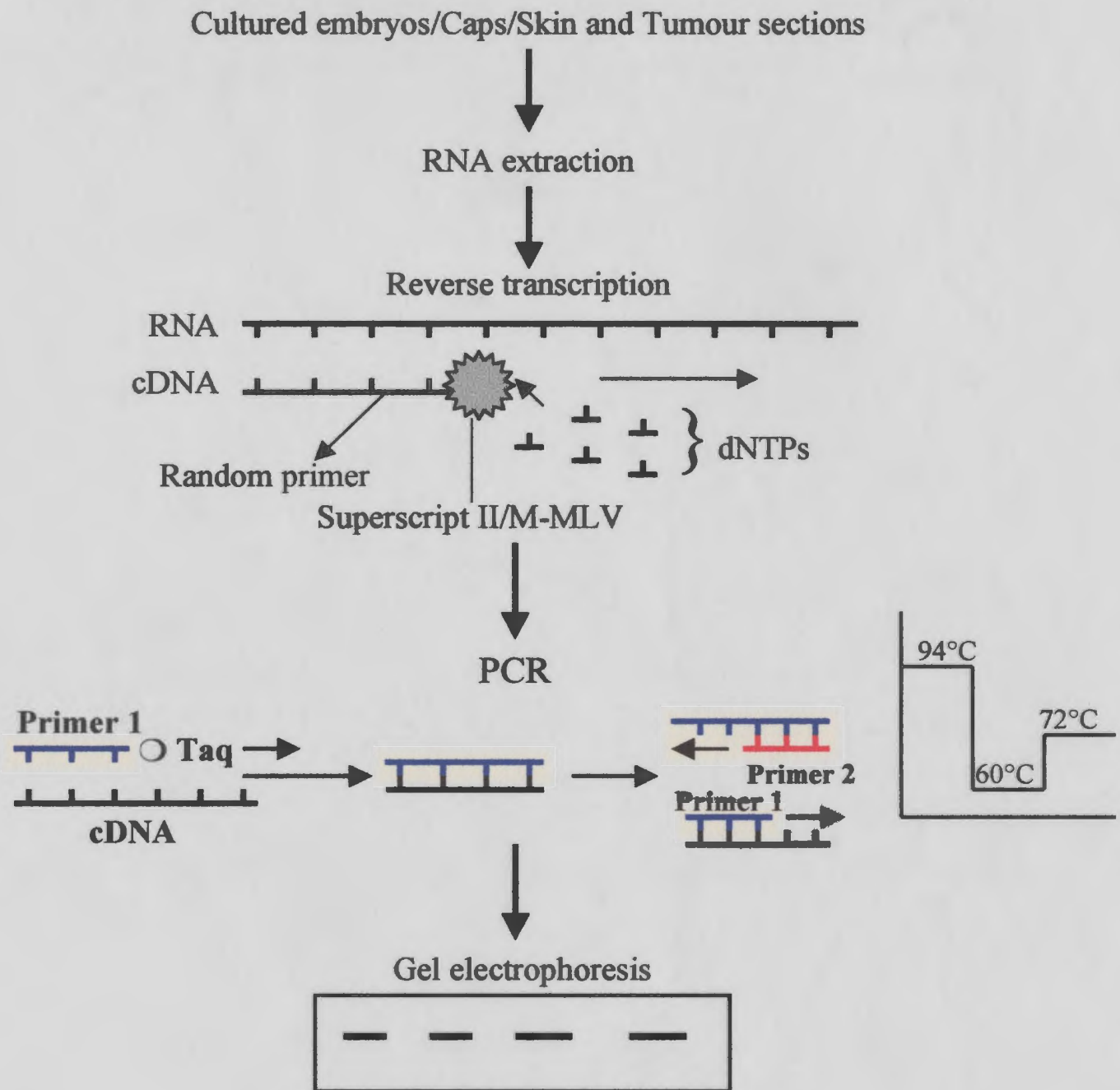


**Figure 2.4:** A schematic diagram outlining RT-PCR analysis

was stored at  $-70^{\circ}\text{C}$  before use, it was first thawed on ice. Once resuspended, the RNA was denatured at  $65^{\circ}\text{C}$  in a  $\text{H}_2\text{O}$  bath for 10 minutes, after which the RNA was removed and immediately placed on ice to prevent internal pairing of RNA strands. To each tube of RNA, a reverse transcription mixture of RNAGuard RNase inhibitor (Pharmacia), 5X first strand buffer (Gibco BRL), deoxyribonucleotide triphosphates (dNTPs, Pharmacia), random hexanucleotide primers (Boehringer Mannheim), DTT (Gibco BRL) and Superscript II or M-MLV (Gibco BRL) were added (see Table 2.3 for volumes and final concentrations of each). The reaction mixtures were then incubated for 1 hour at  $38^{\circ}\text{C}$ , followed by a 10 minute incubation at  $95^{\circ}\text{C}$  in order to inactivate the reverse transcriptase enzyme. Once made, the cDNA samples were stored at  $-20^{\circ}\text{C}$ .

**Table 2.3: Reverse transcription reaction mixture volumes and final concentrations in a  $22\mu\text{l}$  total**

<b>Volume of Reverse Transcription Components per Reaction</b>	<b>Final Concentration per <math>22\mu\text{l}</math> Total Volume</b>
$1\mu\text{l}$ RNAGuard (100U/ml)	4.5U/ml
$4\mu\text{l}$ 5X First Strand Buffer	45.5mM Tris-HCl 68.2mM KCl 2.7mM $\text{MgCl}_2$
$2\mu\text{l}$ 10mM dNTPs	0.23mM of each of dATP, dCTP, dGTP and dTTP
$2\mu\text{l}$ $0.1\mu\text{g}/\mu\text{l}$ random primers	$9.1\text{ng}/\mu\text{l}$
$2\mu\text{l}$ 0.1M DTT	9.1mM
$1\mu\text{l}$ Superscript II (200U/ $\mu\text{l}$ ) or M-MLV	$9.1\text{U}/\mu\text{l}$
$10\mu\text{l}$ RNA in DEPC $\text{dH}_2\text{O}$	-

## **2.6.2 PCR of reverse transcription products (cDNAs)**

Amplification reactions (Figure 2.4) were assembled into thin-walled 0.5ml eppendorf tubes, using the following components: 10x PCR buffer (Gibco BRL), magnesium chloride (Gibco BRL), dNTPs (Pharmacia), 1 set of specific primers (Table 2.5), platinum Taq DNA polymerase (Gibco BRL), cDNA sample, and dH<sub>2</sub>O (Table 2.4).

Each reaction mixture was vortexed briefly and 50 $\mu$ l of light mineral oil added as a layer on top of the reaction mixture to prevent evaporation during the thermocycling program. Each reaction tube was assembled into a Perkin Elmer Thermal Cycler. The general PCR thermocycling program used was as follows:

- 1 cycle:        94°C, 5 minutes for activation of enzyme
- 30 cycles:     57-60°C, 1 minute for annealing of primers  
                  72°C, 1 minute for primer extension  
                  94°C, 1 minute for denaturation
- 1 cycle:        57-60°C, 1 minute for annealing of primers  
                  72°C, 7 minutes for primer extension

For the Histone primer set, however, 23 rather than 30 cycles was used.

Once the program was completed the PCR products were stored at 4°C until run on an 1.8-2.0% agarose gel.

**Table 2.4: Volumes and final concentrations of the PCR components in a 50 $\mu$ l reaction mixture**

<b>Volume of PCR Components Added per Reaction</b>	<b>Final Concentration of PCR Components per 50<math>\mu</math>l Volume of Reaction</b>
5 $\mu$ l 10x PCR buffer	50mM KCl 10mM Tris-HCl (pH 9.0) 0.1% Triton X-100
1.5 $\mu$ l 50mM MgCl <sub>2</sub>	1.5mM
4 $\mu$ l 10mM dNTPs	200 $\mu$ M of each of dATP, dCTP, dGTP and dTTP
2 $\mu$ l Primer #1 (100 $\mu$ g/ml)	4 $\mu$ g/ml
2 $\mu$ l Primer #2 (100 $\mu$ g/ml)	4 $\mu$ g/ml
0.2 $\mu$ l Platinum <i>Taq</i> DNA polymerase (5U/ $\mu$ l)	0.02U/ $\mu$ l
2-4 $\mu$ l cDNA	-
dH <sub>2</sub> O up to 50 $\mu$ l	-

**Table 2.5: Oligonucleotide Primers used for RT-PCR Assay**

Primer Name	Primer Sequence	Expected Size of Product	References
API	5' CTGATCCATG 3'	NA	-
AP2	5' CTGCTCTCAG 3'	NA	-
Cephalic Hedgehog (Chh) U Cephalic Hedgehog (Chh) D	5' TTCTGCTATCTGCTGCGGG 3' 5' AACCTTTCTGAGCCCCGGTG 3'	196bp	Ekker et al., 1995
Crp 18 Crp 20	5' GCAGTTCCATCACATCCA 3' 5' GCAATTGGAAACCTGCCCCAC 3'	153bp	Yang et al., 1998
Cardiac Muscle Actin U Cardiac Muscle Actin D	5' GCTGACAGAATGCAGAAAG 3' 5' TTGCTTGGAGGAGTGTGT 3'	666bp	Mohun et al., 1986
EfgR(i) U EfgR(i) D	5' TGAACCGGCGATGGGAGACC 3' 5' GCCTTATAGTTGTTGGGCAG 3'	329bp	Issacs et al., 1992
EfgR(ii) U EfgR(ii) D	5' CGGACGGAAAGGATAAATGAC 3' 5' CGTGGCAAGAAATGGGTGAG 3'	315bp	Issacs et al., 1992
Fgf-8 U Fgf-8 D	5' GAACATACATCACCTCCATCC 3' 5' CCTTCCATTAGTCTTCCCA 3'	315bp	Christen et al., 1997
Oli1 U Oli1 D	5' GGATGGCCTGATGACTTGG 3' 5' AGTTCGGTTTGGTGCTTG 3'	424bp	Ruiz i Altaba et al., 1996
Oli3 U Oli3 D	5' ATGAACAATGAGCAAGCCCG 3' 5' ACATTCCAAACATGCCCGGC 3'	270bp	Marine et al., 1996
Histone - H4-1 - H4-2	5' CGGATAACATTCAGGTATCACT 3' 5' ATCCATGCCCGTAACGTCTTCCT 3'	191bp	Niehrs et al., 1994
Hox B9 U Hox B9 D	5' GAGGCCACAGTGAATGTTGG 3' 5' ATCCGCTCTGCCAATTCCT 3'	269bp	Wright et al., 1990
Nrp-1 U Nrp-1 D	5' GGGTTTCTTGAACAAGC 3' 5' ACTGTUCAGGAACACAAG 3'	284bp	Richter et al., 1990
Otx-2 U Otx-2 D	5' CGGGATGGAATTGTTGCA 3' 5' TTGAACCAGACCTGGACT 3'	201bp	Pannese et al., 1995
P1 P2	5' ACGCACTGACTGTCCC 3' 5' CAATGGTGAGCAGCTG 3'	446bp	Yang et al., 1998
Radical Fringe (r-fng) U Radical Fringe (r-fng) D	5' CCAAACACCAAAACAAGGCG 3' 5' CCCCCAAGAAACCAACAGTA 3'	394bp	Wu et al., 1996
Sonic Hedgehog (Shh) U Sonic Hedgehog (Shh) D	5' TCTTCAGTCTCACCACCAAG 3' 5' GGCTCTTCCCTTTAGTGTG 3'	308bp	Ekker et al., 1995
Twist U Twist D	5' GTCCAGCTCGCCAGTCTC 3' 5' CCGGTGCTGCTCGCCTTC 3'	168bp	Hopwood et al., 1989
TllAC	5' TTTTITTTTAC 3'	NA	-
Wnt-7a U Wnt-7a D	5' GAAAACCTGTTGGACCAACC 3' 5' CCTCTCCCAACACATCA 3'	303bp	Wolda et al., 1992
XAG-1 U XAG-1 D	5' GTATGATGTGGGACAGTTCC 3' 5' CGTCCTGCTCTCCAGGTAG 3'	199bp	Sive et al., 1989
DDFrag (A1.1aT) U DDFrag (A1.1aT) D	5' AACCAATGCTTCCAGTCCCT 3' 5' AGCAGAAGATAAGTCCAGGG 3'	304bp	-



## **2.7 Differential display**

The differential display technique was used to screen mRNA pools for differential gene expression in *Xenopus* skin and tumour samples (Paterno et al., 1997; Liang and Pardee, 1992). This approach involved a combination of reverse transcription, PCR and denaturing polyacrylamide gel electrophoresis (Figure 2.5). Each skin and tumour set, representing three stages in *Xenopus* development (refer to Table 2.2), were analysed two to three times with each of five primer combinations used for PCR amplification.

### **2.7.1 Reverse transcription of skin and tumour RNA**

Skin and tumour RNA (made as previously described) was diluted to a final concentration of approximately 0.1 µg/µl with DEPC dH<sub>2</sub>O. One of four possible degenerate anchored oligo(dT) primers, T<sub>11</sub>AC, was added to the mixture. The reaction mix was then heated to 70°C for 10 minutes, followed by a quick chill on ice for 5 minutes. A reverse transcription mixture of 5X first strand buffer, dNTPs, DTT, RNAGuard RNase inhibitor, M-MLV and DEPC dH<sub>2</sub>O was added to each tube of RNA (see Table 2.6 for final volumes and concentrations). The samples were then incubated for 1 hour in a 37°C H<sub>2</sub>O bath. The resulting cDNA was stored at -20°C.

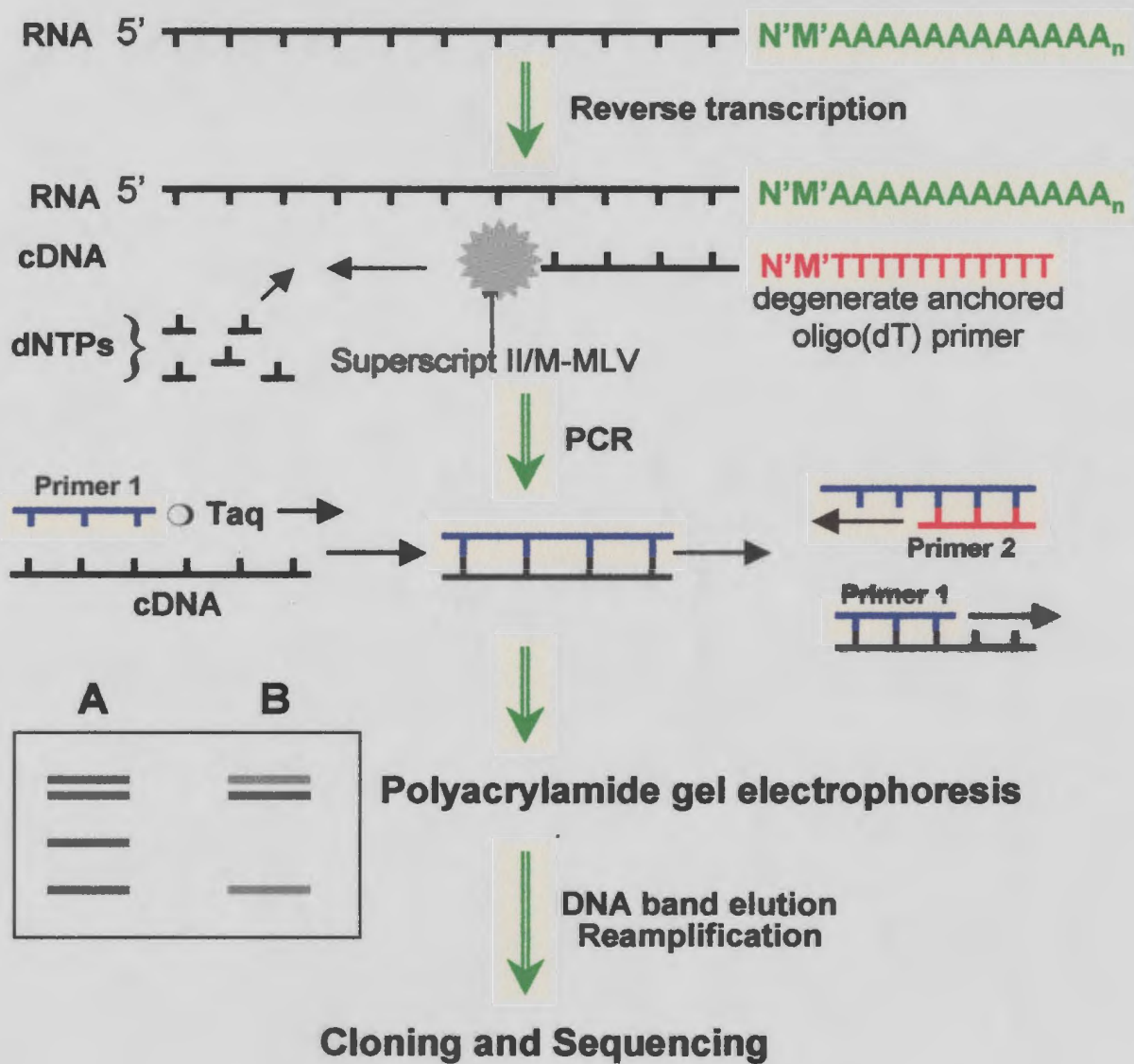


Figure 2.5: A schematic representation of Differential Display

**Table 2.6: Volumes and final concentrations of the differential display reverse transcription components in a 42µl reaction mixture**

<b>Components of Reverse Transcription</b>	<b>Final Concentration of Reverse Transcription Components per 42µl Total Volume</b>
17µl RNA (0.1µg/µl)	0.04µg/µl
2µl 100ng/µl T <sub>11</sub> AC primer	4.8ng/µl
8µl 5X first strand buffer	47.6mM Tris-HCl 71.4mM KCl 2.9mM MgCl <sub>2</sub>
2µl 10mM dNTPs	0.12mM each of dATP, dCTP, dGTP and dTTP
2µl 100mM DTT	4.8mM
1µl RNAGuard (100U/ml)	2.4U/ml
2µl M-MLV (200U/µl)	9.5U/µl
6µl DEPC dH <sub>2</sub> O	-

**2.7.2 PCR of skin and tumour cDNA**

For each skin and tumour cDNA sample, five primer combinations were used (AP<sub>1</sub>/AP<sub>1</sub>, AP<sub>1</sub>/AP<sub>2</sub>, AP<sub>2</sub>/AP<sub>2</sub>, T<sub>11</sub>AC/AP<sub>1</sub>, T<sub>11</sub>AC/AP<sub>2</sub>), involving two arbitrary decamer primers (AP<sub>1</sub> and AP<sub>2</sub>) and the anchored oligo(dT) primer (see Table 2.5 for primer sequences). For each primer set a 20µl reaction mix was prepared (see Table 2.7 for components and final concentrations).

**Table 2.7: Volumes and final concentrations of the differential display PCR components in a 20 $\mu$ l reaction mixture**

<b>Components of Differential Display PCR</b>	<b>Final Concentration of PCR Components per 20<math>\mu</math>l Total Volume</b>
2 $\mu$ l RT mix	-
2 $\mu$ l 10X PCR buffer	50mM KCl 10mM Tris-HCl (pH 9.0) 0.1% Triton X-100
0.6 $\mu$ l 50mM MgCl <sub>2</sub>	1.5mM MgCl <sub>2</sub>
1.6 $\mu$ l 2.5 $\mu$ M each dNTP	0.2 $\mu$ M each dNTP
2 $\mu$ l 2 $\mu$ M AP <sub>1</sub> or AP <sub>2</sub>	0.2 $\mu$ M AP <sub>1</sub> or AP <sub>2</sub>
2 $\mu$ l 10 $\mu$ M T <sub>11</sub> AC or 2 $\mu$ M AP <sub>1</sub> or 2 $\mu$ M AP <sub>2</sub>	1 $\mu$ M T <sub>11</sub> AC or 0.2 $\mu$ M AP <sub>1</sub> or AP <sub>2</sub>
1 $\mu$ l [ $\alpha$ - <sup>35</sup> S]dATP	-
0.2 $\mu$ l Platinum <i>Taq</i> DNA polymerase (5U/ $\mu$ l)	0.05U/ $\mu$ l
dH <sub>2</sub> O up to 20 $\mu$ l	-

The reaction mixtures were overlain with mineral oil and subjected to the following thermocycling program:

40 cycles: 94°C, 30 seconds for denaturation  
40°C, 2 minutes for annealing  
72°C, 30 seconds for extension

1 cycle: 72°C, 5 minutes for extension

PCR products were stored at 4°C until run on a 6% polyacrylamide denaturing gel.

### 2.7.3 Polyacrylamide gel electrophoresis

The radiolabelled differential display PCR products were mixed with sequencing gel loading buffer (for every 3.5 $\mu$ l of PCR product, 2 $\mu$ l of loading buffer was added and approximately 4 to 5  $\mu$ l was then added to the gel wells) and run on 6%

acrylamide/bisacrylamide, 8M urea denaturing sequencing gels. For 100ml of sequencing gel mix, 48g Urea, 15ml 40% acrylamide/bisacrylamide (BioRad, Mississauga, Ontario), 10ml 10X TBE and dH<sub>2</sub>O up to 100ml is required. A [ $\gamma^{32}$ P]ATP (Mandel Scientific Ltd., Guelph, Ontario) labelled 100bp ladder was also run as a molecular weight marker (refer to section 2.7.3.1). Polymerization of the gels was initiated by the free radicals supplied by 10% ammonium persulfate (APS; 0.1g in 1ml dH<sub>2</sub>O) and stabilized by N, N, N', N' - tetramethylethylenediamine (TEMED, BioRad; for 75-80ml of sequencing mix, added 440 $\mu$ l 10% APS and 44 $\mu$ l TEMED). The gels were run at a constant power of 55 Watts with 1X TBE buffer (89mM Tris base, 89mM boric acid and 2mM EDTA, pH 8.0) and left to run for approximately 3-4 hours or until the xylene dye front had migrated to the bottom. The gels were then transferred onto 3mm Whatman paper (Millipore, Mississauga, Ontario). The gels were dried on a Bio-Rad Model 583 gel dryer at 80°C for approximately 1 hour, packed in a Fisher Biotech Autoradiography Cassette - FBXC 810, with Dupont REFLECTION Autoradiography Film and left at RT for about 2-3 days.

Exposed films were developed with a Kodak RP X-OMAT Processor within the Radiology Department of the Health Sciences Centre.

#### *2.7.3.1 100bp end-labelling reaction*

In a 1.5ml eppendorf tube, assembled the following components: 0.5 $\mu$ l of 500 $\mu$ g/ml dephosphorylated DNA fragments (100bp ladder, New England Biolabs), 5 $\mu$ l 5X forward reaction buffer (Gibco BRL), 10U (1 $\mu$ l) T4 polynucleotide kinase (Gibco BRL), 2.5 $\mu$ l [ $\gamma^{32}$ P]ATP and dH<sub>2</sub>O up to 25 $\mu$ l. After brief mixing and centrifuging,

incubated the reaction in a 37°C Fisher H<sub>2</sub>O bath for 30 minutes. The reaction was stopped by adding EDTA to a final concentration of about 5mM (approximately 0.25μl of 0.5M EDTA). The ladder was then precipitated with one tenth of a volume of 3M sodium acetate, pH 5.2 (2.5μl), 2.5 volumes of 95-100% ethanol (62.5μl) and 0.02mg tRNA (2μl, Boehringer Mannheim) by incubating at -20°C for 1 hour. A pellet was obtained after centrifuging for 5-10 minutes in a Fisher Scientific Model 235C Microcentrifuge. The supernatant was removed and the pellet washed with 70% ethanol. The pellet was air dried briefly and then resuspended in 40μl dH<sub>2</sub>O. To ensure that the 100bp ladder had been labelled properly, 1μl was taken for analysis and the number of counts per minute (cpm)/μl was determined with the use of a scintillation counter. The labelled ladder was stored at -20°C.

#### **2.7.4 Differential display DNA recovery**

Differential display bands of interest were excised from the gels with a razor blade and placed in 0.5ml eppendorf tubes with holes punctured in the bottoms. The 0.5ml eppendorf tubes were then placed in 1.5ml eppendorf tubes in which the lids had been removed. The gel slices were soaked in 100μl of dH<sub>2</sub>O for 30 minutes and then moved to a boiling H<sub>2</sub>O bath where they remained for 20 minutes. After centrifugation at 13200rpm for 5 minutes, the supernatants that had collected at the bottoms of the 1.5ml eppendorf tubes were transferred to fresh 1.5ml tubes. The supernatants were then precipitated with 2.5 volumes of 95-100% ethanol, one tenth of a volume of 3M sodium acetate, pH 5.2 and 0.02mg (1μl) of glycogen at -20°C for approximately 2-3 hours. The

DNA was recovered after centrifugation at 4°C for 15 minutes and then washed with 70% ethanol. The DNA pellets were vacuum dried briefly and resuspended in 10µl of dH<sub>2</sub>O.

#### **2.7.5 Re-amplification of eluted differential display bands**

To ensure that the extraction of DNA from the differential display gels had been successful, 4µl of the eluted DNA sample was PCR amplified in a 50µl reaction volume.

The same primer set and PCR conditions were used as in the original differential display PCR amplification (section 2.7.2), except that a mixture of 250µM of each dNTP (20µM final of each dNTP) was added, the <sup>35</sup>S isotope (Mandel) was omitted and 30 instead of 40 cycles were used in the thermocycling program.

The resulting PCR products were run on a 1.5% agarose gel stained with ethidium bromide and the remaining products were stored at 4°C.

#### **2.7.6 Characterization of differential display PCR products**

Once the differential display bands of interest had been successfully eluted from the gel it was necessary to try and identify what they were. The first step in trying to characterize these DNA fragments was to identify their sequences. In order for this to be done the eluted DNA fragments had to first be cloned into a suitable vector, followed by a DNA minipreparation and finally DNA sequencing.

##### **2.7.6.1 TA cloning**

The eluted differential display DNA was PCR amplified and so a TA Cloning®

Kit with pCR<sup>®</sup> 2.1 vector (Invitrogen, CA, USA) was used (Figure 2.6). TA Cloning was chosen because the *Taq* DNA Polymerase used in the PCR amplifications has a nontemplate-dependent activity, which causes a single deoxyadenosine (A) to be added to the 3' ends of PCR products. The pCR<sup>®</sup> 2.1 vector supplied with the TA Cloning kit is linearized and has a single 3' deoxythymidine (T) residue overhang at both ends. This, therefore, allows PCR product inserts to ligate with cohesive ends into the vector.

#### **I. Ligation:**

The re-amplified, eluted differential display products were ligated into the pCR<sup>®</sup>2.1 vector in a 1:1 (vector:insert) ratio. The ligation reaction mix contained the following components: approximately 4.5-5ng fresh (less than 24 hours old) PCR product, 1μl 10X ligation buffer, 50ng(2μl) pCR<sup>®</sup>2.1 vector, 1μl T<sub>4</sub> DNA ligase and sterile dH<sub>2</sub>O up to a total volume of 10μl. The ligation reaction was then incubated overnight at 14°C.

#### **II Transformation:**

Once the PCR products were successfully ligated with the vector, the ligation products were then transformed into INVαF' one-shot competent cells, which were also provided with the kit.

After incubation, the ligation reactions were placed on ice. For each ligation reaction, one vial of 50μl INVαF' one-shot competent cells was thawed on ice. To each vial of competent cells 2μl of 0.5M β-mercaptoethanol was added and mixed gently by stirring with the pipette tip. This was followed by the addition of 2μl of ligation product and again was mixed gently with stirring. The vials were incubated on ice for 30 minutes before being heat shocked at 42°C for exactly 30 seconds. The vials were then placed on



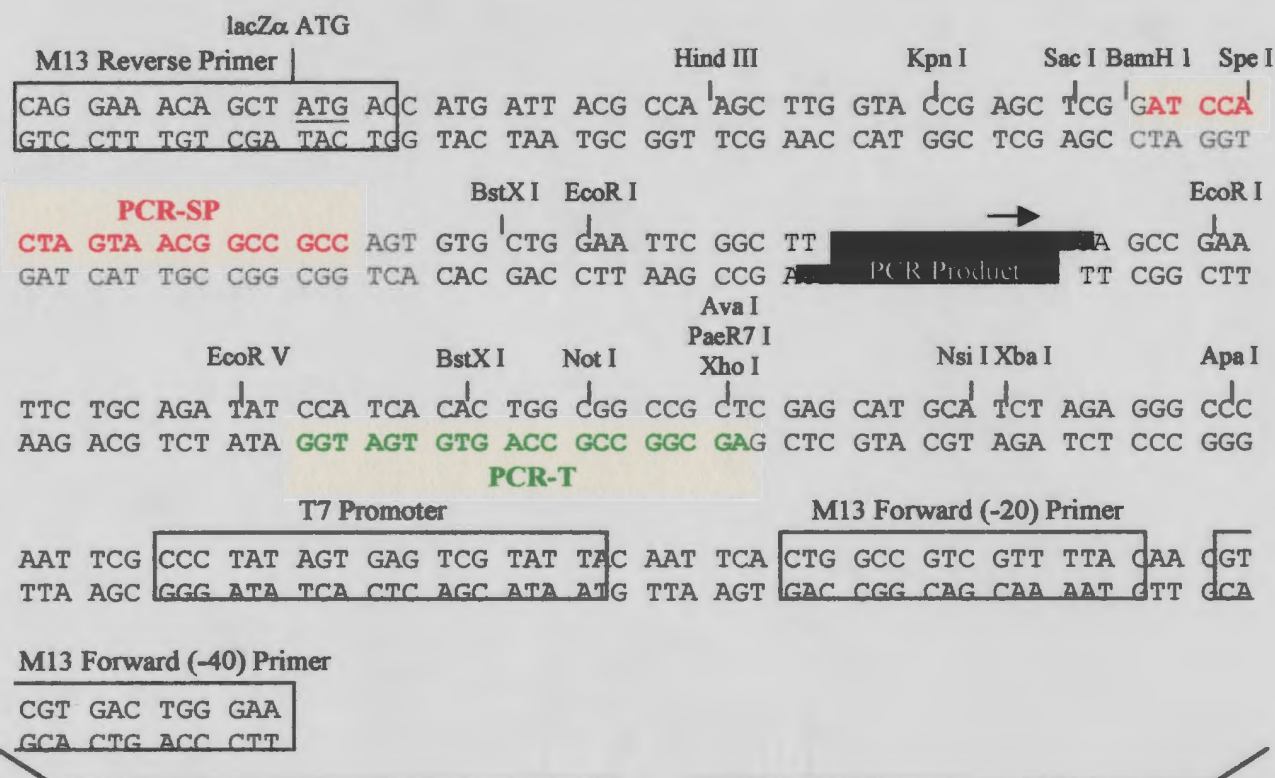


**Figure 2.6:** Map of the TA cloning pCR2.1 vector, showing the sequence of the multiple cloning site and the position of the DNA insert. The red and green highlighted regions, either side of the insert, represent the primers used in the sequencing reactions.

ice for a further 2 minutes. Addition of 250µl RT SOC medium to each vial followed and the vials were shaken horizontally at 37°C for 1 hour at 225rpm. The transformants were then grown overnight at 37°C on LB agar plates containing 100µg/ml ampicillin (sigma).

### **III Colony screening:**

The resulting white colonies from the transformation were then PCR screened to check for the insert of interest. From each plate, 9-10 colonies were randomly selected and analysed using the differential display primer AP1. Each reaction mix contained 2µl 10X PCR buffer, 0.6µl 50mM MgCl<sub>2</sub>, 1.6µl 250µM each dNTPs, 4µl 2µM AP1 primer, 0.2µl Platinum Taq and dH<sub>2</sub>O up to 20µl. The PCR reaction was carried out using 30 cycles of 94°C for 30 seconds, 40°C for 2 minutes and 72°C for 30 seconds and 1 cycle of 72°C for 10 minutes. The size and concentration of the PCR products were then analysed via agarose gel electrophoresis. Estimation of concentration involved comparing the PCR products with the 1650bp band of the 1Kb plus ladder (Gibco BRL), 1µl of which was run along side as a marker, as the 1650bp band is of a known concentration of 80ng.

#### ***2.7.6.2 DNA minipreparation***

Of the screened colonies containing the inserts of interest, two colonies representing each DNA band that was originally cut out of the differential display gel, were grown up overnight at 37°C in 5-6ml of LB broth containing 100µg/ml ampicillin. A glycerol stock was made from 1ml of the bacterial culture and was stored at -70°C.

The remaining culture was used for isolation and purification of the transformed DNA. The Wizard®Plus SV Miniprep DNA Purification System (Promega) was used. The remaining 4-5ml of bacterial culture were pelleted at 4°C for 10 minutes at 10,000 x g. The supernatant was poured off and blotted upside down on a paper towel to remove any excess fluid. The cells were resuspended in 250µl of Cell Resuspension Fluid. At this time the suspensions were transferred to 1.5ml eppendorf tubes and 250µl of Cell Lysis Solution was added. Mixing involved inverting the tubes four times, after which the cell suspensions were allowed to incubate at RT for approximately 1-5 minutes, until they had cleared. Alkaline protease was then added, 10µl to each tube, and mixing again involved inverting four times. The tubes were allowed to incubate at RT for 5 minutes before 350µl of Neutralization Solution was added, with inversion 4 times to mix. The bacterial lysates were then centrifuged at RT for 10 minutes at 10,000rpm. The resulting cleared lysates were transferred to miniprep spin columns attached to 2ml collection tubes and centrifuged again at 10,000rpm for 1 minute at RT. The flowthrough was discarded and 750µl of Column Wash Solution was added to the spin columns. The samples were re-centrifuged at RT for 1 minute at 10,000rpm. The flowthrough was discarded again and 250µl of Column Wash Solution was added to each spin column. Re-centrifugation occurred for 2 minutes this time. The spin columns were transferred to fresh, sterile 1.5ml eppendorf tubes and the plasmid DNA was eluted in a final volume of 100µl, which was stored at -20°C. The concentration of the DNA was determined via agarose gel electrophoresis, as previously described.

### 2.7.6.3 DNA Sequencing

DNA sequencing was performed by the dideoxynucleotide (ddNTP) chain termination method (Sanger et al., 1977) with the use of the USB Sequenase Version 2.0 sequencing kit (Pharmacia). Approximately 4-5 $\mu$ g of plasmid DNA was used in the sequencing reactions. The reactions involved the use of the primers pCR-SP and pCR-T which were designed against the pCR<sup>®</sup>2.1 vector (Figure 2.6), as well as Manganese (Mn) buffer.

Sequencing was initiated with the assembly of 5 $\mu$ g miniprep plasmid DNA, 2 $\mu$ l 0.2N sodium hydroxide/0.2M EDTA solution (100 $\mu$ l 10N sodium hydroxide, 2 $\mu$ l 0.5M EDTA and 398 $\mu$ l dH<sub>2</sub>O) and dH<sub>2</sub>O up to 20 $\mu$ l. Each reaction was incubated at 37°C for 20 minutes. Precipitation followed with incubation at -70°C for 15 minutes, after the addition of 2.2 $\mu$ l 3M sodium acetate, pH 5.2 and 60 $\mu$ l 95-100% ethanol. Pellets were formed after centrifugation at 4°C for 20 minutes in a Fisher Scientific Model 235C Microcentrifuge. The supernatants were poured off, the pellets washed with 70% ethanol, vacuum dried and then resuspended in 7 $\mu$ l dH<sub>2</sub>O.

#### **L. Annealing:**

To each tube of resuspended DNA, 2 $\mu$ l of sequence reaction buffer was added, in addition to 1 $\mu$ l 10ng/ $\mu$ l SP or T primer. The reactions were then heated for 2 minutes in a 65°C H<sub>2</sub>O bath, after which the bath was cooled slowly at RT for approximately 15-30 minutes, until the temperature of the H<sub>2</sub>O in the bath had reached about 30°C. The bath, still containing the reactions, was then put on ice.

## **II Labelling:**

To each annealed primer-DNA reaction tube, the following components were added: 1µl DTT, 2µl diluted labelling mix (1µl mix and 4µl dH<sub>2</sub>O), 1µl <sup>35</sup>S-dATP, 1.75µl enzyme dilution buffer, 1µl Mn buffer and 0.25µl sequenase enzyme. The tubes were then incubated for 5 minutes at RT.

## **III Termination:**

To each set of four 37°C pre-heated tubes, containing 2.5µl of either ddATP, ddCTP, ddGTP or ddTTP, added 3.5µl of labelled reaction mix and incubated at 37°C for 5 minutes. To stop the reactions, 4µl of stop solution was added to each set of ddNTP tubes. Tubes were either stored at -20°C or run on 6% polyacrylamide denaturing gels immediately (see section 2.7.3). The gels were run at a constant power of 55 Watts with 0.5XTBE in the buffer chamber of the gel plate and 1M Sodium Acetate, made with 1XTBE, in the bottom chamber. The gels were left to run for about 2-3 hours or until the bromophenol blue dye front had migrated to the bottom. The gels were then fixed with 10% Methanol:10% glacial acetic acid before being transferred onto 3mm Whatman paper. The gels were dried and exposed to film as per section 2.7.3.

### *2.7.6.4 Sequence Analysis*

The sequences obtained were translated using a sequence analysis tool program from the University of Washington – Biological Information Resource (version 2.0). Further sequence analysis involved the use of the National Center for Biotechnology Information's (NCBI) BLAST (Basic Local Alignment Search Tool) program, in which the sequence query, either DNA or protein, is compared to GenBank/EMBL/DBJ

databases.

#### ***2.7.6.5 Primer design***

Primers specific to the differential display sequences obtained were designed with the use of the Oligo Tech, version 1.00 (Copyright © 1995; Oligos Etc.) and the Amplify, version 1.2 for Macintosh (Copyright © 1993) computer software packages. The Oligo Tech computer program assessed random 19-20bp stretches of DNA that were entered into the program for homodimerization, hairpin formation, GC content, melting temperature ( $T_m$ ) and internal stability. Once appropriate regions of DNA were selected for primer design, these sequences were then entered into the Amplify program to assess their annealing strength to the DNA template in a typical PCR reaction and also to check for multiple annealing sites within the DNA template. The primers were then sent to Oligos, Etc., where the primers were manufactured.

## Chapter 3: Results

### 3.1 Overexpression of *Xrel3* induces tumorigenesis

Synthetic *Xrel3* mRNA (cRNA) injected at 500pg-1ng at the two-cell stage has been previously shown to produce tumour-like lesions on the surfaces of embryos when injected into animal and vegetal regions of *Xenopus laevis* (see Figure 1.5; Yang et al., 1998). The tumours that form from animal pole injection, however, are not visible on the surface of the embryo until early neurula stage (~St. 15). These tumours persist through to tail bud stages but eventually regress and disappear. Initially St. 20 tumours were chosen for analysis because they were the largest in size and the easiest to dissect.

To determine whether injected *Xrel3* mRNA was present in the tumours, RT-PCR was performed on RNA extracted from 20 tumours and from 20 control-injected epidermal samples using primers specific to the coding region of *Xrel3*. Figure 3.1A is representative of three experiments and clearly shows that *Xrel3* is significantly upregulated in the tumour sections. Endogenous levels of *Xrel3* (*Xrel3<sub>e</sub>*) were also tested using primers specific to the non-coding region of *Xrel3*, not found in *Xrel3* cRNA. Figure 3.1A shows that the levels of endogenous *Xrel3* were not affected by *Xrel3* mRNA injection. Thus *Xrel3* does not activate itself in embryos.

### 3.2 Tissue origin of the tumours

To determine what embryonic tissue type the tumours represent, I performed RT-PCR using primers specific to terminally differentiated tissues including muscle mesoderm (cardiac actin), neural tissue (*nrp-1* and *hox b9*) and epidermis (epidermal keratin). Figure 3.1B, representative of three experiments, reveals that no or very low basal levels

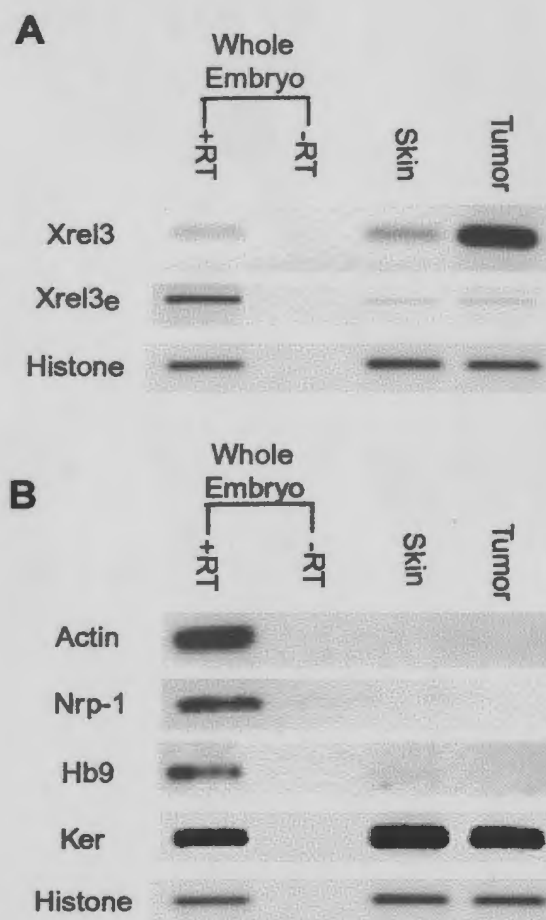


**Figure 3.1:** Expression analysis of Xrel3-induced St. 20 tumours as observed through RT-PCR. A. Twenty tumour and twenty skin samples were excised and analyzed for the expression of total exogenous (Xrel3) and endogenous (Xrel3<sub>e</sub>) Xrel3. B. mRNA expression levels from twenty tumour and skin samples of various terminally differentiated tissues - muscle mesoderm (cardiac actin), neural (Nrp-1 and HoxB9) and epidermis (epidermal keratin). Histone levels were used as a standard for RNA loading.



of *hoxb9*, *cardiac actin*, and *nrp-1* are expressed equivalently in both skin and tumour sections. *Epidermal keratin*, on the other hand, was very highly expressed in both skin and tumour sections, indicating that the tumours were likely of epidermal type.

### **3.3 *Xrel3*-induced tumours express body patterning genes**

The initial analysis of *Xrel3*-induced tumours for genes that are regulated by *Xrel3* came from three lines of evidence. Firstly, epidermal tumours resembling our *Xrel3*-induced tumours were observed when *gli1* was overexpressed in *Xenopus* embryos (Dahmane et al., 1997). Secondly, both Gli1 and Shh have been associated with cellular proliferation and certain types of cancer, in particular, the skin cancer Nevroid Basal Cell Carcinoma (for reviews, see Matise and Joyner, 1999; Ruiz i Altaba, 1999; Wicking et al., 1999; Britto et al., 2000). Finally, cRel is required to activate Twist and Shh signalling in chick limb development (Kanagae et al., 1998 and Bushdid et al., 1998). These lines of evidence suggested that perhaps *Xrel3* is promoting cell proliferation via the Shh signalling pathway in the *Xrel3*-induced tumours. Both *gli1* and *shh* were, therefore, analyzed for their expression levels and were found to be consistently upregulated in the St. 20 tumours of five separate experiments (Figure 3.2). Based on the chicken limb bud evidence, *twist* was also analyzed for expression and it too was consistently upregulated five times in the St. 20 tumours (Figure 3.2).

Interestingly, the normal expression patterns of *gli1*, *shh* and *twist* in *Xenopus* overlaps that of *Xrel3* in neurula stage embryos. Our previous work showed expression of *Xrel3* mRNA in the notochord, forebrain and dorsal aspect of the mid-hind brain in

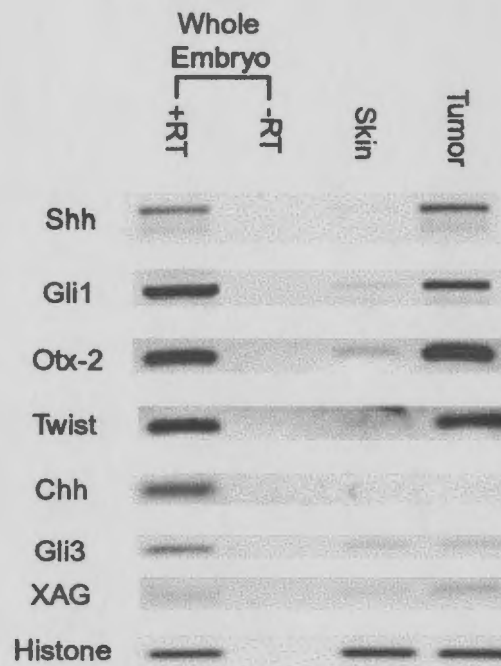


**Figure 3.2:** Expression of various body patterning genes in St. 20 *Xrel3*-induced tumours as observed through RT-PCR analysis. RNA was extracted and analyzed for expression from each of twenty excised skin samples and tumours. Histone levels were used as a standard for RNA loading.

late neurula and larval stage embryos (Yang et al., 1998). *Shh* is expressed in the notochord, has been shown to have activity in the presumptive hindbrain and is involved in patterning the ventral forebrain (Weed et al., 1997; Rubenstein and Beachy, 1998). *Gli1* is a downstream target of the Shh signalling pathway and is expressed in the floor plate of the neural tube. It is also expressed in the developing brain, where it is involved in inducing neuron differentiation in the forebrain, midbrain and hindbrain (Lee et al., 1997; Ruiz i Altaba, 1998). *Twist* is a mesodermal marker that is normally expressed in the non-muscle mesoderm (Stoetzel et al., 1998). The expression of *otx-2* in the St. 20 tumours was also analyzed because *otx-2* is an anterior marker that is normally expressed in the head region of *Xenopus* embryos (Pannese et al., 1995; Andreazzoli et al., 1997; for review, see Acampara et al., 2000). In five independent experiments, RT-PCR analysis revealed an upregulation of *otx-2* in the St. 20 tumours (Figure 3.2). Another anterior marker analyzed was *XAG*, which is expressed in the cement gland of neurula stage *Xenopus* embryos. The cement gland is an organ that forms from the most anterior portion of the ectoderm and also expresses *otx-2* (Sive & Bradley, 1996; Gammil & Sive, 1997). In three independent experiments, RT-PCR analysis revealed that *XAG* was not upregulated in the St. 20 tumours (Figure 3.2). Analysis of other members of the Hedgehog and Gli families, *chh* and *gli3* respectively, showed no upregulation in the tumour sections, after three attempts.

### **3.4 *Xrel3*-induced tumours at different stages in development**

Tumours from a number of other stages of embryos were tested to determine if *otx-2*, *shh*, *gli1* and *twist* were consistently expressed in development. In three independent

experiments both *otx-2* and *shh* were upregulated in the tumours dissected from St. 16/17 embryos. However, both *twist* and *gli1* levels were low and relatively even with their corresponding basal skin levels (Figure 3.3A). At St. 26/27, when the tumours were starting to regress, *shh*, *gli1*, *otx-2* and *twist* levels all remained upregulated in the tumours as compared to the skin (Figure 3.3B). These experiments were repeated three times.

### **3.5 Marker expression does not require any inductive interactions from underlying tissue**

We next tested whether expression of the above markers can be induced by *Xrel3* in animal cells in isolation. Embryos were injected as usual at the two-cell stage and at St. 8 ten to twelve animal regions (caps) were dissected away from the rest of the embryos. The caps were allowed to heal and were processed for RT-PCR analysis at two stages: one prior to tumour formation/initiation (St. 10) and one at a time when tumours are normally visible on the embryo (St. 20). Figure 3.4B represents the results of three independent experiments and shows that there is no change in levels of *Xrel3*. In addition, after three attempts, the levels of *otx-2*, *twist*, *gli1* and *shh* mRNA were not affected by the increased levels of *Xrel3* immediately after injection (Figure 3.4A). However, if the *Xrel3*-injected caps are allowed to develop to a stage when tumours are normally visible on the embryo, the pattern of gene expression for *shh*, *gli1*, *otx-2* and *actin* parallels that of the dissected tumours (Figure 3.4B). *Twist*, on the other hand, unlike the results from the tumour assay (Figure 3.2), was not upregulated in response to *Xrel3* injection. These results, with the exception of *twist*, indicate that inductive



**Figure 3.3:** RT-PCR analysis of St. 16/17 (A) and St. 26/27 (B) tumours for the expression of the body patterning genes sonic hedgehog (Shh), Gli1, Otx-2 and Twist, after RNA extraction from fifteen to twenty excised tumours and skin samples. A. Gli1 and Twist levels were not affected by increased levels of Xrel3 in St. 16/17 tumours. B. Levels of Shh, Gli1, Otx-2 and Twist were all upregulated in the St. 26/27 tumours. Histone levels were used as a standard for RNA loading.

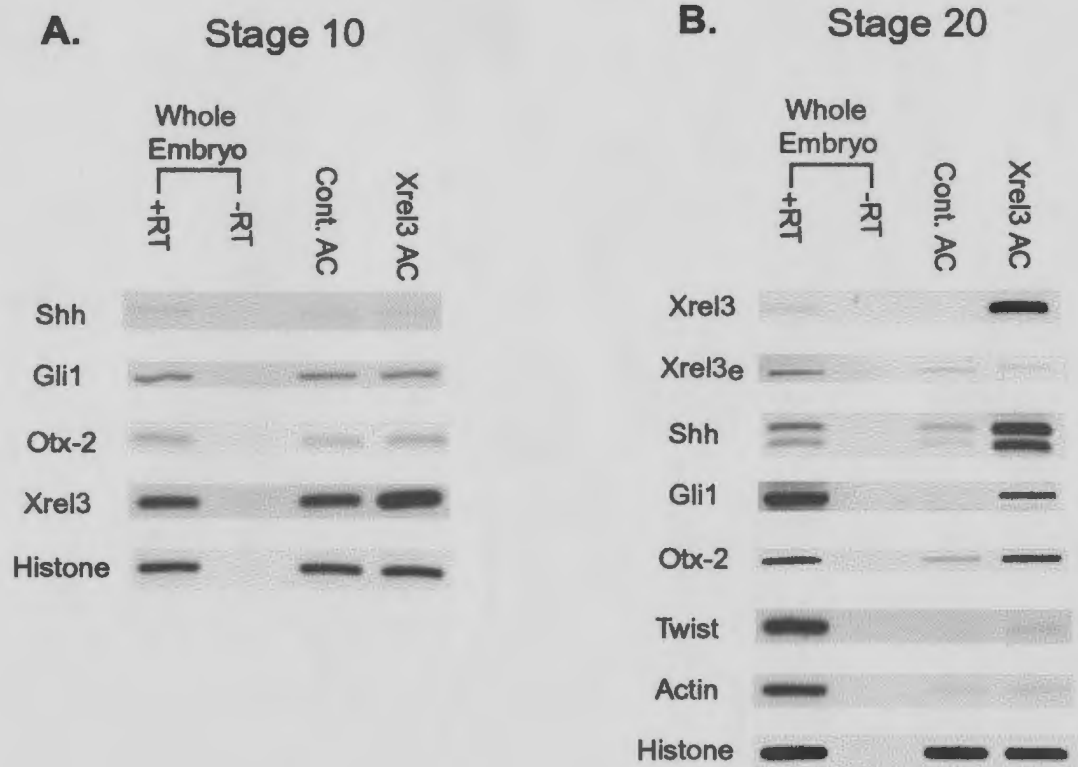


**Figure 3.4:** Expression analysis of *Xrel3* injected animal caps (AC) that have been allowed to develop to St. 10 (A) and St. 20 (B). RNA was extracted from ten to twelve injected *Xrel3* and control ACs. **A.** Expression of the body patterning genes *Shh*, *Gli1*, *Otx-2* and *Twist* (not shown) are not affected by the increased levels of *Xrel3* in the *Xrel3* injected ACs. **B.** Expression of the body patterning genes *Shh*, *Gli1*, and *Otx-2* are upregulated in response to elevated levels of *Xrel3*, while endogenous levels of *Xrel3* (*Xrel3<sub>e</sub>*) and cardiac actin (*Actin*) are not. Histone was used as a standard for RNA loading.

interactions from the underlying tissue were not required for the activation of the patterning genes.

### **3.6 A potential role for FGFs in *Xrel3*-induced tumour formation**

In chick embryos, NF- $\kappa$ B was found to have a role in limb development, in particular in the progress zone (or zone of proliferation). In the development of avian limb buds, NF- $\kappa$ B appears to be involved in regulating the genes *twist*, *shh* and *gli1*. This led me to the hypothesis that the *Xrel3*-induced tumours might actually be premature limb buds. Eight to ten hind limb buds from *Xenopus* tadpoles were extracted, homogenized and processed for RT-PCR analysis. A number of limb bud markers involved in vertebrate limb development, *Xfgf-8*, *XR-fng*, *Xwnt-7a*, *twist*, *gli1* and *shh*, were tested and in three separate experiments, all were found to be expressed as expected (Figure 3.5). Primers for the coding and non-coding regions of *Xrel3*, *Xrel3<sub>c</sub>* and *Xrel3<sub>nc</sub>* respectively, were also tested and both were found to be expressed in the developing limb buds. When the St. 20 tumours were tested for the presence of the vertebrate limb bud markers, however, after three attempts, only *Xfgf-8* and *Xefgf(ii)* were upregulated (Figure 3.6).

### **3.7 A number of differences in gene expression between normal skin and tumour sections**

Analysis of the *Xrel3*-induced tumours for genes that are regulated by *Xrel3* has implicated a number of patterning genes. However, the expression of these genes in response to *Xrel3* overexpression does not appear to be an immediate effect. A PCR-based comparative technique known as 'Differential Display' was, therefore, employed in

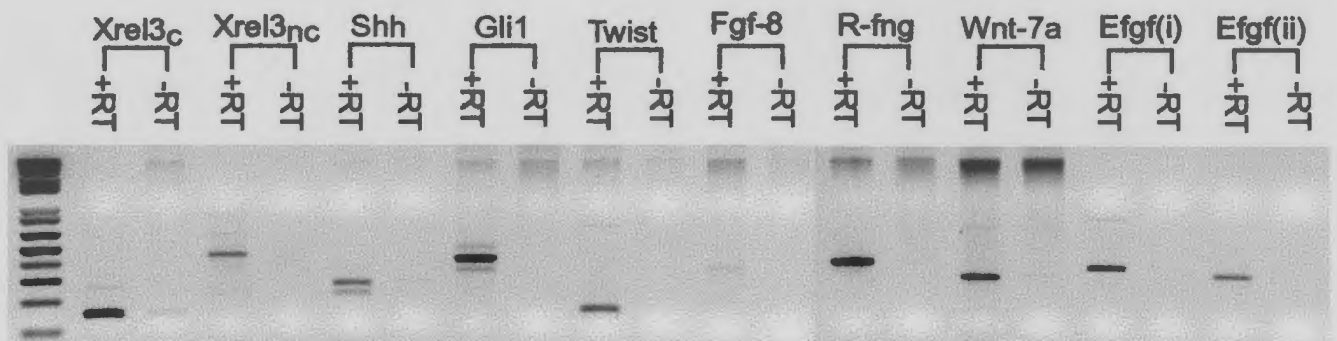


**Figure 3.5:** RT-PCR analysis of Stage 52-53 *Xenopus* hind limb buds, showing expression of *Xrel3* (*Xrel3<sub>C</sub>* and *Xrel3<sub>nc</sub>*). RNA was extracted and analyzed from eight to ten limb buds. The expression of various vertebrate limb bud markers (*Shh*, *Gli1*, *Twist*, *Fgf-8*, *R-fng*, *Wnt-7a*) served as positive controls.



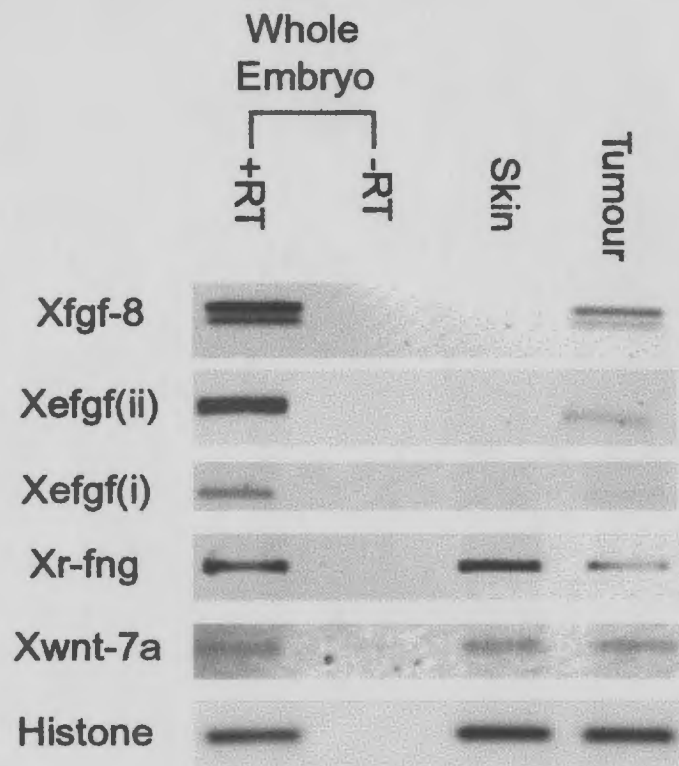


**Figure 3.6:** Expression of vertebrate limb bud markers in St. 20 *Xrel3*-induced tumours. RNA was extracted from each of fifteen to twenty excised tumours and skin samples. *Fgf8* and *efgf(ii)* are upregulated in the tumours. Histone served as a control for RNA loading.

an attempt to identify early genes that are regulated in response to *Xrel3* mRNA overexpression. Skin and tumour total RNA extracts from Stages 20 and 26/27 were tested, in addition to RNA extracts from St. 10 control and *Xrel3* injected animal caps. There were three different sources of St. 20 RNA extracts and all three were analyzed. Reverse transcription was performed on each RNA sample using one of four possible degenerate anchored oligo(dT) primers. Each resulting cDNA sample then underwent PCR amplification with five sets of primers involving arbitrary decamer primers or an arbitrary decamer primer in combination with the anchored oligo(dT) primer. Separation of the resulting PCR products on a denaturing polyacrylamide gel revealed a number of differences between skin and tumour samples and control animal cap and *Xrel3* injected animal cap samples (Figure 3.7). Differential display analysis was repeated two to three times for each RNA sample with each of the five primer sets. The resulting gel banding patterns were examined carefully and bands that were consistently upregulated in either the skin and control animal cap or the tumour and *Xrel3* injected animal cap, in all three embryonic stages tested, were marked for interest (Table 3.1).

### **3.8 A potentially novel gene upregulated in response to *Xrel3* overexpression**

Initially, one band of interest, A1.1aT, was chosen for further characterization. This band represented almost 400bp of a gene that was upregulated consistently in all the tumour samples and in the *Xrel3* injected animal caps. A1.1aT, from each of the five samples analyzed, was subsequently eluted from the gels and PCR re-amplified using the AP1/AP1 primer set that had pulled out the original A1.1aT band of interest. Re-

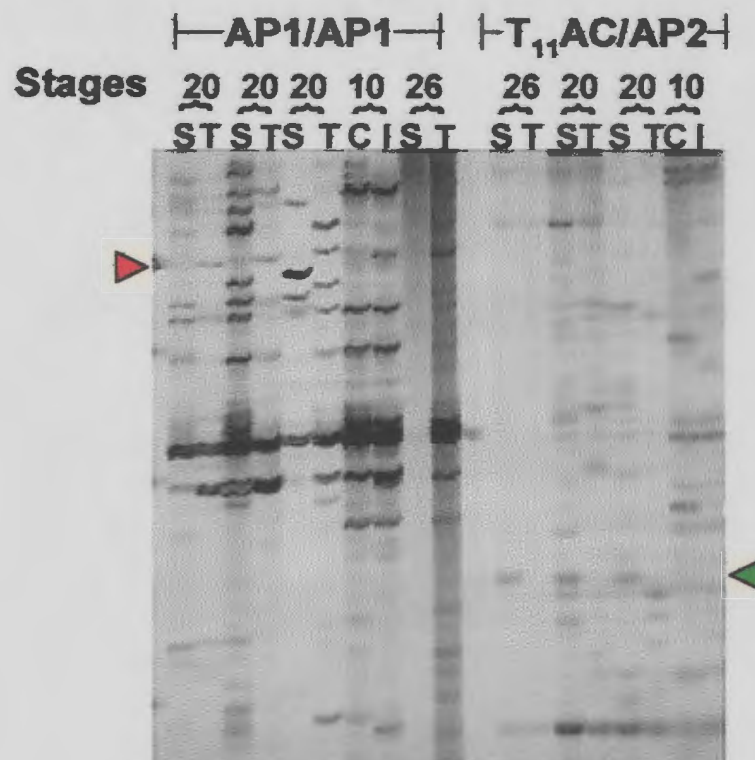


**Figure 3.7:** An example of a differential display gel showing multiple banding patterns in the skin (S), tumour (T), injected (I) or control (C) animal caps from three stages of *Xenopus* embryos, after PCR amplification with the primer sets AP1/AP1 and T<sub>11</sub>AC/AP2. The red arrow points to one type of band that is upregulated in the tumours and the green arrow points to another type of band that is upregulated in the skin.

**Table 3.1:** The sizes and expression of a number of genes, identified from differential display gels after PCR amplification with either one of five primer sets, that are either upregulated ( $\uparrow$ ) in the skin/control animal caps or tumours/*Xrel3* injected animal caps.

Primer Sets	Bands of Interest	Name of Band
Ap1/Ap1	300-400bp $\uparrow$ tumours	A1.1aT
	600bp $\uparrow$ tumours	A1.1bT
Ap1/Ap2	450bp $\uparrow$ tumours	A1.2aT
	650bp $\uparrow$ skin	A1.2aS
Ap2/Ap2	350bp $\uparrow$ skin	A2.2aS
	550bp $\uparrow$ tumours	A2.2aT
	300bp $\uparrow$ skin	A2.2bS
T <sub>11</sub> AC/Ap1	—	
T <sub>11</sub> AC/Ap2	350bp $\uparrow$ tumours	TA2aT

amplification revealed that in all five instances, the correct band had been excised. These resulting PCR products were then cloned and sequenced.

The sequence obtained (Figure 3.8), excluding the pCR2.1 vector portion of the sequence, was entered into a DNA Sequence Translator program in which three reading frames were assessed. An open reading frame, however, was not obtained, as indicated by the asterisks, which correspond to stop codons (Figure 3.9).

Nucleotide sequence and each of the three protein sequences were entered for comparison into the GenBank/EMBL/DDBJ EST databases. No significant sequence identity was obtained in any of the cases, indicating that I had isolated a fragment from a potentially novel gene.

### **3.9 Expression of differential display product in *Xrel3*-induced tumours**

To determine whether the tumour-specific isolated differential display product, A1.1aT, was expressed in *Xrel3* overexpressed tissues, RT-PCR analysis, using nested primers designed against the A1.1aT sequence (Figure 3.8), was performed. Initially, St. 20 skin and tumour sections were assayed. Figure 3.10A shows that A1.1aT is expressed solely in the *Xrel3* overexpressing tumours. At an earlier stage in development, such as St. 10, however, two PCR products were obtained after RT-PCR analysis in the *Xrel3* injected animal caps (Figure 3.10B). Upon comparison with the molecular weight 1kb plus ladder, the higher PCR product corresponded to the PCR product in the St. 20 tumours. The lower PCR product corresponded to the PCR products that were also found in the St. 10 whole embryo and control animal cap samples.

```

1   GAATTCGGCT TCTGATCCAT GCGGAAAACC CATAAACCAA TGCTTCCAGT 50
51  CCGTTGTCAT ACTGGGGTCG GCATCCAAAG GCCGGGGGAA TCCAAAGCTA 100
101 AAAGAAAATT CAAATGTTAT TAATGTGGGA ACAGTGAGCT GAATTTTAGC 150
151 AGCTTTATTA AATGCTCAGG TTAACAGATA AAAAGGCACA CGAGGAAAAA 200
201 GGTGTTATAT CGGGAAAATG TAGGTTTAGT TTATTATAAG TAAAAAAAAA 250
251 CCCTACCCAC ACAGACACAA CCCACCAACA CATCTGCTAA TTCCAAGGAC 300
301 ATTACTCTAT TCTCATTCCC CTGGACTTAT CTTCTGCTTT CAGTACTATT 350
351 AACCATCCTT TTCTAATGCA AATTCTCAAT TTAATTGGTA TCATGGATCA 400
401 GAAGCCGAAT T                                     411

```

RED Letters indicates AP1 primer sequence used in Differential Display

BLUE Letters indicates primers designed from sequence

GREEN Letters indicates pCR2.1 vector sequence

**Figure 3.8:** Nucleotide sequence of the differential display cDNA product A1.1aT that was upregulated in tumours.



Sequence name: A1.1aT  
Sequence length: 390 bp

```

L I H G E N P * T N A S S P L S Y W G R
* S M A K T H K P M L P V R C H T G V G
D P W R K P I N Q C F Q S V V I L G S A
CTGATCCATGGCGAAAACCCATAAACCAATGCTTCCAGTCCGTTGTCATACTGGGGTCGG
-----|-----|-----|-----|-----|-----| 60

H P K A G G I Q S * K K I Q M L L M W E
I Q R P G E S K A K R K F K C Y * C G N
S K G R G N P K L K E N S N V I N V G T
CATCCAAAGGCCGGGGGAATCCAAAGCTAAAAGAAAATTCAAATGTTATTAATGTGGGAA
-----|-----|-----|-----|-----|-----| 120

Q * A E F * Q L Y * M L R L T D K K A H
S E L N F S S F I K C S G * Q I K R H T
V S * I L A A L L N A Q V N R * K G T R
CAGTGAGCTGAATTTTAGCAGCTTTATTAAATGCTCAGGTAAACAGATAAAAAGGCACAC
-----|-----|-----|-----|-----|-----| 180

E E K G V I S G K C R F S L L * V K K N
R K K V L Y R E N V G L V Y Y K * K K T
G K R C Y I G K M * V * F I I S K K K P
GAGGAAAAAGGTGTTATATCGGGAAAATGTAGGTTTAGTTTATTATAAGTAAAAAAAAC
-----|-----|-----|-----|-----|-----| 240

P T H T D T T H Q H I C * F Q G H Y S I
L P T Q T Q P T N T S A N S K D I T L F
Y P H R H N P P T H L L I P R T L L Y S
CCTACCCACACAGACACAACCCACCAACACATCTGCTAATTCCAAGGACATTACTCTATT
-----|-----|-----|-----|-----|-----| 300

L I P L D L S S A F S T I N H P F L M Q
S F P W T Y L L L S V L L T I L F * C K
H S P G L I F C F Q Y Y * P S F S N A N
CTCATTCCCTGGACTTATCTTCTGCTTTCAGTACTATTAACCATCCTTTTCTAATGCAA
-----|-----|-----|-----|-----|-----| 360

I L N L I G I M D Q
F S I * L V S W I
S Q F N W Y H G S
ATTCTCAATTTAATTGGTATCATGGATCAG
-----|-----|-----|-----|-----|-----| 420

```

**Figure 3.9:** DNA translation of the differential display product A1.1aT in three reading frames. Asterisks represent stop codons. No open reading frame was found.

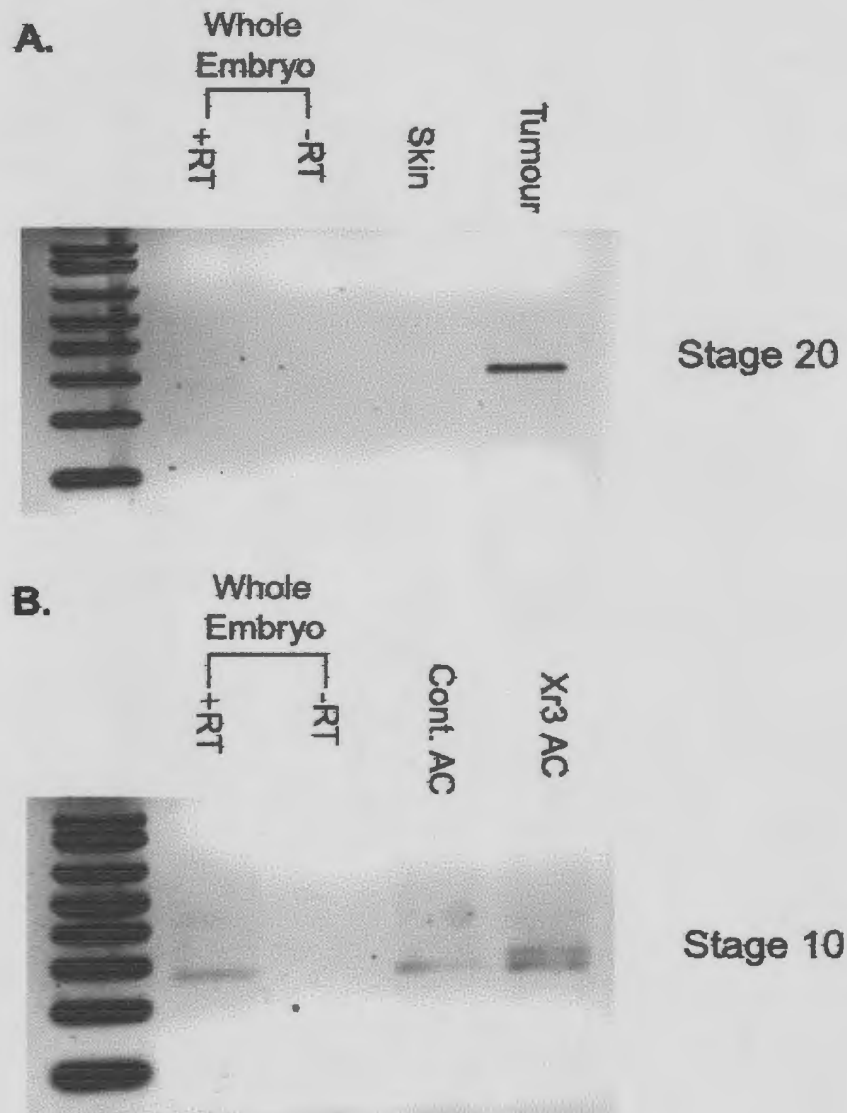


**Figure 3.10:** RT-PCR analysis of *Xrel3*-induced tumours (A) and *Xrel3*-injected ACs (B) for the expression of the isolated differential display product A1.1aT. A. In RNA extracted from fifteen to twenty excised tumours and skin samples, the differential display product is expressed in only the tumours. B. In RNA extracted from ten to twelve ACs, at St. 10 in development, two PCR products were obtained in the *Xrel3* injected ACs. The lower PCR product was also expressed in the whole embryo and control ACs.



To determine the identities of the two PCR products in the St. 10 *Xrel3* injected animal caps, the PCR products were cloned into the pCR2.1 vector and sequenced. The resulting sequences (Figure 3.11) were compared with each other and with the original A1.1aT sequence (Figure 3.8) using a sequence alignment program known as 'ClustalW'. The results from this nucleotide sequence analysis revealed that the higher PCR product in the St. 10 *Xrel3* injected samples was the same as the original differential display products (A1.1aT) sequenced. The lower PCR product in the St. 10 *Xrel3* injected sample was not identical to either the original A1.1aT differential display sequence or the higher PCR product in the St. 10 sample (Figure 3.12).

Further sequence analysis of the two St. 10 PCR products involved DNA sequence translation and comparison with the GenBank/EMBL/DDBJ EST databases. For the higher PCR product (tumour-specific sequence), as with the A1.1aT sequence, no open reading frame was obtained (Figure 3.13). The lower PCR product (embryo-specific sequence), however, did have an open reading frame (Figure 3.14). No significant nucleotide or protein sequence similarities were obtained after searching the GenBank/EMBL/DDBJ EST databases.

Embryo 1	AATTCGGCTT	AACCAATGCT	TCCAGTCCGT	TTGCAGGGGC	40	
Tumour 1	AATTCGGCTT	AACCAATGCT	TCCAGTCCGT	TGTCATACTG	40	
Embryo 41	CGACCAAAGC	TTTCCCCCGG	GGGTTGAAGA	ACACGGCAAG	80	
Tumour 41	GGGTCGGCAT	CCAAAGGCCG	GGGGAATCCA	AAGCTAAAAG	80	
Embryo 81	AACATCAACC	CTCCCAGCAA	CACGTTTAAT	CAAGACCAGC	120	
Tumour 81	AAAATACAAA	TGTTATTAAT	GTGGGAACAG	TGAGCTGAAT	120	
Embryo 121	ATGTTGGGTC	GCCTTCTGCC	GTCAATGGGA	ACCAACCAAA	160	
Tumour 121	TTTAGCAGCT	TTATTAAATG	CTCAGGTAA	CAGATAAAAA	160	
Embryo 161	CTTCACTCCC	AACAACCTCCA	CGCGGGGCAA	CAGCAGCACC	200	
Tumour 161	GGCACACGAG	GGAAAAGGTG	ATTGTCTGGG	AAAATGTATG	200	
Embryo 201	CCCGAAGTCA	ACAACATCCC	TCCCCCGAGC	AACCCACTGG	240	
Tumour 201	GTTTAGTTTA	TTATAAGTTA	AAAAAAAACC	CTACCCACAC	240	
Embryo 241	CAACTGCGTG	GCAGCCAGCC	GCCCCCTCGT	GACATTATCG	280	
Tumour 241	AGACACAACC	CACCAACACA	TCTGCTAAGG	CCAAAGGACA	280	
Embryo 281	TTACTGCTAA	GCCGAATT			298	
Tumour 281	TTACTCTATT	CTCATTC	CCC	TGGACTTATC	TTCTGCTAAG	320
Tumour 321	CCGAATT				327	

GREEN letters indicate pCR2.1 vector sequence

RED letters indicate primers designed towards the A1.1aT sequence

BLUE letters indicate nested primers for each of the embryo-specific and tumour-specific sequences

**Figure 3.11:** Nucleotide sequences of the two PCR products obtained from RT-PCR analysis of St. 10 *Xrel3* injected ACs, with nested A1.1aT primers. The higher PCR product is designated 'Tumour', while the lower PCR product is designated 'Embryo'.

```

Embryo  AACCAATGCTTCCAGTCCGTT----TGCAGGGGCGGAC---CAAAGCTTTCC----CCCG 49
Tumour  AACCAATGCTTCCAGTCCGTTGTCTACTGGGGTCGGCATCCAAAGGCCGGGGGAATCCA 60

Embryo  GGGGTTGAAGAACACGGCAAGAACATCAACCCCTCCCAGCAACACGTTTAAATCAAGACCAG 109
Tumour  AAGCTAAAAGAAAATACAAATGTTATTAATG-TGGGAACAGTGAGCTGAATTTTAGCAGC 119

Embryo  CATGTTGGGTCGCCT--TCTGCCGTCAATGGGAACCA----ACCAACTTCACTCCCAAC 163
Tumour  TTTATTAAATGCTCAGGTTAACAGATAAAAAGGCACACGAGGGAAGGTGATTGTCTGG 179

Embryo  AACTCCACGCGGGGCAACAGCAGCACCCCGAAGTCAACAACATCCCTCCCCCGA-GCAA 222
Tumour  GAAATGTATGGTTTAGTT-TATTATAAGTTAAAAAAAACCTACCCACACAGACACAA 238

Embryo  CCCACTGGCACTGCGTGGCAGCCAGCCGCCCCCTCGTGACATTATCGTTACTGCT---- 278
Tumour  CCCACCAACACATCTGCTAAGGCCAAAGGACATTACTC--TATTCTCATTCCTGACT 296

Embryo  -----
Tumour  TATCTTCTGCT 307
                Alignment score: 8 out of 100

Embryo  -----AACCAATGCTTCCAGTCCGTT----TGCAGGGGCGGA 33
A1.1aT  CTGATCCATGGCGAAAACCCATAAACCAATGCTTCCAGTCCGTTGTCTACTGGGGTCGG 60

Embryo  C---CAAAGCTTTCC----CCCGGGGGTTGAAGAACACGGCAAGAACATCAACCCCTCCA 86
A1.1aT  CATCCAAAGGCCGGGGGAATCCAAAGCTAAAAGAAAATTCAAATGTTATTAATG-TGGGA 119

Embryo  GCAACACGTTTAAATCAAGACCAGCATGTTGGGTCGCCTTCTGCCGTCAATGGGAACCAAC 146
A1.1aT  ACAGTGAGCTGAATTTTAGCAGCTTTATTAAT-GCTCAGGTTAACAGATAAAAAGGCAC 178

Embryo  CAACTTCACTCCCAACAACTCCACGCGGGGCAACAGCAGCACCCCGAAGTCAACAACA 206
A1.1aT  ACGAGGAAAAGGTGTTATATCGGGGAAATGTAGGTTTAGTTTATTATAAGTAAAAAAA 238

Embryo  TCCCTCCCCGAGCAACCCACTGGCACTGCGTGGCAGCCAGCCGCCCCCTCGTGACATT 266
A1.1aT  ACCCTACCCACACAGACACAACC-CACCAACACATCTGCTAATTCCAAGGACATTACTCT 297

Embryo  ATCGTTACTGCT----- 278
A1.1aT  ATTCTCATTCCCCTGGACTTATCTTCTGCTTTCAGTACTATTAACCATCCTTTTCTAATG 357

Embryo  -----
A1.1aT  CAAATTCTCAATTTAATTGGTATCATGGATCAG 390
                Alignment Score: 8 out of 100

Tumour  -----AACCAATGCTTCCAGTCCGTTGTCTACTGGGGTCGG 37
A1.1aT  CTGATCCATGGCGAAAACCCATAAACCAATGCTTCCAGTCCGTTGTCTACTGGGGTCGG 60

Tumour  CATCCAAAGGCCGGGGGAATCCAAAGCTAAAAGAAAATACAAATGTTATTAATGTGGGAA 97
A1.1aT  CATCCAAAGGCCGGGGGAATCCAAAGCTAAAAGAAAATTCAAATGTTATTAATGTGGGAA 120

Tumour  CAGTGAGCTGAATTTTAGCAGCTTTATTAATGCTCAGGTTAACAGATAAAAAGGCACAC 157
A1.1aT  CAGTGAGCTGAATTTTAGCAGCTTTATTAATGCTCAGGTTAACAGATAAAAAGGCACAC 180

Tumour  GAGGGAAAAGGTGATTGTCTGGGAAAATGTATGGTTAGTTTATTATAAGTTAAAAAAA 217
A1.1aT  GAGGAAAAGGTGTTATATCGGGAAAATGTA-GGTTAGTTTATTATAAGT-AAAAAAA 238

Tumour  ACCCTACCCACACAGACACAACCCACCAACACATCTGCTAAGGCCAAAGGACATTACTCT 277
A1.1aT  ACCCTACCCACACAGACACAACCCACCAACACATCTGCTAATTCCAA-GGACATTACTCT 297

Tumour  ATTCTCATTCCCCCTGGACTTATCTTCTGCT----- 307
A1.1aT  ATTCTCATTCCCCTGGACTTATCTTCTGCTTTCAGTACTATTAACCATCCTTTTCTAATG 357

Tumour  -----
A1.1aT  CAAATTCTCAATTTAATTGGTATCATGGATCAG 390
                Alignment Score: 95 out of 100

```

**Figure 3.12:** Sequence alignments between the original differential display sequence (A1.1aT) and the two sequences (Embryo and Tumour) obtained from the St. 10 *Xrel3* injected PCR sample. The sequence alignment analysis shows that the Tumour and A1.1aT sequences are the same, while the Embryo and Tumour/A1.1aT sequences are different. The blue sequence represents regions of similarity.



Sequence name: Tumour-specific  
Sequence length: 307 bp

```

N Q C F Q S V V I L G S A S K G R G N P
T N A S S P L S Y W G R H P K A G G I Q
P M L P V R C H T G V G I Q R P G E S K
AACCAATGCTTCCAGTCCGTTGTCATACTGGGGTCGGCATCCAAAGGCCGGGGGAATCCA
-----|-----|-----|-----|-----|-----| 60

K L K E N T N V I N V G T V S * I L A A
S * K K I Q M L L M W E Q * A E F * Q L
A K R K Y K C Y * C G N S E L N F S S F
AAGCTAAAAGAAAATACAAATGTTATTAATGTGGGAACAGTGAGCTGAATTTTAGCAGCT
-----|-----|-----|-----|-----|-----| 120

L L N A Q V N R * K G T R G K R * L S G
Y * M L R L T D K K A H E G K G D C L G
I K C S G * Q I K R H T R E K V I V W E
TTATTAAATGCTCAGGTTAACAGATAAAAAGGCACACGAGGGAAAAGGTGATTGTCTGGG
-----|-----|-----|-----|-----|-----| 180

K M Y G L V Y Y K L K K N P T H T D T T
K C M V * F I I S * K K T L P T Q T Q P
N V W F S L L * V K K K P Y P H R H N P
AAAATGTATGGTTTAGTTTATTATAAGTTAAAAAAAACCCTACCCACACAGACACAACC
-----|-----|-----|-----|-----|-----| 240

H Q H I C * G Q R T L L Y S H S P G L I
T N T S A K A K G H Y S I L I P L D L S
P T H L L R P K D I T L F S F P W T Y L
CACCAACACATCTGCTAAGGCCAAAGGACATTACTCTATTCTCATTCCCCTGGACTTATC
-----|-----|-----|-----|-----|-----| 300

F C
S A
L
TTCTGCT
-----|-----|-----|-----|-----|-----| 360

```

**Figure 3.13:** DNA translation of the higher PCR product sequenced from the St. 10 *Xrel3* injected sample, in three reading frames. Asterisks represent stop codons. No open reading frame was found.

Sequence name: Embryo-specific  
Sequence length: 278 bp

```

N Q C F Q S V C R G R P K L S P G G * R
T N A S S P F A G A D Q S F P P G V E E
P M L P V R L Q G P T K A F P R G L K N
AACCAATGCTTCCAGTCCGTTTGCAGGGGCCGACCAAAGCTTCCCCCGGGGGTTGAAGA
-----|-----|-----|-----|-----|-----| 60

T R Q E H Q P S Q Q H V * S R P A C W V
H G K N I N P P S N T F N Q D Q H V G S
T A R T S T L P A T R L I K T S M L G R
ACACGGCAAGAACATCAACCCTCCAGCAACACGTTTAATCAAGACCAGCATGTTGGGTC
-----|-----|-----|-----|-----|-----| 120

A F C R Q W E P T K L H S Q Q L H A G Q
P S A V N G N Q P N F T P N N S T R G N
L L P S M G T N Q T S L P T T P R G A T
GCCTTCTGCCGTCAATGGGAACCAACCAAACTTCACTCCCAACAACCTCCACGCGGGGCAA
-----|-----|-----|-----|-----|-----| 180

Q Q H P R S Q Q H P S P E Q P T G N C V
S S T P E V N N I P P P S N P L A T A W
A A P P K S T T S L P R A T H W Q L R G
CAGCAGCACCCCCGAAGTCAACAACATCCCTCCCCGAGCAACCCACTGGCAACTGCGTG
-----|-----|-----|-----|-----|-----| 240

A A S R P L V T L S L L
Q P A A P S * H Y R Y C
S Q P P P R D I I V T A
GCAGCCAGCCGCCCCCTCGTGACATTATCGTTACTGCT
-----|-----|-----|-----|-----|-----| 300

```

**Figure 3.14:** DNA translation of the lower PCR product from the St.10 *Xrel3* injected sample, in three reading frames. Asterisks represent stop codons. The green lettering represents an open reading frame.

## **Chapter 4: Discussion**

### **4.1 The use of RT-PCR in gene expression studies**

Many techniques have been utilized by molecular biologists in gene expression studies. Some of the more common techniques include Northern blot analysis, RNase protection assays and *in situ* hybridizations. RT-PCR still remains a relatively new technique and work on the optimization of this technology is ongoing. In its favour, it has proven to be a more sensitive and discriminating procedure than those mentioned above, as it permits the analysis of very small amounts of RNA. It is also a fairly rapid and simple procedure, in which simultaneous analysis of several transcripts from total RNA and quantitation of RNA can be achieved.

One major pitfall in using RT-PCR is the high degree of variability associated with it. In addition to greatly amplifying the target, any errors or contaminations present are also amplified, thus affecting the accuracy and reliability of the result. However, with proper experimental design, it can be a very useful technique.

RT-PCR sensitivity has helped in the confirmation that fibrinogen is not synthesized by megakaryocytes (Louache et al., 1991) and that atrial natriuretic factor (ANF) is in fact present in the adrenal medulla (Nunez et al., 1990). The discriminatory nature of RT-PCRs can be observed by their ability to distinguish between closely related transcripts. For instance, RT-PCRs have been used to demonstrate that the dystrophin primary transcript can create many different species through alternative splicing (Feener et al., 1989). Recently, RT-PCR has been involved with the detection of disseminated

tumour cells in the peripheral blood and bone marrow of patients with solid tumours (Nollau et al., 1995; Ghossein et al., 2000; Zippelius & Pantel, 2000).

There are many examples of how RT-PCR has helped to improve our knowledge in certain areas of molecular biology. One area of study in which RT-PCR is becoming more commonly employed is early vertebrate embryogenesis. In this project, RT-PCR was used to investigate the expression of genes in response to *Xrel3* overexpression in *Xenopus* embryos. Although my RT-PCR procedure did not allow for quantitative comparisons between primer sets, the use of histone to standardize the amount of cDNA used in PCR amplification with each primer set, did allow for the comparison of samples within each primer set. All experiments were repeated at least three times to ensure reproducibility of the results. The expression results of *otx-2*, *shh* and *gli1* in tumours of neurula stage embryos have subsequently been confirmed by *in situ* hybridization (Lake, Ford & Kao, In press).

## **4.2 Xrel3 and tumorigenesis**

### **4.2.1 Overexpression of Xrel3 leads to the formation of tumour-like lesions**

The *Xenopus* Rel gene *Xrel3* was first identified two years ago by Yang et al. (1998). Initial analysis of this gene led to the discovery that it has a spatiotemporally restricted pattern of expression. The localization of maternal messages of *Xrel3* to dorsoanterior structures of larval and tadpole stages suggested that *Xrel3* has a role in neural development, particularly that of the head and brain. Overexpression of *Xrel3* mRNA in the animal pole of *Xenopus* embryos, however, unexpectedly yielded lumpy

pigmented patches of tissue in either the ventral epidermis or along the flanks of neurula and tadpole stage embryos (Figure 1.5).

Evidence confirming that these lesions were in fact due to synthetic *Xrel3* mRNA injections was illustrated via RT-PCR, in which *Xrel3* mRNA was more abundant in the tumour-like lesions as compared to control skin samples (Figures 3.1A). As previously mentioned, *Xrel3* is a member of the c-Rel subfamily, however, unlike mouse and avian c-Rel, where the c-Rel promoter is autoregulated (Grumont et al., 1993; Bushdid et al., 1998), my data show that endogenous levels of *Xrel3* are not influenced by *Xrel3* mRNA injection (Figure 3.1A). Consistent with the fact that these lesions are due to exogenous *Xrel3* mRNA injection is the observation that the tumour-like lesions eventually disappear as the embryo develops, implying that the injected RNA eventually degrades. Hence, once the source of injected *Xrel3* mRNA has disappeared, the effect is lost.

Although I have not provided a direct correlation between the injection of *Xrel3* mRNA and increased levels of the encoded protein, the use of the CS2+ expression vector has provided a means through which to produce functional mRNA for injection. The CS2+ vector was designed by Dave Turner and Ralph Rupp primarily for expression studies in *Xenopus* embryos (the *Xenopus* Molecular Marker Resource (XMMR) homepage). One of the factors influencing the generation of proteins from injected mRNA is stability. Most injected mRNAs last up until the gastrula stage of *Xenopus* embryos (Vize et al., 1991). However, the half-lives can be extended with the addition of 5' methyl caps and 3' poly(A) tails. Rupp, Snider and Turner (unpublished; XMMR homepage) have observed that capped SP6 mRNAs from the CS2+ vector which include the SV40 poly A site at the 3' end are more stable and produce a much higher yield of



protein than more conventional synthetic mRNAs when injected into *Xenopus* embryos. In addition, our lab has shown *Xrel3* mRNA to translate efficiently *in vitro* using the SP6 transcription/translation (TnT) coupled rabbit reticulocyte lysate system (Promega) and that the protein produced is functional, as demonstrated by Electrophoretic Mobility Shift Assays (EMSAS; Lake, Ford & Kao, In press). The inability of *Xrel3* mRNAs lacking significant regions of their transcriptional activation domains (carboxy terminus) to induce tumours after injection into *Xenopus* embryos (Yang et al., 1998; Lake, Ford & Kao, In press) provides further evidence for the association of wild-type *Xrel3* and tumour formation.

#### **4.2.2 *Xrel3*-induced tumours express genes involved with promoting cell proliferation**

An intriguing aspect of these *Xrel3*-induced lesions is their close similarity to epidermal tumours that have previously been induced in *Xenopus* embryos by *gli1* overexpression and p53 inhibition (Dahmane et al., 1997; Wallingford et al., 1997). My RT-PCR results have shown that as with these other *Xenopus* tumours, the *Xrel3*-induced tumour-like lesions are of epidermal type (Figure 3.1B).

The finding that overexpressing *Xrel3* in *Xenopus* embryos led to the formation of tumours was interesting because apart from the founding member of the Rel/NF- $\kappa$ B family of proteins, v-Rel, no other family member has been found to be oncogenic. In an attempt to elucidate the signalling circuitry through which *Xrel3* induces tumorigenesis, my data show that the Shh signalling pathway (Figure 4.1) is involved. Both *gli1* and *shh* were upregulated in the *Xrel3*-induced tumours (Figures 3.2 & 3.3). Upregulation of both Gli1 and the Shh signalling pathway is responsible for the autosomal dominant human

disease Nevoid Basal Cell Carcinoma Syndrome (NBCCS) or Gorlin syndrome (for reviews, see Matisse & Joyner, 1999; Ruiz i Altaba, 1999; Wicking et al., 1999).

Individuals with this disease are characterized by a predisposition to a variety of tumour types, including basal cell carcinomas, medulloblastomas, ovarian fibromas, and meningiomas (Kraemer et al., 1984; Gorlin, 1995; Raffel et al., 1997; Xie et al., 1997).

The identification of consistent mutations localized to chromosome 9q22 in NBCCS patients and the subsequent mapping of the *Patched* (*PTC*) gene to this region, led to the discovery that mutations resulting in a truncated PTC protein was the primary genetic anomaly involved with this disease (Hahn et al., 1996; Johnson et al., 1996).

PTC is a multipass transmembrane protein and serves as a receptor for Shh in the Shh signalling pathway (Figure 4.1; Marigo et al., 1996; Stone et al., 1996). Inactivation of PTC, through mutation, mimics the effect of Shh binding to the PTC receptor and results in activation of the signalling pathway. Thus, patients with NBCCS suffer from a constitutively active Shh signalling pathway, which ultimately leads to constant activation of downstream target genes, such as Gli 1.

The most common tumour type, as the name of the disease suggests, are basal cell carcinomas, where constant activation of the Shh signalling pathway leads to uncontrolled cell proliferation. In addition to NBCCS, members of the Shh signalling pathway, including PTC, have also been implicated in sporadic cases of BCCs.

Smoothed (SMO), another transmembrane receptor involved in transmitting the Shh signal, normally interacts with PTC (Figure 4.1; Alcedo et al., 1996; van den Heuvel & Ingham, 1996). In the absence of Shh this interaction inhibits SMO and prevents

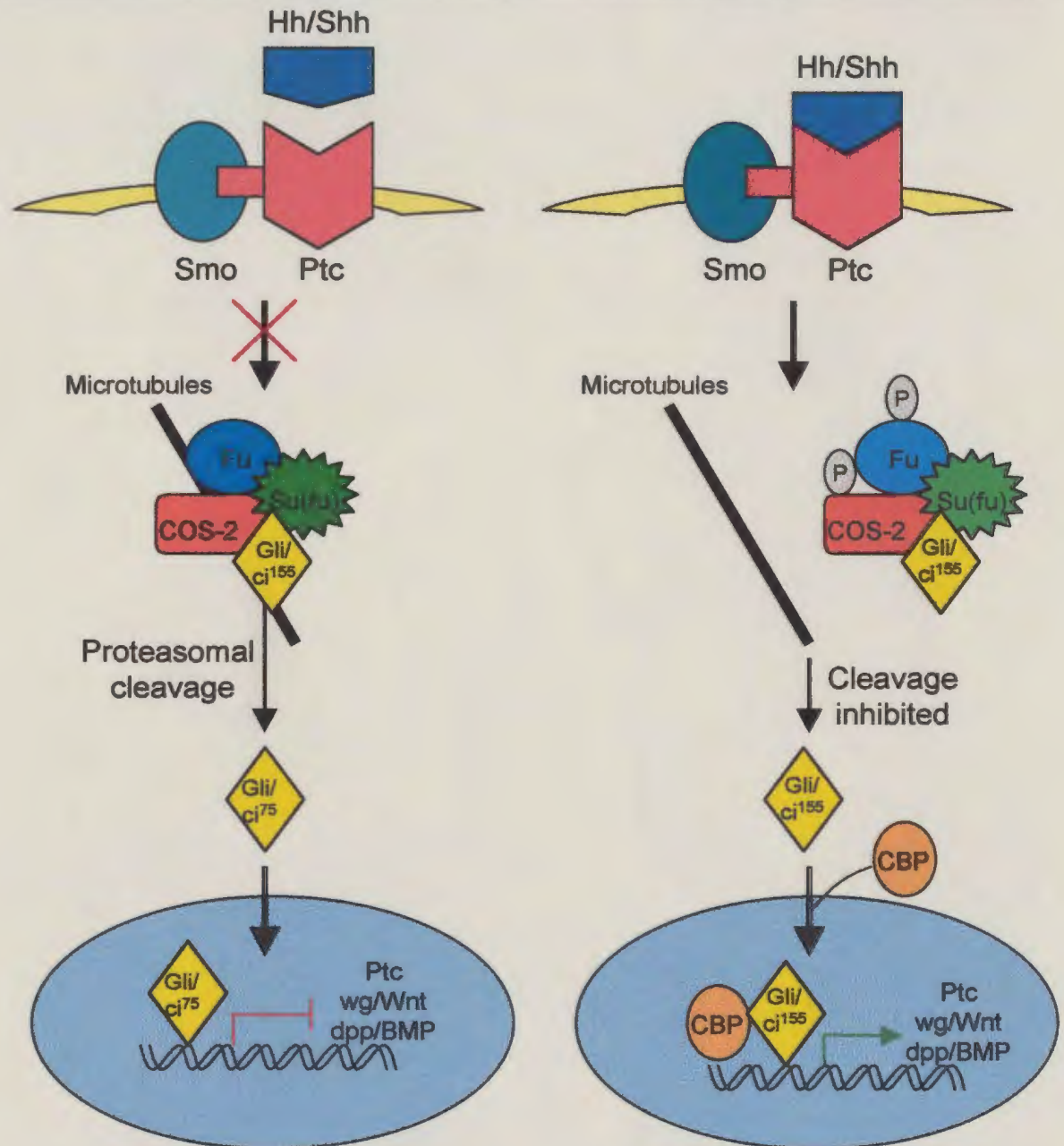


**Figure 4.1:** The Hedgehog (Hh)/Sonic hedgehog (Shh) signalling pathway, established primarily from *Drosophila*. Full length cubitus interruptus (ci<sup>155</sup>) or the vertebrate counterpart Gli, forms a complex with Fused (Fu), Costal-2 (COS-2) and Suppressor of fused (Su(fu)), and associates with a microtubule complex. In the absence of Hh/Shh induction, ci<sup>155</sup> is targeted for proteasomal cleavage and ci<sup>75</sup> is released. Translocation of this molecule to the nucleus leads to the repression of transcription. The binding of Hh/Shh to Ptc inactivates Ptc and releases Smo from repression. COS-2 and Fu become phosphorylated and the complex dissociates from the microtubules. Cleavage of ci<sup>155</sup> is blocked and this full-length form or some other related form translocates to the nucleus, where it associates with CREB-binding protein (CBP) and activates downstream target genes such as Ptc, decapentaplegic (dpp; BMP in vertebrates) and wingless (wg; Wnt in vertebrates; Ingham, 1998; Ming et al., 1998).

activation of the pathway. The binding of Shh to PTC releases SMO from repression and leads to the transduction of the Shh signal (Alcedo & Noll, 1997; Ingham, 1998).

Recently, mutations in the SMO gene, leading to its constant activation, have been found in a number of sporadic BCC cases (Xie et al., 1998; Lam et al., 1999). Overexpression of Shh itself and the downstream target, Gli1 have been found to induce BCCs as well (Dahmane et al., 1997; Oro et al., 1997; Ghali et al., 1999).

The Hedgehog signalling pathway has also been implicated in the etiology of a number of CNS tumours. In fact, Gli1 was initially identified by its oncogenic activity in gliomas (Kinzler et al., 1988).

Not only is the hedgehog signalling pathway involved in promoting proliferation and cell survival during tumorigenesis, but some recent reports provide evidence that the Shh signalling pathway has a role in promoting cell proliferation during normal development (for review, see Britto et al., 2000). Ahlgren and Bronner-Fraser (1999), through studies involving neural development in the chick, found that inhibition of Shh signalling led to extensive cell death in the neural tube and neural crest cells, leading to a significantly reduced head phenotype, suggesting that Shh may normally play a role in promoting the survival and proliferation of these cells. Studies involving mice have also shown that Shh signalling is involved in regulating the division and hence differentiation of cerebellar granule precursor cells (Wallace, 1999; Wechsler-Reya & Scott, 1999), as well as being an important mitogenic factor of retinal precursor cells (Jensen & Wallace, 1997). In addition, Shh plays a role in vertebrate limb development, where it is expressed in the posterior mesenchyme of the developing limb bud and is involved in maintaining

limb bud outgrowth, possibly by promoting mesodermal proliferation (Bushdid et al., 1998; Kanegae et al., 1998).

This evidence suggests that perhaps Hedgehog signalling plays a general role in regulating the cell cycle. What this role exactly is and how the downstream effectors of the Hedgehog signalling pathway, such as Gli1, are involved is unknown. My results provide evidence that there is a possible relationship between the Shh signalling pathway and Rel/NF- $\kappa$ B. It would be interesting to see if the Gli1-induced tumours and the tumours induced by p53 inhibition in *Xenopus* show an upregulation in *Xrel3* expression or perhaps the expression of another Rel family member. This would provide insight into the possibility that these three tumour types, generated in *Xenopus* embryos, might have arisen due to a common pathway/mechanism and as such would provide further insight into the regulation of the cell cycle.

*Drosophila* DORSAL, a homologue of the vertebrate Rel/NF- $\kappa$ B family, is known to directly activate *twist*. Evidence linking the Rel/NF- $\kappa$ B family and Twist also comes from vertebrate limb development, where the abolition of c-Rel in developing chick limbs results in the arresting of limb outgrowth and a marked decline in *twist* expression (Bushdid et al., 1998; Kanegae et al., 1998). As with *c-Rel*, *twist* appears to be expressed in the proliferating mesenchymal region of the developing limb bud. In fact a recent report suggests that *twist* is a potential oncogene (Maestro et al., 1999). Twist interferes with p53 mediated growth arrest and apoptosis, primarily through down-regulating ARF, a tumour suppressor and up-stream regulator of p53 in the cell cycle. In addition, the misregulation of Twist is involved in rhabdomyosarcomas, which arises from a failure of mesenchymal cells to terminally differentiate into skeletal muscle cells.

Misregulation of the *twist* gene also has been linked to the human Saethre-Chotzen syndrome, a hereditary disorder characterized by craniofacial and limb anomalies (el Gouzzi et al., 1997; Howard et al., 1997). The significance of this finding is that normal sutural genesis is highly correlated with apoptosis and many craniosynostosis syndromes result from a deregulation in these apoptotic programs (Bourez et al., 1997). Thus, perhaps Twist also plays a role in regulating the cell cycle during normal development.

My results show that even though *twist* is upregulated in the *Xrel3*-induced tumours (Figures 3.2 & 3.3), it is not upregulated in the *Xrel3*-induced animal caps (Figure 3.4B). This illustrates that the expression of *twist* in the tumours either results from an error in tumour dissection or requires interactions with underlying tissues. Twist, as well as being expressed in the notochord at neurula stages in *Xenopus*, is also expressed in the lateral plate mesoderm. Thus, it is highly probable that when dissecting the tumours, I took some of the underlying mesodermal cells as well. Even though there is overwhelming support for a link between Twist and Rel/NF- $\kappa$ B and that Twist is a factor involved with regulating the cell cycle, my results, regarding the regulation of *twist* by *Xrel3*, are equivocal. It is possible that another *Xenopus* Rel family member is involved with regulating *twist* expression. An investigation into the expression levels of *twist* in the other two *Xenopus* tumour phenotypes might prove useful.

### **4.3 *Xrel3* and neural patterning**

An intriguing aspect of these *Xrel3*-induced tumours is that they express a number of genes that are involved in neural patterning (Figures 3.2, & 3.3), whose normal

expression patterns overlap that of *Xrel3* in neurula and larval embryo stages. These tumours do not become visibly apparent until early neurula stages and the upregulation of the patterning genes *shh*, *gli1* and *otx-2*, in response to *Xrel3* overexpression, occurs at a time when *Xrel3* transcripts normally start to become localized to neural structures in the *Xenopus* embryos (Figure 3.4). These observations indicate that *Xrel3* plays a role in neural development, perhaps by regulating the expression of certain neural patterning genes.

As previously mentioned, *Otx-2* is an anterior neural marker normally expressed in the otocysts and head region of *Xenopus* embryos (Pannese et al., 1995; Andreazzoli et al., 1997). *Otx-2* is also expressed in the *Xenopus* cement gland. In fact, the ectopic expression of *otx-2* in *Xenopus* leads to the formation of secondary cement glands and the activation of the cement gland markers XCG and XAG, as well as severely reduced posterior structures (Pannese et al., 1995; Gammill & Sive, 1997). Paradoxically, my results show that while *otx-2* is upregulated in the *Xrel3*-induced tumours, *XAG* is not (Figure 3.2). This illustrates that although the tumours are of epidermal type, they do not represent secondary cement glands.

The strong correlation between high levels of *Otx-2* and cement gland formation, however, suggest that some other factor must be involved that is preventing the activation of the cement gland. A recent report by Gammill and Sive (2000) has shown a tight relationship between BMP-4 signalling and *Otx-2* activity, which ultimately determines whether neural tissue is induced or cement gland forms.

BMP-4 is a major factor involved in neural induction. Blocking BMP-4 signalling by binding to neuralizing factors such as chordin and noggin leads to the

neuralization of ectoderm. BMP-4 is thought to be expressed in the ectoderm in a graded fashion. In this way, it can be involved in the generation of many ectodermal derivatives (Weinstein & Hemmati-Brivanlou, 1999).

BMP-4, as well as Otx-2, is expressed in the cement gland. BMP-4 is a potent inhibitor of Otx-2 and neural induction and their relationship within the cement gland is likely a tenuous one. The mechanism believed to be involved is that BMP-4 is required to regulate Otx-2 activity within the cement gland, thereby preventing neural tissue induction (Gammill & Sive, 2000). If BMP-4 levels are too high, Otx-2 activity is suppressed and cement gland formation is inhibited. On the other hand, if BMP-4 levels are too low, cement gland formation is also prevented, but the resulting increase in Otx-2 levels would induce neural tissue to form.

It is possible that BMP-4 levels might be high enough in *Xrel3*-induced tumours to prevent cement gland formation and neural induction by ectopically expressed *otx-2*, but not high enough to inhibit Otx-2 activity completely. This would explain the apparent epidermal nature of the tumours and the lack of cement gland marker expression. One way in which to test this theory would be to compare the levels of BMP-4 in the tumours, if any, with that of BMP-4 normally in the cement gland and surrounding epidermis.

#### **4.4 Relationship between Rel/NF- $\kappa$ B signalling and FGFs**

During the course of gene expression analysis of the *Xrel3*-induced tumours, one hypothesis that emerged was that since the species *Xenopus laevis* is not direct developing, the tumours might actually represent attempts by the *Xenopus* embryo to



produce limbs prematurely. Indeed, evidence involving avian embryogenesis has shown that c-Rel plays a crucial role in limb development, which may or may not be conserved throughout vertebrates. What is conserved among vertebrates is the role that Shh and members of the FGF family play during limb morphogenesis.

A proposed mechanism of the signals and factors involved in limb development are illustrated in Figure 4.2. At the crux of vertebrate limb outgrowth, initiation and maintenance is regulatory feedback loop(s) between the AER, a specialized region of ectoderm at the tip of the limb bud and the underlying zone of proliferating mesenchymal cells (progress zone). It is thought that the length of time a cell spends in the progress zone determines its differentiation status along the proximal-distal axis. The shorter the time a cell spends in the progress zone, the more proximal a structure it will specify. The longer a cell spends in the progress zone, the more distal the structure (for reviews, see Johnson & Tabin, 1997; Zeller & Duboule, 1997).

In vertebrate limb development, *shh* is expressed in the posterior mesenchyme of the limb bud and is believed to be the morphogen involved in establishing the anterior/posterior axis of the limb. Regions of high Shh concentration will form posterior structures, while those exposed to little or no Shh will form more anterior structures. Ectopic expression of *shh* in the anterior region of the limb bud induces mirror-image digit duplications (Riddle et al., 1993; Endo et al., 1997; for review, see Johnson & Tabin, 1997). Several studies have provided evidence for the interaction of Shh and Fgfs during limb development (Laufer et al., 1994; Bueno et al., 1996). It has been suggested that Shh initiates *fgf-4* expression in the posterior portion of the overlying AER and that

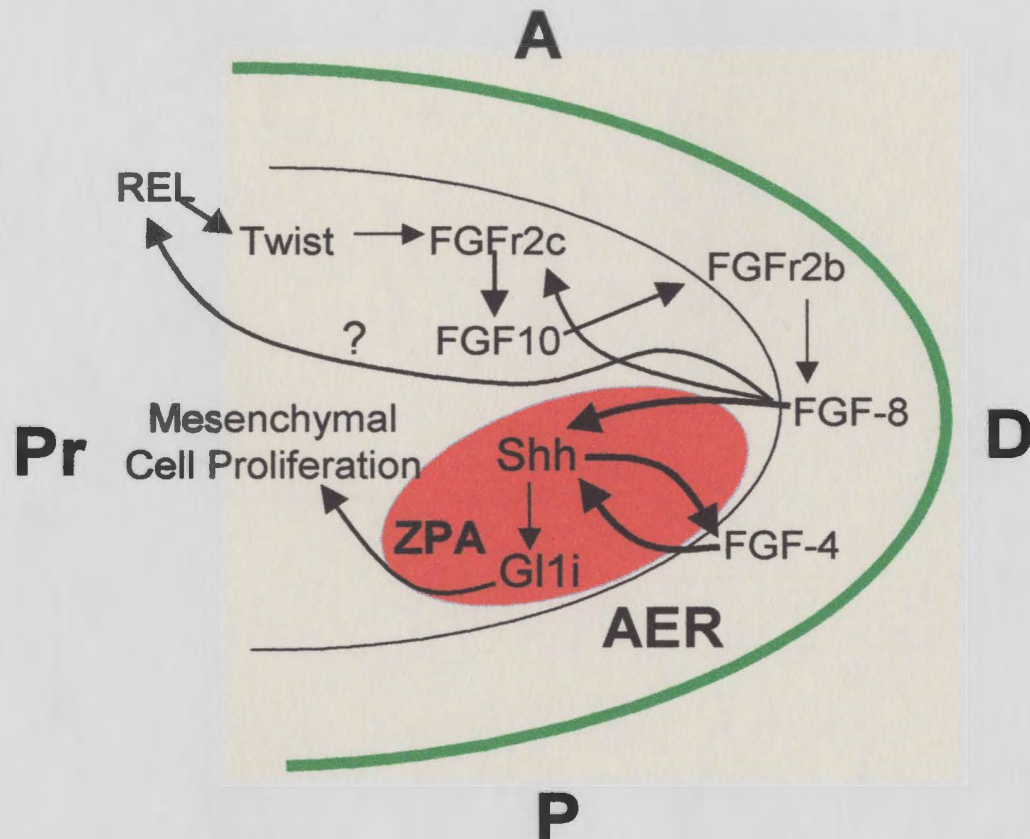


**Figure 4.2:** A schematic representation of a developing limb bud, illustrating some of the possible signalling events involved. A=Anterior; P=Posterior; Pr=Proximal; D=Distal; AER=Apical Ectodermal Ridge; ZPA=Zone of Polarizing Activity.

continued expression of both of these genes is regulated in a positive feedback loop. In this way, not only does Shh help to pattern the mesoderm of the limb, but, indirectly, promotes mesodermal proliferation. In addition, Fgf-10, a vertebrate limb mesenchymal factor is thought to initiate and maintain limb bud outgrowth through interaction with the apical ectodermal factor Fgf-8 (Ohuchi et al., 1997; Xu et al., 1998). Fgf-8, in turn, acts on the underlying mesoderm to maintain *fgf-10* expression and is also thought to induce *shh* expression in the posterior margin of the limb mesoderm (Crossely et al., 1996; Vogel et al., 1996; Ohuchi et al., 1997; Xu et al., 1998). It has also been postulated that there are possible signalling pathways from Shh to Fgf-10 and from Fgf-10 to Fgf-4 (Ohuchi et al., 1997).

Genetic evidence has recently emerged to show that the reciprocal regulation between FGF-8 and FGF-10 during limb morphogenesis requires FGF receptor 2 (FGFR2; Xu et al., 1998). FGFRs are transmembrane tyrosine kinases that function by mediating FGF signals. FGFRs are expressed in a variety of tissues and organs throughout development and share a number of common structural domains. Alternative splicing in some of these domains has been shown to give rise to a variety of isoforms (Givol & Yayon, 1992).

Within the developing limb bud two isoforms of FGFR2 exist, FGFR2b, which is expressed in the surface ectoderm and AER and FGFR2c, which is restricted to the underlying mesenchyme. Induction of *fgf-8* expression by Fgf-10 is mediated through the activation of FGFR2b, while Fgf-8 interacts with FGFR2c in the underlying mesenchyme to maintain *fgf-10* expression and promote continuous proliferation (Xu et al., 1998).

Studies in *Drosophila* embryos have provided evidence to suggest that FGFRs are downstream targets of Twist (Shishido et al., 1993; Emori & Saigo, 1993; El Ghouzzi et al., 1997; Howard et al., 1997). Since Twist in the chick limb is linked to Rel/NF- $\kappa$ B signalling and limb truncations due to inhibition of Rel/NF- $\kappa$ B activity can be rescued by FGFs, perhaps there is a link between Rel/NF- $\kappa$ B and FGF signalling.

My results show that *Xrel3* is indeed expressed in developing *Xenopus* limb buds (Figure 3.5). However, a common feature of most Rel/NF- $\kappa$ B family members is that they tend to be ubiquitously expressed. While *Xrel3* is restricted to particular dorsal and anterior structures in larval and tadpole stages, nothing is known about its spatial and temporal expression during metamorphosis and in adult tissues. It will be necessary to determine initially the spatial expression of *Xrel3* using *in situ* hybridisation in St. 52-53 limb buds.

If these *Xrel3*-induced tumours do actually represent prematurely developing limbs, expression of vertebrate limb bud markers would be expected to be upregulated in the tumours. My results show that the limb bud markers *Xfgf-8* and *Xefgf(ii)* are indeed upregulated (Figure 3.6).

While nine members of the FGF family have been identified in mammals, only five members are known to presently exist in *Xenopus* (Christen & Slack, 1997; Issacs, 1997). Most are direct homologues of their mammalian counterparts, however, eFGF, which exists as two pseudoalleles, due to the tetraploid nature of *Xenopus laevis*, is most closely related to mammalian FGF-4 and FGF-6 (Issacs et al., 1992). Expression data seem to suggest, however, that eFGF is more like FGF-4 than FGF-6 (Slack et al., 1996). Therefore, since there was no direct homologue of FGF-4, which plays a very important

role in vertebrate limb development, I chose to test eFGF(i) and (ii), both of which are expressed in *Xenopus* limb buds (Figure 3.5).

The upregulation of FGFs in the *Xrel3*-induced tumours provide preliminary evidence for a role of FGFs in the Rel/NF- $\kappa$ B signalling pathway. As their name suggests, FGFs are mitogenic factors involved in promoting proliferation, such as in the developing limb bud, and hence are involved in various forms of cancer, including skin carcinogenesis (Kurtz et al., 1997). As previously mentioned, in addition to having a role in mesoderm induction, FGFs also play a role in neural induction. Interestingly, FGF-8 is expressed in several domains in the head, including the forebrain and mid-hindbrain, as well as in the optic vesicle, regions to which *Xrel3* normally becomes localized during neural development (Rubenstein & Beachy, 1998; Vogul-Hopker et al., 2000; Xu et al., 2000). In addition, other members of the FGF family, such as FGF-3, FGF-6 and FGF-7, play an important role in brain development by regulating growth and morphogenesis (Ozawa et al., 1996; Vaccarino et al., 1999). This provides a further potential link between Rel/NF- $\kappa$ B and FGFs, perhaps in regulating proliferation during neural tissue patterning, in particular brain development.

Further investigations into the relationship between FGFs and Rel/NF- $\kappa$ B proteins might include whether treatment of *Xenopus* animal caps with FGF can induce *Xrel3* expression and whether co-injection of a dominant negative FGFR with *Xrel3* can inhibit tumour formation.

## 4.5 Identification of novel downstream targets of *Xrel3*

My results indicate that *Xrel3*-induced tumours do not appear until after gastrulation. Furthermore, upregulation of *shh*, *glil*, *twist* and *otx-2*, does not occur until the formation of the tumours, long after injection of *Xrel3* mRNA. Thus, it was evident that something else had to be occurring prior to the visible phenotypic effect of *Xrel3* overexpression. Histological analysis of late blastula and gastrula stage embryos, has subsequently revealed that in embryos injected with *Xrel3* mRNA in the animal pole there is a definite thickening of the blastocoel roof or prospective ectoderm, where the cells retain an undifferentiated morphology and become unable to migrate normally (Kao et al., manuscript in progress). This provides evidence to suggest that perhaps *Xrel3* has two roles during the course of *Xenopus* development, an early role where it is involved in regulating pre-gastrula differentiation and a later role where it is involved in neural patterning.

In an attempt to identify some immediate target genes of *Xrel3*, a relatively new technique, known as differential display, was utilized.

Differential display technology was developed by Liang and Pardee (1992) as a means of identifying and isolating genes that are differentially expressed in various cells or throughout development or under altered conditions. Although this technique has been used successfully to identify a number of novel genes, there are two major problems associated with it. Firstly, confirmation of the differential expression pattern of a differentially expressed gene of interest, excised from the original display gel, often cannot be reproduced on Northern blots (Sun et al., 1994; Sompayrac et al., 1995). In other words, a lot of false positives tend to be generated with this technique. Secondly,

the differentially expressed gene of interest often represents cDNA from the 3' untranslated region, which is frequently not included in GenBank (Liang et al., 1994; Sompayrac et al., 1995).

To help overcome the possibility of false positives, I identified genes of interest that were consistently up-regulated or down-regulated in either control animal caps and skin or *Xrel3*-induced animal caps and tumours throughout blastula and neurula stages in development. In addition, in an attempt to avoid isolating 3' untranslated regions, I used decamer-decamer primer combinations, as well as oligo(dT)-decamer primer combinations.

My results show that a number of genes are differentially expressed throughout *Xenopus* development and in response to *Xrel3* overexpression (Figure 3.7 and Table 3.1). The initial isolation of a gene fragment that is up-regulated in response to *Xrel3* overexpression proves promising as a novel immediate target gene. Although an attempt to confirm its differential expression pattern through Northern blot analysis was unsuccessful, RT-PCR results showed that this gene was exclusively expressed in response to *Xrel3* overexpression (Figure 3.10). Interestingly, at a late blastula stage in development (St. 10), RT-PCR analysis revealed an additional lower molecular weight fragment that was amplified in control as well as *Xrel3*-induced animal caps (Figure 3.10B). Sequence analysis has revealed it to be distinct from the *Xrel3*-induced gene (Figure 3.11) and it is currently part of an on-going investigation involving the screening of a Stage 10 lambda zap II cDNA library.

The complete sequencing and hence identification of the isolated up-regulated fragment remains to be elucidated. In addition, a more extensive analysis of its

expression pattern throughout development needs to be investigated. It is hoped that the recent emergence of cDNA microarray technology might help provide some of the answers. cDNA chip or microarray technology involves the spotting of cDNAs or expressed sequence tags (ESTs) onto known positions on a glass slide, using a machine known as an arrayer. Fluorescently labelled cDNA probes are then passed over the chip and allowed to hybridise to defined spots on the chip. The resulting fluorescent emissions can then be analysed with computer assistance (for review, see Khan et al., 1999; Kurian et al., 1999). The primary advantage of this technology is that it allows for the simultaneous analysis of thousands of genes (for review, see Khan et al., 1999; Kurian et al., 1999). The major limitations, however, are that, at present, there is a lack of publicly available sequence-validated cDNA clones and ESTs that can be spotted on a chip. Secondly, the use of equipment such as an arrayer, a laser scanner/reader, a computer and computer software for analysis, makes this technology extremely expensive and therefore, out of the realm of most individual researchers (Kurian et al., 1999). Despite the disadvantages, cDNA microarray technology has tremendous potential and as modifications occur, it is likely to become much more accessible, affordable and an invaluable tool for such things as gene expression analysis, genotyping and gene mapping.

At present a *Xenopus* chip exists that contains 900 clones (Hemmati-Brivanlou & Altmann, XMMR homepage), which were obtained from a gastrula expression library and also includes a number of tissue-specific markers. It is hoped that eventually most known *Xenopus* genes will be included on this chip. Perhaps, in the future, this



microarray technology may provide a more efficient and precise method of identifying differentially expressed genes than the current differential display method.

## 4.6 Conclusion

My investigation into the genes involved in *Xrel3*-induced tumorigenesis provides preliminary evidence for a role of *Xrel3* in neural differentiation, possibly by promoting cell proliferation to ensure that adequate numbers of cells are present in the structures in which it is expressed. Although Shh and Gli1 are involved in patterning the neural floor plate and regions of the brain, they are also involved in other developmental processes, including somite formation. Further expression analysis is required to determine whether other neural patterning genes, are also upregulated in *Xrel3*-induced tumours.

Not only can *Xrel3* overexpression in the animal pole induce tumours, but it also can induce tumours after injection into the vegetal pole (Yang et al., 1998). This suggests that a conserved pathway or mechanism is involved in *Xrel3*-induced tumorigenesis. Investigations into *Xrel3*-induced tumorigenesis after vegetal pole injection is required. Perhaps the identification of some of the early response target genes will help provide some of the answers. In addition, the identification of down-regulated genes in response to *Xrel3* overexpression might provide an important insight into *Xrel3* activity.

It is evident that the mechanism of *Xrel3*-induced tumorigenesis and how this reflects on its role during embryonic development is quite complex and likely to involve more than one pathway. In addition, it is also highly likely that other Rel/NF- $\kappa$ B proteins are involved. More direct methods of assessing protein function such as the development

of anti-Xrel3 antibodies and the generation of dominant negative mutants to knock-out Xrel3 activity may help to provide some additional insight.

---

## References

- Acampora, D., Gulisano, M. and Simeone, A. (2000). Genetic and molecular roles of Otx homeodomain proteins in head development. *Gene* **246**: 23-35.
- Alcedo, J., Ayzenzon, M., Von Ohlen, T., Noll, M. and Hooper, J.E. (1996). The *Drosophila smoothened* gene encodes a seven-pass membrane protein, a putative receptor for the hedgehog signal. *Cell* **86**(2): 221-32.
- Alcedo, J. and Noll, M. (1997). Hedgehog and its patched-smoothened receptor complex: a novel signalling mechanism at the cell surface. *Biol. Chem.* **378**(7): 583-90.
- Ahlgren, S.C. and Bronner-Fraser, M. (1999). Inhibition of sonic hedgehog signaling *in vivo* results in craniofacial neural crest cell death. *Curr. Biol.* **9**(22): 1304-14.
- Amaya, E., Musci, T.J. and Kirschner, M.W. (1991). Expression of a dominant negative mutant of the FGF receptor disrupts mesoderm formation in *Xenopus* embryos. *Cell* **66**: 257-270.
- Andreazzoli, M., Pannese, M. and Boncinelli, E. (1997). Activating and repressing signals in head development: the role of *Xotx1* and *Xotx2*. *Development* **124**: 1733-1743.
- Ang, S-L. and Rossant, J. (1994). HNF-3 $\beta$  is essential for node and notochord formation in mouse development. *Cell* **78**: 561-574.
- Barkett, M. and Gilmore, T.D. (1999). Control of apoptosis by Rel/NF-kappaB transcription factors. *Oncogene* **18**: 6910-6924.
- Barth, T.F., Dohner, H., Werner, C.A., Stilgenbauer, S., Schlotter, M., Pawlita, M., Lichter, P., Moller, P. and Bentz, M. (1998). Characteristic pattern of chromosomal gains and losses in primary large B-cell lymphomas of the gastrointestinal tract. *Blood* **91**(11): 4321-30.
- Bearer, E.L. (1994). Distribution of Xrel in the early *Xenopus* embryo: a cytoplasmic and nuclear gradient. *Eur. J. Cell Biol.* **63**(2): 255-268.
- Berry, D. L., Schwartzman, R. A. and Brown, D. D. (1998). The expression pattern of thyroid hormone response genes in the tadpole tail identifies multiple resorption programs. *Dev. Biol.* **203**: 12-23.
- Bourez, R.L., Mathijssen, I.M., Vaandrager, J.M. and Vermeij-Keers, C. (1997). Apoptotic cell death during normal embryogenesis of the coronal suture: early detection of apoptosis in mice using annexin V. *J. Craniofac. Surg.* **8**(6): 441-5.

- Branford, W.W., Essner, J.J. and Yost, H.J. (2000). Regulation of gut and heart left-right asymmetry by context-dependent interactions between *Xenopus* lefty and BMP4 signaling. *Dev. Biol.* **223**: 291-306.
- Britto, J. M., Tannahill, D. and Keynes, R. J. (2000). Life, death and sonic hedgehog. *BioEssays* **22**(6), 499-502.
- Brown, D. D., Wang, Z., Furlow, J. D., Kanamori, A., Schwartzman, R. A., Remo, B. F. and Pinder A. (1996). The thyroid hormone-induced tail resorption program during *Xenopus laevis* metamorphosis. *Proc. Natl. Acad. Sci. USA* **93**: 1924-1929.
- Bueno D., Skinner J., Abud H. and Heath, J.K. (1996). Spatial and temporal relationships between *Shh*, *Fgf4*, and *Fgf8* gene expression at diverse signalling centers during mouse development. *Dev Dyn.* **207**(3): 291-9.
- Burstein, J. and Braunstein, G.D. (1995). Urine pregnancy tests from antiquity to the present. *Early Pregnancy* **1**(4): 288-296.
- Bushdid, P. B., Brantley, D. M., Yull, F. E., Blaeuer, G. L., Hoffman, L. H., Niswander, L. and Kerr, L. D. (1998). Inhibition of NF- $\kappa$ B activity results in disruption of the apical ectodermal ridge and aberrant limb morphogenesis. *Nature* **392**: 615-618.
- Caamaño, J.H., Rizzo, C.A., Durham, S.K., Barton, D.S., Raventos-Suarez, C., Snapper, C.M. and Bravo, R. (1998). Nuclear factor (NF)-Kappa B2 (p100/p52) is required for normal splenic microarchitecture and B cell-mediated immune responses. *J. Exp. Med.* **187**(2): 185-196.
- Cabannes, E., Khan, G., Aillet, F., Jarrett, R.F. and Hay, R.T. (1999). Mutations in the *IkBa* gene in Hodgkin's disease suggest a tumour suppressor role for *IkappaB* alpha. *Oncogene* **18**(20): 3063-70.
- Cameron, J.A. and Fallon, J.F. (1977). Evidence for polarizing zone in the limb buds of *Xenopus laevis*. *Dev Biol.* **55**(2): 320-30.
- Capdevila, J. and Izpisua Belmonte, J.C. (2000). Knowing left from right: the molecular basis of laterality defects. *Mol. Med. Today* **6**: 112-118.
- Chang, P., Perez-mongiovi and Houlston, E. (1999). Organisation of *Xenopus* oocyte and egg cortices. *Microsc. Res. Tech.* **44**(6): 415-29.
- Chen, C., Edelstein, L.C. and Gelinas, C. (2000). The Rel/NF- $\kappa$ B family directly activates expression of the apoptosis inhibitor Bcl-x(L). *Mol. Cell. Biol.* **20**: 2687-2695.

- Chen, F. E and Ghosh, G. (1999). Regulation of DNA binding by Rel/NF- $\kappa$ B transcription factors: structural views. *Oncogene* **18**, 6845-6851.
- Chen, R-H., Ding, W.V. and McCormick, F. (2000). Wnt signaling to  $\beta$ -catenin involves two interactive components. Glycogen synthase kinase-3 $\beta$  inhibition and activation of protein kinase C. *J. Biol. Chem.* **275**(23): 17894-9.
- Christen, B. and Slack, J. M. W. (1997). FGF-8 is associated with anteroposterior patterning and limb regeneration in *Xenopus*. *Dev. Biol.* **192**: 455-466.
- Connolly, D.J., Patel, K., Withington, S. and Cooke, J. (2000). Effects of follistatin and BMP4 proteins on early dorso-ventral patterning in chick. *Int. J. Dev. Biol.* **44**: 129-140.
- Cox, W.G. and Hemmati-Brivanlou, A. (1995).. Caudalization of neural fate by tissue recombination and bFGF. *Development* **121**(12): 4349-4358.
- Crossley, P.H., Minowada, G., MacArthur, C.A., and Martin, G.R. (1996). Roles for FGF8 in the induction, initiation, and maintenance of chick limb development. *Cell* **84**(1): 127-36.
- Dahmane, N., Lee, J., Robins, P., Heller, P. and Ruiz i Altaba, A. (1997). Activation of the transcription factor Gli1 and the sonic hedgehog signalling pathway in skin tumours. *Nature* **389**, 876-881.
- Dale, L. and Jones, C.M. (1999). BMP signalling in early *Xenopus* development. *BioEssays* **21**(9): 751-760.
- Damjanovski, S., Puzianowska-Kuznicka, M., Ishizuya-Oka, A. and Shi, Y.B. (2000). Differential regulation of three thyroid hormone-responsive matrix metalloproteinase genes implicates distinct functions during frog embryogenesis. *FASEB J.* **14**(3): 503-510.
- Danilchik, M. V. and Gerhart, J. C. (1987). Differentiation of the animal-vegetal axis in *Xenopus laevis* oocytes. I. Polarized intracellular translocation of platelets establishes the yolk gradient. *Dev. Biol.* **122**(1): 101-12.
- Dean, M. (1998). Cancer as a complex developmental disorder--nineteenth Cornelius P. Rhoads Memorial Award Lecture. *Cancer Res.* **58**(24): 5633-6.
- Deconinck, A.E., Mead, P.E., Tevosian, S.G., Crispino, J.D., Katz, S.G., Zon, L.I. and Orkin, S.H. (2000). FOG acts as a repressor of red blood cell development in *Xenopus*. *Development* **127**: 2031-2040.

- Dejardin, E., Bonizzi, G., Bellahcene, A., Castronovo, V., Merville, M.P. and Bours, V. (1995). Highly-expressed p100/p52 (NFKB2) sequesters other NF-kappa B related proteins in the cytoplasm of human breast cancer cells. *Oncogene* **11**(9): 1835-41.
- Dejardin, E., Deregowski, V., Chapelier, M., Jacobs, N., Gielen, J., Merville, M.P. and Bours, V. (1999). Regulation of NF-kappaB activity by I kappaB-related proteins in adenocarcinoma cells. *Oncogene* **18**(16): 2567-77.
- deMartin, R., Schmid, J. A. and Hofer-Warbinek, R. (1999). The NF- $\kappa$ B/Rel family of transcription factors in oncogenic transformation and apoptosis. *Mutat. Res.* **437**, 231-243.
- Devalaraja, M. N., Wang, D.Z., Ballard, D.W. and Richmond, A. (1999). Elevated constitutive I kappaB kinase activity and I kappaB-alpha phosphorylation in Hs294T melanoma cells lead to increased basal MGSA/GRO-alpha transcription. *Cancer Res.* **59**(6): 1372-7.
- Doi, T.S., Marino, M.W., Takahashi, T., Yoshida, T., Sakakura, T., Old, L.J. and Obata, Y. (1999). Absence of tumor necrosis factor rescues Rel A-deficient mice from embryonic lethality. *Proc. Natl. Acad. Sci. USA* **96**(6): 2994-2999.
- Doniach, T. (1995). Basic FGF as an inducer of anteroposterior neural pattern. *Cell* **83**(7): 1067-1070.
- Drier, E.A. and Steward, R. (1997). The dorsoventral signal transduction pathway and the Rel-like transcription factors in *Drosophila*. *Sem. Cancer Biol.* **8**: 83-92.
- Drier, E.A., Govind, S. and Steward, R. (2000). Cactus-independent regulation of Dorsal nuclear import by the ventral signal. *Curr. Biol.* **13**: 23-26.
- Echelard, Y., Epstein, D.J., St-Jacques, B., Shen, L., Mohler, J., McMahon, J.A. and McMahon, A.P. (1993). Sonic hedgehog, a member of a family of putative signaling molecules, is implicated in the regulation of CNS polarity. *Cell* **75**(7): 1417-30.
- Edwards, P.A. (1999). The impact of developmental biology on cancer research: an overview. *Cancer Metastasis Rev.* **18**(2): 175-80.
- Ekker, S.C., McGrew, L.L., Lai, C.J., Lee, J.J., von Kessler, D.P., Moon, R.T. and Beachy, P.A. (1995). Distinct expression and shared activities of members of the hedgehog gene family of *Xenopus laevis*. *Development* **121**(8): 2337-47.

- el Ghouzzi, V., Le Merrer, M., Perrin-Schmitt, F., Lajeunie, E., Benit, P., Renier, D., Bourgeois, P., Bolcato-Bellemin, A.L., Munnich, A. and Bonaventure, J. (1997). Mutations of the TWIST gene in the Saethre-Chotzen syndrome. *Nat. Genet.* **15**(1): 42-6.
- Elinson, R.P. (1975). Site of sperm entry and a cortical contraction associated with egg activation in the frog *Rana pipiens*. *Dev. Biol.* **47**: 257-268.
- Emori, Y. and Saigo, K. (1993). Distinct expression of two *Drosophila* homologs of fibroblast growth factor receptors in imaginal discs. *FEBS Lett.* **332**: 111-4.
- Endo, T., Yokoyama, H., Tamura, K., and Ide, H. (1997). *Shh* expression in developing and regenerating limb buds of *Xenopus laevis*. *Dev Dyn.* **209**(2): 227-32.
- Essner, J.J., Branford, W.W., Zhang, J. and Yost, H.J. (2000). Mesendoderm and left right brain, heart and gut development are differentially regulated by *pitx2* isoforms. *Development* **127**: 1081-1093.
- Feener C.A., Koenig, M. and Kunkel, L.M. (1989). Alternative splicing of human dystrophin mRNA generates isoforms at the carboxy terminus. *Nature* **338**: 509-511.
- Ferrell, Jr., J. E. (1999). *Xenopus* oocyte maturation: new lessons from a good egg. *BioEssays* **21**(10): 833-842.
- Ferrier, R., Nougarede, R., Doucet, S., Kahn-Perles, B., Imbert, J. and Mathieu-Mahul, D. (1999). Physical interaction of the bHLH LYL1 protein and NF-kappaB1 p105. *Oncogene* **18**(4): 995-1005.
- Foo, S. Y. and Nolan, G. P. (1999). NF- $\kappa$ B to the rescue: RELs, apoptosis and cellular transformation. *Trends Genet.* **15**(6): 229-235.
- Forristall, C., Pondel, M., Chen, L. and King, M.L. (1995). Patterns of localization and cytoskeletal association of two vegetally localized RNAs, *Vgl* and *Xcat-2*. *Development* **121**: 201-208.
- Franzoso, G., Carlson, L., Poljak, L., Shores, E.W., Epstein, S., Leonardi, A., Grinberg, A., Tram, T., Scharon-Kersten, T., Anver, M., Love, P., Brown, K. and Siebenlist, U. (1998). Mice deficient in nuclear factor (NF)-kappa B/p52 present with defects in humoral responses, germinal center reactions, and splenic microarchitecture. *J.Exp. Med.* **187**(2): 147-159.
- Furlow, J.D. and brown, D.D. (1999). In vitro and in vivo analysis of the regulation of a transcription factor gene by thyroid hormone during *Xenopus laevis* metamorphosis. *Mol. Endocrinol.* **13**(12): 2076-2079.

- Gammill L. S. and Sive H. (1997). Identification of *otx2* target genes and restrictions in ectodermal competence during *Xenopus* cement gland formation. *Development* **124**: 471-481.
- Gammill, L. S. and Sive, H. (2000). Coincidence of *otx2* and BMP4 signaling correlates with *Xenopus* cement gland formation. *Mech. Dev.* **92**: 217-226.
- Gerondakis, S., Grossmann, M., Nakamura, Y., Pohl, T. and Grumont, R. (1999). Genetic approaches in mice to understand Rel/NF- $\kappa$ B and I $\kappa$ B function: transgenics and knockouts. *Oncogene* **18**, 6888-6895.
- Gerhart, J., Ubbels, G., Black, S., Hara, K. and Kirschner, M. (1981). A reinvestigation of the role of the grey crescent in axis formation in *Xenopus laevis*. *Nature* **292**: 511-516.
- Gerhart, J., Danilchik, M., Doniach, T., Roberts, S., Rowning, B. and Stewart, R. (1989). Cortical rotation of the *Xenopus* egg: consequences for the anteroposterior pattern of embryonic dorsal development. *Development* **107**: 37-51.
- Ghali, L., Wong, S.T., Green, J., Tidman, N. and Quinn, A.G. (1999). Gli1 protein is expressed in basal cell carcinomas, outer root sheath keratinocytes and a subpopulation of mesenchymal cells in normal human skin. *J. Invest. Dermatol.* **113**(4): 595-9.
- Ghossein, R.A., Carusone, L. and Bhattacharya, S. (2000). Molecular detection of micrometastases and circulating tumor cells in melanoma prostatic and breast carcinomas. *In Vivo* **14**(1): 237-50.
- Gilmore, T. (1999). The Rel/NF- $\kappa$ B signal transduction pathway: introduction. *Oncogene* **18**, 6842-6844.
- Gilmore, T. D. (1999). Multiple mutations contribute to the oncogenicity of the retroviral oncoprotein v-Rel. *Oncogene* **18**, 6925-6937.
- Givol, D. and Yayon, A. (1992). Complexity of FGF receptors: genetic basis for structural diversity and functional specificity. *FASEB J.* **6**(15): 3362-9.
- Godsave, S.F. and Slack, J.M.W. (1989). Clonal analysis of mesoderm induction in *Xenopus laevis*. *Dev. Biol.* **134**(2): 486-490.
- Gorlin, R.J. (1995). Nevoid basal cell carcinoma syndrome. *Dermatol. Clin.* **13**(1): 113-25.
- Govind, S. (1999). Control of development and immunity by Rel transcription factors in *Drosophila*. *Oncogene* **18**, 6875-6887.



- Grant, P. and Wacaster, J.F. (1972). The amphibian gray crescent region – a site of developmental information? *Dev. Biol.* 28(3): 454-471.
- Grumont, R.J., Richardson, I.B., Gaff, C. and Gerondakis, S. (1993). rel/NF-kappa B nuclear complexes that bind kB sites in the murine c-rel promoter are required for constitutive c-rel transcription in B-cells. *Cell Growth Differ.* 4(9): 731-43.
- Grumont, R.J., Rourke, I.J., O'Reilly, L.A., Strasser, A., Miyake, K., Sha, W. and Gerondakis, S. (1998). B lymphocytes differentially use the Rel and nuclear factor kappa B1 (NF-kappaB1) transcription factors to regulate cell cycle progression and apoptosis in quiescent and mitogen-activated cells. *J. Exp. Med.* 187(5): 663-674.
- Grunz, H. and Tacke, L. (1989). Neural differentiation of *Xenopus laevis* ectoderm takes place after disaggregation and delayed reaggregation without inducer. *Cell Diff. Dev.* 28: 211-218.
- Hansen, C.S., Marion, C.D., Steele, K., George, S. and Smith, W.C. (1997). Direct neural induction and selective inhibition of mesoderm and epidermis inducers by Xnr3. *Development* 124(2): 483-492.
- Hahn, H., Wicking, C., Zaphiropoulos, P.G., Gailani, M.R., Shanley, S., Chidambaram, A., Vorechovsky, I., Holmberg, E., Unden, A.B., Gillies, S., Negus, K., Smyth, I., Pressman, C., Leffell, D.J., Gerrard, B., Goldstein, A.M., Dean, M., Toftgard, R., Chenevix-Trench, G., Wainwright, B. and Bale, A.E. (1996). Mutations of the human homolog of *Drosophila patched* in the nevoid basal cell carcinoma syndrome. *Cell* 85(6): 841-51.
- Hawley, S.H., Wunnenberg-Stapleton, K., Hashimoto, C., Laurent, M.N., Watabe, T., Blumberg, B.W. and Cho, K.W. (1995). Disruption of BMP signals in embryonic *Xenopus* ectoderm leads to direct neural induction. *Genes Dev.* 9(23): 2923-2935.
- He, X., Saint-Jennet, J-P., Woodgett, J.R., Varmus, H.E. and Dawid, I.B. (1995). Glycogen synthase kinase-3 and dorsoventral patterning in *Xenopus* embryos. *Nature* 374: 617-622.
- Heasman, J. (1997). Patterning the *Xenopus* blastula. *Development* 124: 4179-4191.
- Hemmati-Brivanlou, A. and Melton, D.A. (1992). A truncated activin receptor inhibits mesoderm induction and formation of axial structures in *Xenopus* embryos. *Nature* 359: 609-14.
- Hemmati-Brivanlou, A. and Altmann, C.R. [http://vize222.zo.utexas.edu/Marker\\_pages/arrays/microarrays.html](http://vize222.zo.utexas.edu/Marker_pages/arrays/microarrays.html)

- Holowacz, T. and Sokol, S. (1999). FGF is required for posterior neural patterning but not for neural induction. *Dev. Biol.* **205**(2): 296-308.
- Hongo, I., Kengaku, M. and Okamoto, H. (1999). FGF signalling and the anterior neural induction in *Xenopus*. *Dev. Biol.* **216**(2): 561-581.
- Hopwood, N. D., Pluck, A. and Gurdon, J. B. (1989). A *Xenopus* mRNA related to *Drosophila twist* is expressed in response to induction in the mesoderm and the neural crest. *Cell* **59**: 893-903.
- Houldsworth, J., Mathew, S., Rao, P.H., Dyomina, K., Louie, D.C., Parsa, N., Offit, K. and Chaganti, R.S. (1996). REL proto-oncogene is frequently amplified in extranodal diffuse large cell lymphoma. *Blood* **87**(1): 25-9.
- Howard, T.D., Paznekas, W.A., Green, E.D., Chiang, L.C., Ma, N., Ortiz de Luna, R.I., Garcia Delgado, C., Gonzalez-Ramos, M., Kline, A.D. and Jabs, E.W. (1997). Mutations in TWIST, a basic helix-loop-helix transcription factor, in Saethre-Chotzen syndrome. *Nat. Genet.* **15**(1): 36-41.
- Hunt, T. (1989). Maturation promoting factor, cyclin and the control of M-phase. *Curr. Opin. Cell. Biol.* **1**(12): 268-274.
- Iemura, S., Yamamoto, T.S., Takagi, C., Uchiyama, H., Natsume, T., Shimaski, S., Sugino, H. and Ueno, N. (1998). Direct binding of follistatin to a complex of bone-morphogenetic protein and its receptor inhibits ventral and epidermal cell fates in early *Xenopus* embryo. *Proc. Natl. Acad. Sci. USA* **95**(16): 9337-9342.
- Imbert, V., Rupec, R.A., Livolsi, A., Pahl, H.L., Traenknes, E.B., Mueller-Dieckmann, C., Fariahifar, D., Rossi, B., Auberger, P., Baeuerle, P.A. and Peyron, J.F. (1996). Tyrosine phosphorylation of I kappa B-alpha activates NF-kappa B without proteolytic degradation of I kappa B-alpha. *Cell* **86**(5): 787-798.
- Ingham, P.W. (1998). Boning up on Hedgehog's movements. *Nature* **394**: 16-7.
- Isaacs H. V. (1997). New perspectives on the role of the fibroblast growth factor family in amphibian development. *Cell Mol. Life Sci.* **53**(4): 350-361.
- Isaacs, H.V., Pownall, M.E. and Slack, J.M.W. (1994). eFGF regulates *Xbra* expression during *Xenopus* gastrulation. *EMBO J.* **13**: 4469-4481.
- Isaacs, H.V., Tannahill, D. and Slack, J.M.W. (1992). Expression of a novel FGF in the *Xenopus* embryo. A new candidate inducing factor for mesoderm formation and anteroposterior specification. *Development* **114**: 711-720.
- Jensen, A.M. and Wallace, V.A. (1997). Expression of Sonic hedgehog and its putative role as a precursor cell mitogen in the developing mouse retina. *Development* **124**(2): 363-71.

- Johnson, R.L., Rothman, A.L., Xie, J., Goodrich, L.V., Bare, J.W., Bonifas, J.M., Quinn, A.G., Myers, R.M., Cox, D.R., Epstein, E.H. Jr. and Scott, M.P. (1996). Human homolog of *patched*, a candidate gene for the basal cell nevus syndrome. *Science* **272**: 1668-71.
- Johnson, R.L. and Tabin, C.J. (1997). Molecular models for vertebrate limb development. *Cell* **90**: 979-990.
- Jones, C. M. and Smith, J. C. (1999). An overview of *Xenopus* development. *Methods Mol. Biol.* **97**: 331-40.
- Kanegae, Y., Tavares, A. T., Belmonte, J. C. I. and Verma, I. M. (1998). Role of Rel/NF- $\kappa$ B transcription factors during the outgrowth of the vertebrate limb. *Nature* **392**: 611-614.
- Kao, K.R. and Elinson, R.P. (1988). The entire mesodermal mantle behaves as Spemann's organizer in dorsoanterior enhanced *Xenopus laevis* embryos. *Dev. Biol.* **127**(1): 64-77.
- Kao, K. R. and Lockwood, A. (1996). Negative regulation of dorsal patterning in early embryos by overexpression of XrelA, a *Xenopus* homologue of NF- $\kappa$ B. *Mech. Devel.* **58**, 129-139.
- Karin, M. (1999). How NF- $\kappa$ B is activated: the role of the I $\kappa$ B kinase (IKK) complex. *Oncogene* **18**, 6867-6874.
- Keller, R., Shih, J. and Slater, A. (1992). The cellular basis of the convergene and extension of the *Xenopus* neural plate. *Dev. Dyn.* **193**(3): 218-234.
- Kessler, D.S. and Melten, D.A. (1994). Vertebrate embryonic induction: mesodermal and neural patterning. *Science* **266**: 596-604.
- Khan, J., Saal, L.H., Bittner, M.L., Chen, Y., Trent, J.M., and Meltzer, P.S. (1999). Expression profiling in cancer using cDNA microarrays. *Electrophoresis* **20**(2): 223-9.
- Kimelman, D., Kirschner, M. and Scherson, T. (1987). The events of the midblastula transition in *Xenopus* are regulated by changes in the cell cycle. *Cell* **48**(3): 399-407.
- Kinzler, K.W., Ruppert, J.M., Bigner, S.H. and Vogelstein, B. (1988). The GLI gene is a member of the Kruppel family of zinc finger proteins. *Nature* **332**: 371-4.
- Klein, P.S. and Melton, D.A. (1996). A molecular mechanism for the effect of lithium on development. *Proc. Natl. Acad. Sci. U S A* **93**(16): 8455-9.

- Kofron, M., Demel, T., Xanthos, J., Lohr, J., Sun, B., Sive, H., Osada, S., Wright, C., Wylie, C. and Heaseman, J. (1999). Mesoderm induction in *Xenopus* is a zygotic event regulated by maternal VegT via TGF beta growth factors. *Development* 126(24): 5759-5770.
- Kraemer, B.B., Silva, E.G. and Sneige, N. (1984). Fibrosarcoma of ovary. A new component in the nevoid basal-cell carcinoma syndrome. *Am J Surg Pathol.* 8(3): 231-6.
- Krappmann, D., Emmerich, F., Kordes, U., Scharschmidt, E., Dorken, B. and Scheidereit, C. (1999). Molecular mechanisms of constitutive NF-kappaB/Rel activation in Hodgkin/Reed-Sternberg cells. *Oncogene* 18(4): 943-53.
- Kurian, K.M., Watson, C.J., and Wyllie, A.H. (1999). DNA chip technology. *J Pathol.* 187(3): 267-71.
- Kurtz, A., Wang, H.L., Darwiche, N., Harris, V. and Wellstein, A. (1997). Expression of a binding protein for FGF is associated with epithelial development and skin carcinogenesis. *Oncogene* 14(22): 2671-81.
- Lake, B.B., Ford, R. and Kao, K.R. (2000). *Xrel3* is required for head development of *Xenopus laevis*. *Development* (In press).
- Lam, C.W., Xie, J., To, K.F., Ng, H.K., Lee, K.C., Yuen, N.W., Lim, P.L., Chan, L.Y., Tong, S.F. and McCormick, F. (1999). A frequent activated smoothened mutation in sporadic basal cell carcinomas. *Oncogene* 18(3): 833-6.
- Larrain, J., Bachiller, D., Lu, B., Agius, E., Piccolo, S. and De Robertis, E.M. (2000). BMP-binding modules in chordin: a model for signalling regulation in the extracellular space. *Development* 127(4): 821-830.
- Laufer, E., Nelson, C. E., Johnson, R. L., Morgan, B. A. and Tabin, C. (1994). *Sonic hedgehog* and *Fgf-4* act through a signalling cascade and feedback loop to integrate growth and patterning of the developing limb bud. *Cell* 79: 993-1003.
- Lee, J., Platt, K.A., Censullo, P. and Ruiz i Altaba, A. (1997). Gli1 is a target of sonic hedgehog that induces ventral neural tube development. *Development* 24(13): 2537-52.
- Lemaire, P., Garrett, N. and Gurdon, J.B. (1995). Expression cloning of *Siamois*, a *Xenopus* homeobox gene expressed in dorsal-vegetal cells of blastulae and able to induce a complete secondary axis. *Cell* 81(1): 85-94.
- Leyns, L., Bouwmeester, T., Kim, S-H., Piccolo, S. and De Robertis, E.M. (1997). *Frzb* 1 is a secreted antagonist of Wnt signalling expressed in the spermann organizer. *Cell* 88: 747-756.

- Li, N. and Karin, M. (1998). Ionizing radiation and short wavelength UV activate NF-kappa B through two distinct mechanisms. *Proc. Natl. Acad. Sci. USA* **95**(22): 13012-7.
- Liang, P. and Pardee, A.B. (1992). Differential display of eukaryotic messenger RNA by means of the polymerase chain reaction. *Science* **257**: 967-970.
- Liang, P., Zhu, W., Zhang, X., Guo, Z., O'Connell, R.P., Averboukh, L., Wang, F. and Pardee, A.B. (1994). Differential display using one-base anchored oligo-dT primers. *Nucleic Acids Res.* **22**(25): 5763-5764.
- Liu, W., Ren, C., Shi, J., Feng, X., He, Z., Xu, L., Lan, K., Xie, L., Peng, Y., Fan, J., Kung, H.F., Yao, K.T. and Xu, R.H. (2000). Characterization of the functionally related sites in the neural inducing gene noggin. *Biochem. Biophys. Res. Commun.* **270**(1): 293-297.
- Louache, F., Debili, N., Cramer, E., Breton-Gorius, J. and Vainchenker, W. (1991). Fibrinogen is not synthesized by human megakaryocytes. *Blood* **77**: 311-316.
- Maestro, R., Dei Tos, A. P., Hamamori, Y., Krasnokutsky, S., Sartorelli, V., Kedes, L., Doglioni, C., Beach, D. H. and Hannon, G. J. (1999). *Twist* is a potential oncogene that inhibits apoptosis. *Genes Dev.* **13**(17): 2207-17.
- Malacinski, G. M., Benford, H. and Chung, H. M. (1975). Association of an ultraviolet irradiation sensitive cytoplasmic localization with the future dorsal side of the amphibian egg. *J. Exp. Zool.* **191**: 97-110.
- Marigo, V., Davey, R.A., Zuo, Y., Cunningham, J.M. and Tabin, C.J. (1996). Biochemical evidence that patched is the hedgehog receptor. *Nature* **384**: 176-9.
- Marine, J.C., Bellefroid, E.J., Pendeville, H., Martial, J.A. and Pieler, T. (1997). A role for *Xenopus* Gli-type zinc finger proteins in the early embryonic patterning of mesoderm and neuroectoderm. *Mech Dev.* **1997** **63**(2): 211-25.
- Masui, V. and Wang, P. (1998). Cell cycle transition in early embryonic development of *Xenopus laevis*. *Biol. Cell.* **90**(8): 337-348.
- Mathew, S., Murty, V.V., Dalla-Favera, R. and Chaganti, R.S. (1993). Chromosomal localization of genes encoding the transcription factors, c-rel, NF-kappa Bp50, NF-kappa Bp65, and lyt-10 by fluorescence *in situ* hybridization. *Oncogene* **8**(1): 191-3.
- Matise, M. P. and Joyner, A. L. (1999). *Gli* genes in development and cancer. *Oncogene* **18**, 7852-7859.

- May, M. J. and Ghosh, S. (1998). Signal transduction through NF- $\kappa$ B. *Immunology Today* 19(2): 80-88.
- McGrew, L.L., Hoppler, S. and Moon, R.T. (1997). Wnt and FGF pathways cooperatively pattern anteroposterior neural ectoderm in *Xenopus*. *Mech. Dev.* 69: 105-114.
- Mercurio, F. and Manning, A. (1999). Multiple signals converging on NF- $\kappa$ B. *Curr. Opin. Cell. Biol.* 11: 226-232.
- Michaux, L., Dierlamm, J., Wlodarska, I., Bours, V., Van den Berghe, H. and Hagemeijer, A. (1997). t(14;19)/BCL3 rearrangements in lymphoproliferative disorders: a review of 23 cases. *Cancer Genet Cytogenet* 94(1): 36-43.
- Mignatti, P., Morimoto, T. and Rifkin, D.B. (1992). Basic fibroblast growth factor, a protein devoid of secretory signal sequence, is released by cells via a pathway independent of the endoplasmic reticulum-Golgi complex. *J. Cell. Physiol.* 151: 81-93.
- Ming, J.E., Roessler, E. and Muenke, M. (1998). Human developmental disorders and the Sonic hedgehog pathway. *Mol. Med. Today* 4(8): 343-9.
- Mohun, T.J., Garrett, N. and Gurdon, J.B. (1986). Upstream sequences required for tissue-specific activation of the cardiac actin gene in *Xenopus laevis* embryos. *EMBO J.* 5(12): 3185-93.
- Moon, R. T. and Kimelman, D. (1998). From cortical rotation to organizer gene expression: toward a molecular explanation of axis specification in *Xenopus*. *BioEssays* 20: 536-545.
- Moon, R.T., Brown, J.D., Yang-Snyder, J.A. and Miller, J.R. (1997). Structurally related receptors and antagonists compete for secreted Wnt ligands. *Cell* 88: 725-728.
- Mosiales, G. and Gilmore, T. D. (1992). V-Rel and c-Rel are differentially affected by mutations at a consensus protein kinase recognition sequence. *Oncogene* 8, 721-730.
- Mukhopadhyay, T., Roth, J.A. and Maxwell, S.A. (1995). Altered expression of the p50 subunit of the NF-kappa B transcription factor complex in non-small cell lung carcinoma. *Oncogene* 11(5): 999-1003.
- Nakamura, O. and Takasaki, H. (1970). Further studies on the differentiation capacity of the dorsal marginal zone in the morula of *Triturus pyrrhogaster*. *Proc. Japan Acad.* 46: 700-705.

- Neri, A., Fracchiolla, N.S., Roscetti, E., Garatti, S., Trecca, D., Boletini, A., Perletti, L., Baldini, L., Maiolo, A.T. and Berti, E. (1995). Molecular analysis of cutaneous B- and T-cell lymphomas. *Blood* **86**(8): 3160-72.
- Newport, J.W. and Kirschner, M.W. (1984). Regulation of the cell cycle during *Xenopus laevis* development. *Cell* **37**: 731-742.
- Newton, T.R., Patel, N.M., Bhat-Nakshatri, P., Stauss, C.R., Goulet, R.J. Jr. and Nakshatri, H. (1999). Negative regulation of transactivation function but not DNA binding of NF-kappaB and AP-1 by IkappaBbeta1 in breast cancer cells. *J. Biol. Chem.* **274**(26): 18827-35.
- Niehrs, C., Steinbeisser, H. and De Robertis, E.M. (1994). Mesodermal patterning by a gradient of the vertebrate homeobox gene *goosecoid*. *Science* **263**: 817-20.
- Nieuwkoop, P.D. (1969). The formation of the mesoderm in urodele amphibians. I. Induction by the endoderm. *Wilhelm Roux Arch. Entw. Org.* **162**: 341-373.
- Nieuwkoop, P.D. and Faber, J. (1994). *Normal Table of Xenopus laevis* (Daudin). Garland Publishing, Inc., New York.
- Nollau, P., Jung, R., Meumaier, M. and Wagener, C. (1995). Tumour diagnosis by PCR based detection of tumour cells. *Scand. J. Clin. Lab. Invest. Suppl.* **221**: 116-21.
- Nuccitelli, R. (1991). How do sperm activate eggs? *Curr. Top. Dev. Biol.* **25**: 1-16.
- Nunez, D.J.R., Davenport, A.P. and Brown, M.J. (1990). Atrial natriuretic factor mRNA and binding sites in the adrenal gland. *Biochem. J.* **271**: 555-558.
- Ohuchi, H., Nakagawa, T., Yamamoto, A., Araga, A., Ohata, T., Ishimaru, Y., Yoshioka, H., Kuwana, T., Nohno, T., Yamasaki, M., Itoh, N. and Noji, S. (1997). The mesenchymal factor, FGF10, initiates and maintains the outgrowth of the chick limb bud through interaction with FGF8, an apical ectodermal factor. *Development* **124**: 2235-2244.
- O'Reilly, M.A., Smith, J.C. and Cunliffe, V. (1995). Patterning of the mesoderm in *Xenopus*: dose-dependent and synergistic effects of Brachyury and Pintallavis. *Development* **121**(5): 1351-1359.
- Oro, A.E., Higgins, K.M., Hu, Z., Bonifas, J.M., Epstein, E.H. Jr. and Scott, M.P. (1997). Basal cell carcinomas in mice overexpressing sonic hedgehog. *Science* **276**: 817-21.
- Orkin, S.H. (1992). GATA-binding transcription factors in hematopoietic cells. *Blood* **80**(3): 575-81.

- Ozawa, K., Uruno, T., Miyakawa, K., Seo, M. and Imamura, T. (1996). Expression of the fibroblast growth factor family and their receptor family genes during mouse brain development. *Brain Res. Mol. Brain Res.* **41**: 279-88.
- Pahl, H. L. (1999). Activators and target genes of Rel/NF- $\kappa$ B transcription factors. *Oncogene* **18**, 6853-6865.
- Pannese, M., Polo, C., Andreazzoli, M., Vignali, R., Kablar, B., Barsacchi, G. and Boncinelli, E. (1995). The *Xenopus* homologue of *otx2* is a maternal homeobox gene that demarcates and specifies anterior body regions. *Development* **121**: 707-720.
- Paterno, G.D., Li, Y., Luchman, H.A., Ryan, P.J. and Gillespie, L.L. (1997). CDNA cloning of a novel, developmentally regulated immediate early gene activated by fibroblast growth factor and encoding a nuclear protein. *J. Biol. Chem.* **272**(41): 25591-5.
- Patterson, K.D., Drysdale, T.A. and Krieg, P.A. (2000). Embryonic origins of spleen asymmetry. *Development* **127**: 167-175.
- Phillips, C.R. (1991). Neural induction. *Methods Cell Biol.* **36**:329-46.
- Piccolo, S., Agius, E., Leyns, L., Bhattacharyya, S., Grunz, H., Bouwmeester, T. and De Robertis, E.M. (1999). The head inducer Cerberus is a multifunctional antagonist of Nodal, BMP and Wnt signals. *Nature* **397**: 707-10.
- Piccolo, S., Sasai, Y., Lu, B. and De Robertis, E.M. (1996). Dorsoventral patterning in *Xenopus*: inhibition of ventral signals by direct binding of chordin to BMP-4. *Cell* **86**: 589-598.
- Pierce, G.B., Arechaga, J. and Wells, R.S. (1986). Embryonic control of cancer. *Prog Clin Biol Res.* **226**: 67-77.
- Poznanski, A., Minsuk, S., Stathopoulos, D. and Keller, R. (1997). Epithelial cell wedging and neural trough formation are induced planarly in *Xenopus*, without persistent vertical interactions with mesoderm.
- Raffel, C., Jenkins, R.B., Frederick, L., Hebrink, D., Alderete, B., Fults, D.W. and James, C.D. (1997). Sporadic medulloblastomas contain *PTC* mutations. *Cancer Res.* **57**(5):842-5.
- Ramsdell, A.F. and Yost, H.J. (1998). Molecular mechanisms of vertebrate left-right development. *Trends Genet.* **14**(11): 459-465.



- Ramsdell, A.F. and Yost, H.J. (1999). Cardiac looping and the vertebrate left-right axis: antagonism of left-sided Vg1 activity by a right-sided ALK2-dependent BMP pathway. *Development* 126(23): 5195-205.
- Rao, P.H., Houldsworth, J., Dyomina, K., Parsa, N.Z., Cigudosa, J.C., Louie, D.C., Popplewell, L., Offit, K., Jhanwar, S.C. and Chaganti, R.S. (1998). Chromosomal and gene amplification in diffuse large B-cell lymphoma. *Blood* 92(1): 234-40.
- Rayet, B. and G  linas, C. (1999). Aberrant rel/nfkb genes and activity in human cancer. *Oncogene* 18(49): 6938-47.
- Richter, K., Good, P.J. and Dawid, I.B. (1990). A developmentally regulated, nervous system-specific gene in *Xenopus* encodes a putative RNA-binding protein. *New Biol.* 2(6): 556-65.
- Riddle, R.D., Johnson, R.L., Laufer, E., and Tabin, C. (1993). *Sonic hedgehog* mediates the polarizing activity of the ZPA. *Cell* 75(7): 1401-16.
- Riddle, R.D. and Tabin, C. (1999). How limbs develop. *Sci Am.* 280(2): 74-9.
- Rubenstein, J. L. R. and Beachy, P. A. (1998). Patterning of the embryonic forebrain. *Curr. Opin. Neurobiol.* 8: 18-26.
- Ruiz i Altaba, A. (1998). Combinatorial *Gli* gene function in floor plate and neuronal inductions by sonic hedgehog. *Development* 125(12): 2203-12.
- Ruiz i Altaba, A. (1999). Gli proteins and hedgehog signalling: development and cancer. *Trends Genet.* 15(10), 418-425.
- Runft, L. L., Watras, J. and Jaffe, L. A. (1999). Calcium release at fertilization of *Xenopus* eggs requires type I IP<sub>3</sub> receptors, but not SH2 domain-mediated activation of PLC $\gamma$  or G<sub>q</sub>-mediated activation of PLC $\beta$ . *Dev. Biol.* 214: 399-411.
- Sachdev, S., Hoffmann, A., Hannink, M. (1998). Nuclear localization of I kappa B alpha is mediated by the second ankyrin repeat: the I kappa B alpha ankyrin repeats define a novel class of cis-acting nuclear import sequences. *Mol. Cell. Biol.* 18(5), 2524-34.
- Saffman, E. E. and Lasko, P. (1999). Germline development in vertebrates and invertebrates. *Cell Mol. Life Sci.* 55: 1141-63.
- Sagata, N. (1998). Introduction: meiotic maturation and arrest in animal oocytes. *Semin. Cell. Dev. Biol.* 9(5): 533-537.
- Sanger, F., Nicklen, S. and Coulson, A.R. (1977). DNA sequencing with chain terminating inhibitors. *Proc. Natl. Acad. Sci. U S A* 74(12): 5463-7.

- Sasai, Y and De Robertis, E. M. (1997). Ectodermal patterning in vertebrate embryos. *Dev. Biol.* **182**(1): 5-20.
- Sato, S.M. and Sargent, T.M. (1989). Development of neural inducing capacity in dissociated *Xenopus* embryos. *Dev. Biol.* **134**: 263-266.
- Schoenwolf, G.C. and Smith, J.L. (1990). Mechanisms of neurulation: traditional viewpoint and recent advances. *Development* **109**(2): 243-270.
- Schulte-Merker, S. and Smith, J.C. (1995). Mesoderm formation in response to *Brachyury* requires FGF signalling. *Curr. Biol.* **5**: 62-67.
- Sen, R. and Baltimore, D. (1986). Multiple nuclear factors interact with the immunoglobulin enhancer sequences. *Cell* **46**, 705-716.
- Sevoian, M., Larose, R. N., and Chamberlain, D. M. (1964). Avian lymphomatosis. VI. A virus of unusual potency and pathogenicity. *Avian Dis.* **8**, 336-347.
- Sha, W.C., Liou, H.C., Tuomanen, E.I. and Baltimore, D. (1995). Targeted disruption of the p50 subunit of NF-kappa B leads to multifocal defects in immune responses. *Cell* **80**(2): 321-330.
- Shi, Y., Katsev, S., Cai, C. and Evans, S. (2000). BMP signalling is required for heart formation in vertebrates. *Dev. Biol.* **224**: 226-237.
- Shih, J. and Keller, R. (1994). Gastrulation in *Xenopus laevis* involution – a current view. *Dev. Biol.* **5**: 85-90.
- Shishido, E., Higashijima, S., Emori, Y. and Saigo, K. (1993). Two FGF-receptor homologues of *Drosophila*: one is expressed in mesodermal primordium in early embryos. *Development* **117**(2): 751-61.
- Shum, A.S., Poon, L.L., Tang, W.W., Koide, T., Chan, B.W., Leung, Y.C., Shiroshi, T. and Copp, A.J. (1999). Retinoic acid induces down-regulation of Wnt-3a, apoptosis and diversion of tail bud cells to a neural fate in the mouse embryo. *Mech. Dev.* **84**: 17-30.
- Sive, H. and Bradley, L. (1996). A sticky problem: the *Xenopus* cement gland as a paradigm for anteroposterior patterning. *Dev. Dyn.* **205**(3): 265-80.
- Skipper, J. K. and Hamilton, T. H. (1977). Regulation by estrogen of the vitellogenin gene. *Proc. Natl. Acad. Sci. USA* **74**(6): 2384-8.
- Slack, J.M. (1991). The nature of the mesoderm-inducing signal in *Xenopus*: a transfilter induction study. *Development* **113**(2): 661-9.

- Slack, J. M.W. (1994). Inducing factors in *Xenopus* early embryos. *Curr. Biol.* **4**(2): 116-26.
- Slack, J.M.W., Isaacs, H.V., Song, J., Durbin, L. and Pownall, M.E. (1996). The role of fibroblast growth factors in early *Xenopus* development. *Biochem. Soc. Symp.* **62**: 1-12.
- Slack, J.M., Isaacs, H.V. and darlington, B.G. (1988). Inductive effects of fibroblast growth factor and lithium ion on *Xenopus* blastula ectoderm. *Development* **103**(3): 581-590.
- Slack, J.M.W., Darlington, B.G., Heath, J.K. and Godsave, S.F. (1987). Mesoderm induction in early *Xenopus* embryos by heparin-binding factors. *Nature* **326**: 197-200.
- Smith, D.L., Xu, W. and Varnold, R.L. (1991). Oogenesis and oocyte isolation. *Meth. Cell Biol.* **36**: 45-60.
- Smith, W.C., Knecht, A.K., Wu, M. and Harland, R.M. (1993). Secreted noggin protein mimics the Spemann organizer in dorsalizing *Xenopus* mesoderm. *Nature* **361**: 547-9.
- Sompayrac, L., Jane, S., Burn, T.C., Tenen, D.G. and Danna, K.J. (1995). Overcoming limitations of the mRNA differential display technique. *Nucleic Acids Res.* **23**(22): 4738-9.
- Song, J. and Slack, J.M. (1996). XFGF-9: a new fibroblast growth factor from *Xenopus* embryos. *Dev. Dyn.* **206**(4): 427-436.
- Song, J. and Slack, J.M.W. (1994). Spatial and temporal expression of basic fibroblast growth factor (FGF-2) mRNA and protein in early *Xenopus* development.
- Spemann, H. and Mangold, H. (1924). Induction of embryonic primordial by implantation of organizers from a different species, in *Foundations of Experimental Embryology*, (Willier, B.H. and Oppenheimer, J.M., 2<sup>nd</sup> ed.). Hafner Press, New York.
- Stoetzel, C., Bolcato-Bellemin, A.L., Bourgeois, P., Perrin-Schmitt, F., Meyer, D., Wolff, M. and Remy, P. (1998). *X-twi* is expressed prior to gastrulation in presumptive neurectodermal and mesodermal cells in dorsalized and ventralized *Xenopus laevis* embryos. *Int. J. Dev. Biol.* **42**(6): 747-56.
- Stone, D.M., Hynes, M., Armanini, M., Swanson, T.A., Gu, Q., Johnson, R.L., Scott, M.P., Pennica, D., Goddard, A., Phillips, H., Noll, M., Hooper, J.E., de Sauvage, F. and Rosenthal, A. (1996). The tumor suppressor gene *patched* encodes a candidate receptor for Sonic hedgehog. *Nature* **384**: 129-34.

- Strong, C.F., Barnett, M.W., Hartman, D., Jones, E.A. and Stott, D. (2000). Xbra3 induces mesoderm and neural tissue in *Xenopus laevis*. *Dev. Biol.* **222**(2): 405-419.
- Sun, B. I., Bush, S. M., Collins-Racie, L. A., LaVallie, E. R., DiBiasio-Smith, E. A., Wolfman, N. M., McCoy, J. M. and Sive, H. L. (1999). *derrière*: a TGF- $\beta$  family member required for posterior development in *Xenopus*. *Development* **126**: 1467-1482.
- Sun, Y., Hegamyer, G. and Colburn, N.H. (1994). Molecular cloning of five messenger RNAs differentially expressed in preneoplastic or neoplastic JB6 mouse epidermal cells: one is homologous to human tissue inhibitor of metalloproteinases-3. *Cancer Res.* **54**(5): 1139-44.
- Suzuki, A., Ueno, N. and Hemmati-Brivanlou, A. (1997). *Xenopus* MSX1 mediates epidermal induction and neural inhibition by BMP4. *Development* **124**(16): 3037-3044.
- Suzuki, K., Tsuchida, J., Yamamoto, T. and Inoue, J. (1998). Identification and expression of the *Xenopus* homolog of mammalian p100-NF $\kappa$ B2. *Gene* **206**, 1-9.
- Taira, M., Jamrich, M., Good, P.J. and David, L.B. (1992). The LIM domain-containing homeobox gene *Xlim-1* is expressed specifically in the organizer region of *Xenopus* gastrula embryos. *Genes Dev.* **6**: 356-366.
- Tannahill, D., Isaacs, H.V., Close, M.J., Peters, G. and Slack, J.M. (1992). Developmental expression of the *Xenopus* int-2 (FGF-3) gene: activation by mesodermal and neural induction. *Development* **115**(3): 695-702.
- Tata, J.R. (1993). Gene expression during metamorphosis: an ideal model for post embryonic development. *BioEssays* **15**: 239-248.
- Tata, J.R. (1996). Metamorphosis: an exquisite model for hormonal regulation of post embryonic development. *Biochem. Soc. Symp.* **62**: 123-136.
- Tata, J.R. (1999). Amphibian metamorphosis as a model for studying the developmental actions of thyroid hormone. *Biochimie* **81**(4): 359-366.
- Thakur, S., Lin, H.C., Tseng, W.T., Kumar, S., Bravo, R., Foss, F., Gelinas, C. and Rabson, A.B. (1994). Rearrangement and altered expression of the NF $\kappa$ B-2 gene in human cutaneous T-lymphoma cells. *Oncogene* **9**(8): 2335-44.
- Thanos, D. and Maniatis, T. (1995). NF- $\kappa$ B: A lesson in family values. *Cell* **80**, 529-532.
- Theilen, G. H., Zeigel and Twiehaus, M. J. (1966). Biological studies with RE virus (strain T) that induces reticuloendotheliosis in turkeys, chickens and Japanese quail. *J. Natl. Cancer Inst.*, **37**, 731-743.

- Thomsen, G.H. and Melton, D.A. (1993). Processed Vg1 protein is an axial mesoderm inducer in *Xenopus*. *Cell* **74**(3): 433-41.
- Tiedemann, H., Asashima, M., Grunz, H., Knöchel, W. and Tiedemann, H. (1998). Neural induction in embryos. *Develop. Growth Differ.* **40**: 363-376.
- Trecca, D., Guerrini, L., Fracchiolla, N.S., Pomati, M., Baldini, L., Maiolo, A.T. and Neri, A. (1997). Identification of a tumor-associated mutant form of the NF kappaB RelA gene with reduced DNA-binding and transactivating activities. *Oncogene* **14**(7): 791-9.
- Turner, D., Snider, L. and Rupp, R. [http://vize222.zo.utexas.edu/Marker\\_pages/PlasMaps/CS2.html](http://vize222.zo.utexas.edu/Marker_pages/PlasMaps/CS2.html)
- Vaccarino, F.M., Schwartz, M.L., Raballo, R., Rhee, J. and Lyn-Cook, R. (1999). Fibroblast growth factor signaling regulates growth and morphogenesis at multiple steps during brain development. *Curr. Top. Dev. Biol.* **46**: 179-200.
- van den Heuvel, M. and Ingham, P.W. (1996). *Smoothed* encodes a receptor-like serpentine protein required for hedgehog signalling. *Nature* **382**: 547-51.
- Vincent, J.P. and Gerhart, J.C. (1989). Subcortical rotation in *Xenopus* eggs: an early step in embryonic axis specification. *Dev. Biol.* **123**(2): 526-39.
- Visconti, R., Cerutti, J., Battista, S., Fedele, M., Trapasso, F., Zeki, K., Miano, M.P., de Nigris, F., Casalino, L., Curcio, F., Santoro, M. and Fusco, A. (1997). Expression of the neoplastic phenotype by human thyroid carcinoma cell lines requires NFkappaB p65 protein expression. *Oncogene* **15**(16): 1987-94.
- Vize P.D., Melton, D.A., Hemmati-Brivanlou, A. and Harland R.M. (1991). Assays for gene function in developing *Xenopus* embryos. *Methods Cell Biol.* **36**: 367-87.
- Vogel, A., Rodriguez, C., and Izpisua-Belmonte, J.C. (1996). Involvement of FGF-8 in initiation, outgrowth and patterning of the vertebrate limb. *Development* **122**(6): 1737-50.
- Vogel-Hopker1, A., Momose1, T., Rohrer, H., Yasuda, K., Ishihara, L., Rapaport, D.H. (2000). Multiple functions of fibroblast growth factor-8 (FGF-8) in chick eye development. *Mech. Dev.* **94**: 25-36.
- von Dasow, G., Schmidt, J.E. and Kimelman, D. (1993). Induction of the *Xenopus* organizer: expression and regulation of *Xnot*, a novel FGF and activin-regulated homeo box gene. *Genes. Dev.* **7**(3): 355-366.

- Wallace, V.A. (1999). Purkinje-cell-derived Sonic hedgehog regulates granule neuron precursor cell proliferation in the developing mouse cerebellum. *Curr. Biol.* **9**(8): 445-8.
- Wallingford, J. B. (1999). Tumors in tadpoles: the *Xenopus* embryo as a model system for the study of tumorigenesis. *Trends Genet.* **15**(10): 385-8.
- Wallingford, J. B., Seufert, D. W., Virta, V. C. and Vize, P. D. (1997). p53 activity is essential for normal development in *Xenopus*. *Curr. Biol.* **7**, 747-757.
- Watanabe, N., Hunt, T., Ikawa, Y. and Sagata, N. (1991). Independent inactivation of MPF and cytosstatic factor (Mos) upon fertilization of *Xenopus* eggs. *Nature* **352**: 247-8.
- Wechsler-Reya, R.J. and Scott, M.P. (1999). Control of neuronal precursor proliferation in the cerebellum by Sonic Hedgehog. *Neuron* **22**(1): 103-14.
- Weed, M., Mundlos, S. and Olsen, B.R. (1997). The role of sonic hedgehog in vertebrate development. *Matrix Biol.* **16**(2): 53-8.
- Weinberg, R.A. (1996). How cancer arises. *Sci Am.* **275**(3): 62-70.
- Weinstein, D. C. and Hemmati-Brivanlou, A. (1999). Neural induction. *Ann. Rev. Cell Dev. Biol.* **15**, 411-33.
- Wicking, C., Smyth, I. and Bale, A. (1999). The hedgehog signalling pathway in tumorigenesis and development. *Oncogene* **18**, 7844-7851.
- Wilson, P.A. and Hemmati-Brivanlou, A. (1995). Induction of epidermis and inhibition of neural fate by BMP-4. *Nature* **376**: 331-333.
- Wolda, S.L. and Moon, R.T. (1992). Cloning and developmental expression in *Xenopus laevis* of seven additional members of the Wnt family. *Oncogene* **7**(10): 1941-7.
- Wolpert, L., Beddington, R., Brockes, J., Jessell, T., Lawrence, P. and Meyerowitz, E. (1998). *Principles of development*. Current Biology Ltd., London, U.K.
- Wood, K.M., Roff, M. and Hay, R.T. (1998). Defective IkappaBalpha in Hodgkin cell lines with constitutively active NF-kappaB. *Oncogene* **16**(16): 2131-9.
- Wright, C.V., Morita, E.A., Wilkin, D.J., De Robertis, E.M. (1990). The *Xenopus* XIHbox 6 homeo protein, a marker of posterior neural induction, is expressed in proliferating neurons. *Development* **109**(1): 225-34.

- Wu, M.X., Ao, Z., Prasad, K.V., Wu, R. and Schlossman, S.F. (1998). IEX-1L, an apoptosis inhibitor involved in NF-kappaB-mediated cell survival. *Science* **281**: 998-1001.
- Xie, J., Johnson, R.L., Zhang, X., Bare, J.W., Waldman, F.M., Cogen, P.H., Menon, A.G., Warren, R.S., Chen, L.C., Scott, M.P. and Epstein, E.H. Jr. (1997). Mutations of the PATCHED gene in several types of sporadic extracutaneous tumors. *Cancer Res.* **57**(12): 2369-72.
- Xie, J., Murone, M., Luoh, S.M., Ryan, A., Gu, Q., Zhang, C., Bonifas, J.M., Lam, C.W., Hynes, M., Goddard, A., Rosenthal, A., Epstein, E.H. Jr. and de Sauvage, F.J. (1998). Activating *Smoothed* mutations in sporadic basal-cell carcinoma. *Nature* **391**: 90-2.
- Xu, J., Liu, Z. and Ornitz, D.M. (2000). Temporal and spatial gradients of Fgf8 and Fgf17 regulate proliferation and differentiation of midline cerebellar structures. *Development* **127**(9): 1833-43.
- Xu, R.H., Kim, J., Taira, M., Sredni, D. and Kung, H. (1997). Studies on the role of fibroblast growth factor signalling in neurogenesis using conjugated/aged animal caps and dorsal ectoderm-grafted embryos. *J. Neurosci.* **17**(18): 6892-6898.
- Xu, R.H., Kim, J., Taira, M., Zhan, S., Sredni, D. and Kung, H. (1995). A dominant negative bone morphogenetic protein 4 receptor causes neuralization in *Xenopus* ectoderm. *Biochem. Biophys. Res. Commun.* **212**(1): 212-219.
- Xu, X., Weinstein, M., Li, C., Naski, M., Cohen, R. I., Ornitz, D. M., Leder, P. and Deng, C. (1998). Fibroblast growth factor receptor 2 (FGFR2)-mediated reciprocal regulation loop between FGF8 and FGF10 is essential for limb induction. *Development* **125**: 753-765.
- Yamamoto, T., Nakayama, Y., Tajima, T., Abe, S. and Kawahara, A. (2000). Cloning of a cDNA for *Xenopus* prolactin receptor and its metamorphic expression profile. *Dev. Growth Diff.* **42**(2): 167-174.
- Yamashita, K., Matsuda, K., Hayashi, H., Hanaoka, Y., Tanaka, S., Yamamoto, K. and Kikuyama, S. (1993). Isolation and characterization of two forms of *Xenopus* prolactin. *Gen. Comp. Endocrinol.* **91**(3): 307-317.
- Yang S., Lockwood, A., Hollett, P., Ford, R. and Kao, K. (1998). Overexpression of a novel *Xenopus* rel gene induces tumors in early embryos. *J. Biol. Chem.* **273**(22): 13746-13752.
- Yokoyama, H., Endo, T., Tamura, K., Yajima, H. and Ide, H. (1998). Multiple digit formation in *Xenopus* limb bud recombinants. *Dev Biol.* **196**(1): 1-10.

- Yokoyama, H., Yonei-Tamura, S., Endo, T., Izpisua Belmonte, J.C., Tamura, K. and Ide, H. (2000). Mesenchyme with *fgf-10* expression is responsible for regenerative capacity in *Xenopus* limb buds. *Dev Biol.* **219**(1): 18-29.
- Zeller, R. and Duboule, D. (1997). Dorso-ventral limb polarity and origin of the ridge: on the fringe of independence? *BioEssays* **19**(7): 541-546.
- Zhang, J., Houston, D. W., King, M. L., Payne, C., Wylie, C. and Heasman, J. (1998). The role of maternal vegT in establishing the primary germ layers in *Xenopus* embryos. *Cell* **94**: 515-524.
- Zhong, H., Su Yang, H., Erdjument-Bromage, H., Tempest, P. and Ghosh, S. (1997). The transcriptional activity of NF-kappaB is regulated by the IkappaB-associated PKAc subunit through a cyclic AMP-independent mechanism. *Cell* **89**(3): 413-424.
- Zhong, H., Voll, R.E. and Ghosh, S. (1998). Phosphorylation of NF-kappa B p65 by PKA stimulates transcriptional activity by promoting a novel bivalent interaction with the coactivator CBP/p300. *Mol. Cell* **5**: 661-671.
- Zimmerman, L.B., De Jesús-Escobar, J.M. and Harland, R.M. (1996). The spermann organizer signal noggin binds and inactivates bone morphogenic protein 4. *Cell* **86**: 599-606.
- Zippelius, A. and Pantel, K. (2000). RT-PCR-based detection of occult disseminated tumor cells in peripheral blood and bone marrow of patients with solid tumors. An overview. *Ann. N.Y. Acad. Sci.* **906**: 110-23.









